

Appendix A. Seismologic and Active Fault Investigations

Appendix A. Seismologic and Active Fault Investigations

Appendix A-1 Seismologic Investigation

Appendix A-1 Seismologic Investigation

Appendix A-1- Seismological Investigation

A.1 Seismotectonic Setting

The project site is located in the Sierran Foothills of central California east of the Sacramento Valley (Figure A-1). The modern tectonic setting of central California is dominated by the transform plate boundary contact between the Pacific and North American plates south of the Mendocino triple junction. The Pacific plate moves north-northwest (N35°W to N38°W) at a rate of about 46 to 47 mm/yr relative to the North American plate (DeMets *et al.*, 1994). Right-lateral strike-slip displacement along the major branches of the San Andreas fault system accommodates most of this plate motion, with the remainder generating Holocene tectonism and seismicity at the western continental margin and to the east in the Sierra Nevada and Basin and Range Provinces (Minster and Jordan, 1987; Atwater, 1970). East of the Coast Ranges, the Great Valley and the adjacent Sierra Nevada form a relatively stable crustal block composed of Mesozoic crystalline basement that dips gently to the west (Hill *et al.*, 1991). The western edge of the Sierra Nevada block, beneath the sediments of the Great Valley, is generally thought to be coincident with the western margin of the Great Valley. This region is referred to as the Coast Ranges-Sierran Block (CRSB) boundary zone (Wong and Ely, 1983; Wong *et al.*, 1988), where compressional deformation occurs on reactivated east-verging, low-angle structures (Unruh and Moores, 1992; Unruh and Lettis, 1998). High slip-rate faults associated with the San Andreas fault system lie to the west of this boundary zone (Figure A-1).

The Sierra Nevada is a 600-km-long by 150-km-wide composite batholith that was emplaced over a period of nearly 100 m.y., from approximately 180 to 80 Ma (Bateman and Eaton, 1967). Uplift of the range to its present elevation occurred in late Cenozoic time around 10 to 3.5 Ma. In the vicinity of the central Sierra Nevada, the fault activity map of California compiled by Jennings (1994) and Jennings and Bryant (2010) shows few Quaternary faults within the 60-km-long zone that extends northwest from the foothills to Lake Tahoe in the east. East of Lake Tahoe, the eastern escarpment of the Sierra Nevada (and the western extent of the Basin and Range Province) is defined by a series of north-to-northwest-striking, eastward-dipping, normal and dextral-oblique faults that have sustained significant Holocene displacement. However, recent research suggests that “internal” faults may be distributed relatively evenly across the Sierra Nevada. The activity rate of faults on the west side of the Sierra Nevada appears to be lower than that on the east side of the range, and cumulative late Cenozoic vertical separations and slip rates on these faults systematically increase eastward towards the frontal fault system along the eastern escarpment of the Sierra (from thousandths of a mm/yr to hundredths of a mm/yr). Only a few of these faults show latest Pleistocene or younger movement. These western late Cenozoic faults are the closest to the project site and typically exhibit normal dip-slip and normal-right-lateral oblique motion. Many of these faults are reactivated portions of the Mesozoic Foothills fault system (PG&E, 1994a) and have been interpreted to have low long-term slip rates (Schwartz *et al.*, 1977; Woodward-Clyde Consultants, 1978; PG&E, 1994a; Page and Sawyer, 2001).

A.2 Sierran Foothills Fault System

The west-central portion of the Sierra Nevada block contains late Cenozoic faults that have reactivated portions of the Mesozoic Foothills fault system (Page and Sawyer, 2001) (Figure A-2). The approximately 360-km-long Foothills fault system appears to have two different structural components. South of the Cosumnes River and south of Folsom Dam, the fault system is relatively narrow (10 to 15 km wide) and composed of continuous faults within two zones: the Melones fault zone to the east and the Bear Mountain fault zone to the west. North of the Cosumnes River, the fault system broadens (50 to 70 km wide) and becomes more diffuse in nature. Individual faults become more discontinuous (< 20 km long) and sinuous. Based on these observations, we consider the Foothills fault system to consist of a “North” and “South” section, with the division between the two situated at the Cosumnes River. The project site is between the two bounding faults in the northern part of the fault system where the Bear Mountain and Melones faults are about 45 km apart (Figure A-2).

The Foothills fault system formed in response to eastward convergence and subduction during Mesozoic time (Clark, 1960). The fault zone is largely composed of Mesozoic structures that have not been active in Cenozoic time. However, some preferentially oriented structures within this older framework have been reactivated in the late Cenozoic and some even in the Quaternary. Although originally developed as reverse faults associated with convergence, the late Cenozoic faults exhibit primarily normal dip-slip motion in response to tectonic extension (LaForge and Ake, 1999). Earthquake focal mechanisms also indicate extensional stresses along the Sierran Foothills (Lahr *et al.*, 1976). Page and Sawyer (2001) estimate that about 1 to 2 mm/yr of dextral shear are also accommodated by faulting within the central Sierra Nevada and some of the more westerly-striking faults within the Foothills fault system are dextral-oblique.

The Foothills fault system is complex and its paleoseismic history is still not well known. This is due to a lack of late Cenozoic deposits over much of the southern part of the zone that prevents evaluation of fault continuity (Schwartz *et al.*, 1996) and erosion rates that exceed fault-slip rates (Tom Sawyer, Piedmont Geosciences, personal communication, 2015). It appears that only faults with multiple late Cenozoic surface-rupturing events are conspicuous, given the geologic conditions that exist in the central Sierra Nevada (Schwartz *et al.*, 1996).

Numerous studies have been conducted along portions of the Foothills fault zone to evaluate its level of activity (e.g. LaForge and Ake, 1999; Tierra Engineering Consultants, 1983; Woodward-Clyde Consultants, 1977; Wong *et al.*, 1994). Page and Sawyer (2001) report several methods that have been used in their studies including: construction of geomorphic and geologic profiles to identify anomalies that may be Cenozoic faults; paleogeographic reconstructions; geomorphic analysis in areas of low erosion rates such as drainage divides; and exploratory trenching for paleoseismic analysis. Page and Sawyer (2001; 2007) compiled reports and studies conducted in the central Sierra Nevada and report that analysis of 34 geomorphic profiles identify 134 late Cenozoic geomorphic anomalies, of which 110 are considered probable late Cenozoic faults. Trenches have been excavated across 59 faults, with some faults requiring multiple trenches. Based on the trenching evidence, eight or nine faults have been shown to have experienced latest Pleistocene to Holocene surface displacement.

Page and Sawyer (2001; 2007) use their compiled data to characterize late Cenozoic faults within the Sierra Nevada as being generally less than 20 km long with predominantly vertical slip and

minor lateral slip. They characterize the faults as having very low slip rates that range from 0.001 to 0.01 mm/yr with repeated displacement events in the past 4 to 5 million years. They estimate recurrence intervals for repeated fault ruptures on the order of tens of thousands of years. They conclude that many of the late Cenozoic faults, but not all, are reactivated parts of the Mesozoic Foothills fault system. They emphasize, however, that most of the Mesozoic faults are not late Quaternary faults.

An examination of the faults within the Foothills fault system by Schwartz *et al.* (1996) for the proposed Auburn Dam led them to concur with PG&E (1994b) that mapped lengths of late Cenozoic faults in the western foothills closely approximate the lengths of seismogenic faulting. Schwartz *et al.* (1996) also stated that long multiple-segment ruptures are not expected because long rupture lengths tend to scale with large displacements, and observed displacements in the Foothills fault zone are generally small (usually < 30 cm and always <1 m) (Tom Sawyer, Piedmont Geosciences, personal communication, 2015).

The faults of the Foothills fault system nearest the project site are the Wolf Creek-Big Bend fault, approximately 6 km west of the dam site area, and the Weimar fault, which crosses the Bear River within the study area. The Wolf Creek fault west of the site constitutes a bedrock fault that juxtaposes Mesozoic and Paleozoic metavolcanic rocks on the east against intrusive rocks of the Smartville Complex on the west (Saucedo and Wagner, 1992). The Wolf Creek basement fault is partially coincident with the late Cenozoic Highway 49 lineament or fault (PG&E, 1994b; Page and Sawyer, 2007). The Highway 49 lineament is a pronounced 21-km-long north-northeast-trending topographic lineament formed by a fault that dips steeply west (Figures A-1 and A-2). In places, the prominent strand parallels a less prominent lineament about 0.5 to 1 km to the east. Alt *et al.* (1977) trenched the lineament at the Smith Property site and determined that the fault displaced late-Quaternary "paleo-B horizon" but was overlain by unfaulted colluvium estimated to be about 50,000 years old (Page and Sawyer, 2007).

The Weimar fault is also a bedrock fault, which juxtaposes Mesozoic and Paleozoic metavolcanic rocks on the west against slate and sandstone of the Mariposa Formation, Logtown Ridge volcanics, serpentinite, and Permo-Triassic metasedimentary rocks. The fault was considered as a possible late Cenozoic fault for inclusion in Page and Sawyer's (2007) compilation but was ultimately excluded (Tom Sawyer, Piedmont Geosciences, personal communication, 2015). The basement fault is coincident with locally pronounced lineaments, which Page and Sawyer interpret to form two segments, separated by a step at the North Fork American River. They found two geomorphic anomalies in erosion surfaces across the fault: the Driver's Flat anomaly, 15 km east of Auburn and just south of the North Fork American, which had a 90-100-m down-to-the-west step on a Tertiary erosion surface; and a possible 35-m step on the Tertiary Mehrten Formation across the fault just south of Bear River (Tom Sawyer, Piedmont Geosciences, written communication, 2015).

A.2.1 Lineament Observations

As part of this investigation, we reviewed Lidar data in the immediate vicinity of the project site and black and white stereo aerial photography in a wider region encompassing the breadth of the Foothills fault system and extending about 25 km north and south of the project site. The aerial photographs were obtained in 1975 and 1978 by the U.S. Geological Survey (USGS) and were taken at a scale of 1:80,000.

Based on the analysis of the photographs and the Lidar, we developed a preliminary lineament map (Figure A-3). The lineaments mapped include topographic lineaments, vegetation and tonal lineaments. They are in places associated with linear erosion features, linear drainages, topographic steps, and range fronts. The map is of lineaments only, and association with faults is possible but not implied. Lineaments can be produced by other processes than faulting including fluvial and gravitational processes, differential erosion of different rock types, and jointing.

The analysis showed that many of the longer and more prominent lineaments are coincident with previously mapped faults of the Foothills fault system (Figure A-3). These are assumed to represent faults. In addition to these long lineaments, however, we have mapped numerous shorter and less prominent lineaments. Due to the short lengths of most of these, and the lack of continuity between them, we do not propose any new faults within the area observed, based on this analysis at small-scale.

The high-resolution Lidar within the project area also revealed several short and not very prominent lineaments (Figure A-3). Most of these are not likely associated with faults, but may bear further investigation if they are near the proposed damsite.

5.2.2 Earthquake magnitude

We consider the maximum earthquake for any faults within the Foothills fault system to be **M** 6.5 based on a surface rupture length of less than ~20 km. This is consistent with the maximum magnitude considered by the Working Group on Northern California Earthquake Probabilities (WGNCEP, 1996), Schwartz *et al.* (1996), Page and Sawyer (2001), and the 2008 USGS National Hazard Maps (Petersen *et al.*, 2008). The UCERF3 (Field *et al.*, 2013) statewide seismic hazard analysis allows much larger ruptures on most faults than previous models, but return times on magnitudes greater than **M** 6.5 are greater than 100,000 years. Schwartz *et al.* (1996) suggest that the information about maximum earthquake magnitude is incomplete and that slightly larger maximum earthquake magnitudes might also be possible. However, Tom Sawyer (personal communication, 2015) argues that the small observed displacements (generally < 30 cm) are consistent with smaller magnitude earthquakes.

A.3 Historical Seismicity

The area of the proposed damsite has experienced very few historical earthquakes (Figure A-4), with only two earthquakes of magnitude **M** 5.0 or larger within 50 km of the proposed damsite during the time period 1855 to 2014. A small cluster of microearthquakes were located about 36 km southwest of the site in the Rocklin-Penrhyn pluton (Figure A-4), which appear to be confined to a very small source volume (Cramer *et al.* 1978). The largest nearby earthquake was a **M** (unknown magnitude scale) 4 event that was reported as felt in 1908 in the Roseville-Auburn area with a maximum Modified Mercalli (MM) intensity of IV (Cramer *et al.* 1978) (Figure A-5). The MM II-III isoseismal encompasses the area of the proposed dam (Figure A-5). The closest event located to the proposed site is a duration magnitude (M_D) 2.1 event that occurred on 17 June 1983 about 5 km to the north-northeast.

The most significant historical earthquake near the site was the 1975 Richter local magnitude (M_L) 5.7 (body-wave magnitude, m_b , 5.9) Oroville earthquake that occurred on 1 August about 60 km to the northwest (Figure A-4). The earthquake was preceded by a sequence of foreshocks

beginning on 28 June, 25 of which were located, and the largest of which was M_L 4.7 (Lahr *et al.*, 1976; Morrison *et al.* 1976). Following the mainshock, 7 earthquakes of $M \geq 5$ and 9 earthquakes between M 4 and 5 were located between 1 August and 27 September. This earthquake is of interest as it occurred close to Oroville Dam, which impounds a reservoir of 4.3 million m^3 . A 16-station temporary network was immediately installed after the mainshock in order to record aftershocks. The network was fully operational by 11 August and recorded many aftershocks of which over 300 were located. The hypocentral locations defined a fault plane surface striking N3°E and dipping 60° to the west to a depth of 10 km (Lahr *et al.*, 1976). A focal mechanism derived from long-period teleseismic compression (P) and shear (S) waves and P wave first motions indicate normal faulting on a 65° west dipping fault plane, striking north-south, with a very small component of left-lateral motion and consistent with the fault plane observed from the aftershock locations (Langston and Butler, 1976). Surface-faulting was observed, consistent with the aftershock locations and focal mechanism, along a north-south oriented zone nearly 3.8 km long within about 5 km of Lake Oroville (Clark *et al.*, 1976). The slip vectors indicated normal faulting with east-west extension with slip on the order of up to 4 to 5 cm horizontally and 5 to 6 cm vertically. The slip appeared to increase with time indicating additional slip after the mainshock (Clark *et al.*, 1976).

The Oroville earthquake mainshock was felt over a large area of northern California and western Nevada and a maximum Modified Mercalli (MM) intensity VII was reported (Stover and Coffman, 1993). Damage mostly consisted of cracks in chimneys and walls, with some broken windows and plaster at schools, hospitals and houses in the Oroville-Thermalito area. Property damage was estimated to be \$2.5 million (Stover and Coffman, 1993). The seismicity occurred 6 years after the first filling of Lake Oroville in 1969 (Lahr *et al.* 1976). No seismicity was observed during the filling and subsequent fluctuations in following years. However, in 1974 the dam was lowered more than 40 m between July 1974 and January 1975, after which it was filled more rapidly than before. Historically, there had been fewer than 40 events of $M \geq 3.5$ within 100 km of the Oroville damsite between 1940 and 1974 with none closer than 40 km (Lahr *et al.* 1976). Seismicity has continued to occur in this area through the 1990's and the epicenters have migrated further to the north defining a north-south zone 15 km long. Since about 2000, another distinct cluster of microearthquakes ($M_D \leq 2.5$) have been located about 17 km north-northwest of the 1975 mainshock. The Oroville earthquake is discussed as a possible case of reservoir-triggered seismicity in Section A.5.1.

In 1966 on September 12, a M 5.9 earthquake occurred near Boca, California, a distance of 55 km east-northeast of the proposed damsite (Figure A-4). This was the mainshock in a series of earthquakes and was felt over an area of 116,500 km^2 (Coffman and von Hake, 1982). Ground cracks were observed in the area northeast of Truckee, in the Russell Valley. Ground cracks were also reported in the Boca and Prosser (earthfill) Dams (Coffman and von Hake, 1982). There was some damage to the I80 highway bridges and some chimneys fell in some towns. Some plaster cracks were observed and a roofline was thrown out of plumb in Calpine (Coffman and von Hake, 1982).

Two other $M \geq 5$ events occurred 41 and 44 km northeast of the damsite in 1909 (Figure A-4). These events are the M_L 5 earthquake of 3 March 1909 and the 23 June 1909 event of M 5.5 (unknown magnitude scale). The latter event was reported as felt (Coffman and von Hake, 1982) in Sierra County with maximum intensities estimated as MM VII. Chimneys were damaged in Downieville and slight damage was reported at Redding and Grass Valley. The principal

damage was to flumes and chimneys and numerous aftershocks were reported (Coffman and von Hake, 1982). The felt area was estimated to be about 130,000 km².

A.4 Deterministic Seismic Hazard Analysis

A deterministic seismic hazard analysis (DSHA) was performed to develop preliminary design ground motions for the proposed water storage facility. This preliminary analysis is based on inputs from the Phase I Geological Investigations including literature review. To carry out the DSHA, we calculated site-specific 5%-damped median, 69th and 84th percentile horizontal acceleration response spectra for a maximum earthquake of **M** 6.5 on the Wolf Creek fault. As discussed in Section A.2, the closest faults of the Foothill fault system are the Wolf Creek-Big Bend and Weimer faults. The existing geomorphic evidence for late Cenozoic fault activity for the Weimer fault is weak, but permissible, with a probability of activity of 0.25 (T. Sawyer, written communication, 2015). Given such a low probability of activity, the Weimer fault is not considered in the DSHA. All other faults within the Foothill fault system are characterized with a maximum magnitude of **M** 6.5 (Section A.2) but are at greater distances than the Wolf Creek-Big Bend fault. Hence, these are not included in the DSHA.

In addition to active faults, state-of-the-art seismic hazard evaluations need to address the hazard from background earthquakes, events that are not associated with known or mapped faults. In probabilistic seismic hazard analysis (PSHA), the hazard from background earthquakes can be handled through the use of seismic source zones or smoothing of the historical seismicity. In DSHA, the hazard from background seismicity cannot be addressed without specifying a distance. Traditionally an arbitrary judgment was made in specifying a distance but that practice has all but disappeared in modern seismic hazard analysis. For the western Sierran Foothills in which the proposed dam is located, a reasonable maximum background earthquake would be a **M** 6.5 event. Such an event would be consistent with the maximum earthquake along the Foothills fault system, given the uncertainty of which segments of the fault system are active. DSOD addresses the hazard from background earthquakes by specifying a “Minimum Earthquake” (Fraser and Howard, 2002) as discussed below.

To estimate the ground motions, we used recently developed ground motion prediction models appropriate for tectonically active crustal regions. The crustal models were developed as part of the NGA-West2 Project sponsored by Pacific Earthquake Engineering Research (PEER) Center Lifelines Program.

The NGA-West1 Project began in 2003 and in 2008 the first set of models became available. The NGA-West1 models had a substantially better scientific basis than past relationships, which generally dated around 1997 (e.g., Abrahamson and Silva, 1997). They were developed through the efforts of five selected ground motion prediction developer teams working in a highly interactive process with other researchers who: (a) developed an expanded and improved database of strong ground motion recordings and supporting information on the causative earthquakes, the source-to-site travel path characteristics, and the site and structure conditions at ground motion recording stations; (b) conducted research to provide improved understanding of the effects of various parameters and effects on ground motions that are used to constrain models; and (c) developed improved statistical methods to develop ground motion relationships including uncertainty quantification. The NGA-West1 models benefited greatly from a large amount of new strong motion data from large earthquakes (**M** > 7) at close distances (< 25 km).

Data include records from the 1999 **M** 7.6 Chi Chi, Taiwan, 1999 **M** 7.4 Kocaeli, Turkey, and 2002 **M** 7.9 Denali, Alaska earthquakes.

The NGA-West2 models were developed based on an expanded strong motion database compared to the initial NGA database. A number of more recent well recorded earthquakes were added to the NGA-West2 database including the Wenchuan, China earthquake, numerous moderate magnitude California events down to **M** 3.0, and several Japanese, New Zealand, and Italian earthquakes. The NGA-West2 models by Chiou and Youngs (2014), Campbell and Bozorgnia (2014), Abrahamson *et al.* (2014), and Boore *et al.* (2014) were used in the DSHA. The models were weighted equally in the DSHA. Input parameters are provided in Table A-1.

One of the main inputs to the NGA-West 2 models is the time-averaged shear-wave velocity (V_s) in the top 30 meters (V_{s30}). At this preliminary phase of the project, site-specific V_s have not been made. As discussed in Section 3, the rock at the site consists of interbedded pyroclastic tuff, tuff-breccia, volcanic flows and epiclastic strata of the middle volcanic unit of the Lake Combie Complex (Tuminas, 1983). Preliminary site investigations indicate that the bedrock at the site is competent. Seismic refraction measurements by NORCAL Geophysical Consultants in 2013 at Combie Dam, approximately 4.5 km to the southwest on the Bear River, show P-wave velocities of 4,000 to 7,000 ft/sec in highly weathered rock over less weathered rock with P-wave velocities of 7,000 to over 11,000 ft/sec (NORCAL Geophysical Consultants, 2013). The highly weathered rock was generally four to six feet thick with some places up to ten feet thick. These P-wave velocities indicate V_s of 3,360 to 5,880 ft/sec (1,020 to 1,790 m/sec) for less weathered rock based on a range of Poisson's ratio of 0.3 to 0.35. For this study a lower bound V_{s30} of 1,000 m/sec was used in the NGA-West2 models. V_{s30} should be verified in future site investigations for final design ground motions.

Figure A-6 illustrates the 69th percentile deterministic spectra for each of the four ground motion models along with the geometric mean. Figure A-7 compares the median, 69th and 84th percentile geometric mean deterministic spectra. The median, 69th and 84th percentile peak horizontal ground accelerations (PGAs) are 0.23, 0.31 and 0.42 g, respectively.

For these preliminary analyses, the proposed water storage facility is assumed to be a “high or extreme consequence” dam. Based on this consequence classification along with the low slip rate of the Wolf Creek-Big Bend fault (< 0.1 mm/yr) (Section A.2), DSOD guidelines recommend the use of 50th to 84th percentile ground motions (Fraser and Howard, 2002). A probabilistic seismic hazard analysis (PSHA) is often used to determine the level of conservatism in the DSHA by providing an estimate of the approximate return period of the deterministically based ground motions. DSOD has used PSHA for over 30 dams in California and estimated return periods ranging from a few hundred years for 50th percentile deterministic ground motions for dams near high slip rate faults to over 20,000 years for the 84th percentile deterministic ground motions for dams near low slip rate faults (Fraser and Howard, 2002). Hence, DSOD recommends that in matrix categories requiring “50th to 84th percentile ground motions”, a PSHA and engineering judgment be used to select the appropriate level of design (Fraser and Howard, 2002). At this phase of the project, a site-specific PSHA has not been performed. It is recommended that a site-specific PSHA be performed when developing final design ground motions.

The 2008 USGS hazard values for PGA for a site class B are provided in Table A-2 for return periods of 5,000, 8,000 and 10,000 years (<http://geohazards.usgs.gov/hazardtool/application.php>). The median deterministic PGA (0.23 g) for the site is similar to the 5,000-year return period PGA from the 2008 USGS hazard analysis and the 69th percentile deterministic PGA (0.31 g) is slightly higher than the 10,000-year PGA. Based on DSOD guidelines (Fraser and Howard, 2002), the Minimum Earthquake PGA for new and existing dams should be 0.25 g. AECOM recommends that the 69th percentile deterministic ground motions be used for design of the proposed water storage facility (Table A-3). This is consistent with DSOD guidelines and recommendations by U.S. Committee on Large Dams (1985; 1998) and the International Committee on Large Dams (2010), which recommend a range of return periods of 3,000 to 10,000 years with the appropriate return period for the design ground motion depending on the risk rating of the dam.

A.5 Reservoir-Triggered Seismicity

As early as 1945, a relationship was recognized between the level of water impounded by Hoover Dam and the frequency of earthquakes occurring in the vicinity of its reservoir, Lake Mead (Simpson, 1976). Since then, numerous cases of reservoir-triggered seismicity (RTS) have been recognized worldwide. The most commonly cited cases are the reservoirs created by Kariba Dam in Zambia, Aswan Dam in Egypt, Koyna Dam in India, and Kremasta Dam in Greece. Of the more than 30,000 reservoirs in the world, a disproportionately large fraction of the largest and deepest reservoirs have been associated with reported cases of RTS (Packer *et al.*, 1979). Through 1996, URS had compiled 145 reported cases of RTS worldwide (Wong and Strandberg, 1996). In the following, the potential for RTS at the proposed reservoir to be impounded by Centennial Dam is examined. The proposed reservoir will have a maximum depth of about 76 m and a total volume of $1.26 \times 10^8 \text{ m}^3$ (110,000 acre-ft).

In California, eight reservoirs have been suggested to be cases of RTS (Wong and Strandberg, 1996; Knudsen *et al.*, 2009), including Lake Oroville, which came to prominence with the occurrence of the 1975 M_L 5.7 Oroville earthquake (Toppozada and Morrison, 1982; Section A.3). Lake Oroville is located in a setting that is geologically, tectonically and seismically similar to the proposed reservoir at Centennial Dam. The possible California RTS cases include: Lake Oroville; Lake Crowley in the Sierra Nevada near the town of Mammoth Lakes; Lake Shasta north of Redding; Lake Mendocino near Ukiah; San Luis Reservoir near Los Banos; Lake Berryessa impounded by Monticello Dam near Vacaville; Del Valle Reservoir near Livermore; and Briones Reservoir in the eastern San Francisco Bay area.

A.5.1 1975 Oroville Earthquake

The 1975 Oroville earthquake occurred 12 km south of Lake Oroville (Section A.3). Aftershocks defined a zone extending 16 km south of the dam, consistent with normal faulting on the Cleveland Hills fault as it has been named subsequent to the earthquake. The fault is likely an element of the Foothill fault system. Early studies of the 1975 earthquake were non-committal on whether Lake Oroville was a case of RTS (Morrison *et al.*, 1976; Lahr *et al.*, 1976) or suggested it was not (Beck, 1976). However, Toppozada and Morrison (1982) suggested that there are two factors that might indicate Lake Oroville is a case of RTS: (1) the proximity of the 1975 earthquake to the lake and the extension of the causative fault to the lake. The presence of

the fault provides an “avenue” of water under pressures as high as 20 bars, resulting from a water depth of more than 200 m, into the fault zone; and (2) the occurrence of the earthquake following the largest seasonal fluctuation in lake level. In the winter of 1974 to 1975, the lake was drawn down to its lowest level since filling, and this was followed by refilling and the 1975 earthquake sequence. Seismic monitoring at Lake Oroville since 1975 showed that local seismicity decreases as the lake fills during winter and spring and the largest earthquakes occur as the lake empties during summer and fall (Toppozada and Morrison, 1982). This pattern was consistent from 1975 to 1982 indicating that seasonal fluctuations in water depth at Lake Oroville control the earthquake occurrence.

Whether the 1975 Oroville earthquake was a RTS event is still controversial. Rajendran and Gupta (1986) suggest that the earthquake was not an example of RTS based on the observed b -values (recurrence parameter defining the slope of the Gutenberg-Richter seismicity model), long delay for the onset of activity, and the fact that no seismicity followed the largest lake fluctuation observed up to that time in 1976 to 1977. Packer *et al.* (1979) and Wong and Strandberg (1996) classified Lake Oroville as a case of RTS.

A.5.2 Probabilistic Approach

A useful approach to assessing the potential for RTS is to make comparisons with other reservoirs which have and have not exhibited RTS. Statistical comparisons have been made using the worldwide database of reservoir characteristics and associated seismicity by Packer *et al.* (1979), Perman *et al.* (1981), Wong *et al.* (1991), and Wong and Strandberg (1996). The database provides the means for use of a multivariate probabilistic model to calculate the conditional probability of triggered seismicity at a reservoir using the parameters of depth, volume, local stress conditions, rock type, and the presence of active faulting (Baecher and Kenney, 1982).

From a preliminary analysis of a small data set of 29 cases of RTS and 205 reservoirs not associated with triggered seismicity, Baecher and Kenney (1982) noted that depth was the best discriminant for determining RTS. However, it should be recognized that the data set used in their study and in subsequent studies, includes only deep, very deep, and/or very large reservoirs (Table A-4). The next best attribute was the reservoir volume. Although in the earlier studies, there was insufficient data on active faulting to consider this parameter probabilistically, Packer *et al.* (1979) studied in detail 11 reservoirs that had exhibited RTS and nine showed evidence of active faults near the reservoir. Packer *et al.* (1979) developed a set of definitions for three categories (or “states”) of the five attributes they used to classify reservoirs (Table A-4).

An important aspect as pointed out by Baecher and Keeney (1982) must be noted in evaluating the results of a probabilistic RTS evaluation. Considerable professional judgment is required in analyzing the data and in applying the methodology. No method for developing a model of the likelihood of RTS can be completely objective. The ultimate goal of such models is to systematize the application of professional judgment and to provide a basis for better understanding the phenomenon of RTS.

Based on the probabilistic model to predict RTS, the mean conditional probability for the 70 cases of RTS (includes questionable cases) is 0.300 with 10th and 90th percentile values of 0.264 and 0.336, respectively (Wong *et al.*, 1991). The mean conditional probability of the 459 non-RTS cases is 0.107 with upper- and lower-bound probabilities of 0.100 and 0.114, respectively.

The significant difference between the two mean values with no overlap indicates that the probability estimated for a given reservoir should clearly discern whether RTS can occur based on the trends reflected in the database of the deep, very deep, and very large reservoirs. The probabilistic model estimates RTS conditional probabilities higher than the mean for several well-known RTS cases (Table A-5).

The proposed reservoir would be classified as a shallow and small reservoir based on Table A-4. The reservoir is located within an extensional tectonic stress field (Sections A.2 and A.3) and the underlying geology is generally volcanic (igneous) (Section A.4). In addition, no historical seismicity has been observed in the vicinity of the proposed reservoir (Section A.3). A critical attribute is that there are lineaments that are located beneath the proposed reservoir, as well as a possible continuation of the Weimar fault (Section A.2.1). Note that there is no evidence of RTS at the existing Combie and Rollins damsites. Based on these attributes and states and previous analyses, we believe that RTS has a low probability of occurrence at the proposed reservoir. However, further investigations of the lineaments in the reservoir area are warranted in addition to performing a formal RTS probabilistic calculation.

A.5.3 Maximum RTS Earthquake

The effects of a reservoir-induced stresses which are only on the order of a few bars are only capable of triggering failure along critically stressed faults. The size of an earthquake is controlled by the geometry and the size of the rupture area along such faults, and the pre-existing imposed state of stress. Because these parameters remain essentially unchanged in the presence of a reservoir, the maximum size of an earthquake on a specific fault will not change. Thus the largest RTS earthquake will not exceed the maximum earthquake already assigned to the faults or background seismicity considered significant to the reservoir. In the case of Centennial Dam, the maximum RTS earthquake will be a **M** 6.5 consistent with the maximum event assigned to faults within the Foothill fault system (Section A.4). The maximum background earthquake for the western Sierran foothills is a **M** 6.5 (Section A.4).

Table A-1. NGA-West2 Input Parameters

Parameter	Definition	Value
M	Moment Magnitude	6.5
R_{RUP} (km)	Closest distance to rupture	5.9
R_{JB} (km)	Closest distance to surface projection of rupture	5.9
R_X (km)	Horizontal distance from top of rupture measured perpendicular to fault strike (km)	-5.9 (not used on footwall)
R_{y0} (km)	The horizontal distance off the end of the rupture measured parallel to the strike	0
V_{s30} (m/sec)	Time-averaged shear wave velocity in top 30 m	1000
U	Unspecified mechanism. 1 = unspecified, 0 otherwise	0
F_{RV}	Reverse-faulting factor: 0 for strike slip, normal, normal-oblique; 1 for reverse, reverse-oblique and thrust	0
F_{NM}	Normal-faulting factor: 0 for strike slip, reverse, reverse-oblique, thrust and normal-oblique; 1 for normal	1
F_{HW}	Hanging-wall factor: 1 for site on down-dip side of top of rupture; 0 otherwise	0
Dip (deg)	Average dip of rupture plane (degrees)	80
Z_{TOR} (km)	Depth to top of coseismic rupture (km)	0
Z_{HYP} (km)	Hypocentral depth from the earthquake	Default (8.9)
Z_{1.0} (km)	Depth to V _s =1 km/sec	0.0
Z_{2.5} (km)	Depth to V _s =2.5 km/sec	0.443
W (km)	Fault rupture width (km)	15.2
V_{s30} Flag	1 for measured, 0 for inferred V _{s30}	0 (Inferred)
F_{AS}	0 for mainshock; 1 for aftershock	0
Region	Specific region	California

Table A-2. 2008 USGS Hazard Values for Site Class B

Return Period (years)	PGA (g)
5,000	0.22
8,000	0.26
10,000	0.29

Table A-3. 69th-Percentile Deterministic Spectrum

Period (s)	Spectral Acceleration (g)
0.010	0.31
0.020	0.33
0.030	0.37
0.050	0.50
0.075	0.63
0.100	0.70
0.150	0.74
0.200	0.70
0.250	0.62
0.300	0.55
0.400	0.44
0.500	0.36
0.750	0.25
1.000	0.18
1.500	0.11
2.000	0.08
3.000	0.05
4.000	0.03
5.000	0.02
7.500	0.01
10.000	0.01

Table A-4. Definitions of Reservoir Attribute States
(from Packer *et al.*, 1979)

Attribute	State		
	1	2	3
Depth	Very deep (over 150 m)	Deep (92 to 150 m)	Shallow (less than 92 m)
Volume	Very large (over $1.00 \times 10^{10} \text{ m}^3$)	Large (1.20 to $10.00 \times 10^9 \text{ m}^3$)	Shallow (less than $1.20 \times 10^9 \text{ m}^3$)
Stress State	Extensional	Compressional	Shear
Fault Activity	Active faults present	No active faults present	Not known
Geology	Sedimentary	Metamorphic	Igneous

Table A-5. Estimated Conditional Probabilities for Several Well-Known RTS Reservoirs

Reservoir	Probability
Oroville, CA, USA	0.464
Hoover (Lake Mead), AZ, USA	0.847
Khao Laem, Thailand	0.610
Srinagarind, Thailand	0.490
La Grande 2, Canada	0.660
Aswan, Egypt	0.537
Kastraki, Greece	0.098
Kremasta, Greece	0.322
Koyna, India	0.314
Kariba, Zambia	0.595
Nurek, Tadjikistan	0.964

References

- Atwater, T., 1970, Implications of plate tectonics for the Cenozoic tectonic evolution of western North America: Geological Society of America Bulletin, v. 81, p. 3513-3536.
- Baecher, G.B. and Kenney, R.L., 1982, Statistical examination of reservoir-induced seismicity, Bulletin of the Seismological Society of America, v. 72, p. 553-569.
- Bateman, P.C. and Eaton, J.P., 1967, Sierra Nevada Batholith: Science, v. 158, p. 1407-1410.
- Beck, J.L., 1976, Weight-induced stresses and the recent seismicity at Lake Oroville, California: Bulletin of the Seismological Society of America, 66, p. 1121-1131.
- Clark, M.M., Sharp, R.V., Castle, R.O., and Harsh, P.W. 1976, Surface Faulting Near Lake Oroville, California in August, 1975: Bulletin of the Seismological Society of America, Vol. 66, No. 4, pp. 1101-1110.
- Coffman, J.L., and Von Hake, C.A., 1982, Earthquake History of the United States, Publication 41-1, Revised Edition (Through 1970) with supplement (1971-1980), U.S. Department of Commerce, National Oceanic and Atmospheric Administration and U.S. Department of the Interior, Geological Survey, 208 p.
- Cramer, C.H., Toppozada, T.R., and Parke, D.L. 1978, Seismicity of the Foothills Fault System of the Sierra Nevada Between Folsom and Oroville, California: Bulletin of the Seismological Society of America, Vol. 68, No. 1, pp. 245-249.
- DeMets, C., Gordon, R.G., Argus, D.F., and Stein, S., 1994, Effect of recent revisions to the geomagnetic reversal time scale on estimates of current plate motions: Geophysical Research Letters, v. 21, p. 2191-2194.
- Field, E.H., Biasi, G.P., Bird, P., Dawson, T.E., Felzer, K.R., Jackson, D.D., Johnson, K.M., Jordan, T.H., Madden, C., Michael, A.J., Milner, K.R., Page, M.T., Parsons, T., Powers, P.M., Shaw, B.E., Thatcher, W.R., Weldon, R.J., II, and Zeng, Y., 2013, Uniform California earthquake rupture forecast, version 3 (UCERF3)—The time-independent model: U.S. Geological Survey Open-File Report 2013–1165, 97 p., California Geological Survey Special Report 228, and Southern California Earthquake Center Publication 1792, <http://pubs.usgs.gov/of/2013/1165/>.
- Fraser, W.A. and Howard, J.K., 2002, Guidelines for use of the consequence – hazard matrix and selection of ground motion parameters: unpublished memorandum, California Division of Safety of Dams, 9 p.
- Hill, D. P., Eaton, J. P., Ellsworth, W. L., Cockerham, R. S., Lester, F. W., and Corbett, E. J., 1991, The seismotectonic fabric of central California, in Slemmons, D. B., Engdahl, E. R., Zoback, M. R., and Blackwell, D. D. (eds.): Neotectonics of North America, Decade of North American Geology: Geological Society of America, p. 107-132.
- ICOLD (International Committee on Large Dams), 2010, Selecting seismic parameters for large dams guidelines: Bulletin 72, 2010 Revision.
- Jennings, C.W., 1994, Fault activity map of California and adjacent areas with locations and ages of recent volcanic eruptions: California Division of Mines and Geology, 1:750,000.

- Jennings, C.W., and Bryant, W.A., 2010, Fault activity map of California: California Geological Survey Geologic Data Map No. 6, map scale 1:750,000.
- Knudsen, K., Thomas, P., Wong, I., and Zachariasen, J., 2009, Updated probabilistic seismic hazard analyses of Shasta and Keswick Dams and evaluation of reservoir-triggered seismicity, Shasta Dam, Central Valley Project, northern California: unpublished report prepared for U.S. Department of the Interior, Bureau of Reclamation.
- LaForge, R. and Ake, J., 1999, Probabilistic seismic hazard analysis: Central Valley Project, Folsom Unit, Mormon Island Auxiliary Dam: U.S. Bureau of Reclamation Seismotectonic Report 94-3, 109 p.
- Lahr, K.M., Lahr, A.G., Lindh, A.G., Bufe, C.G., and Lester, F.W., 1976, The August 1975 Oroville earthquakes: Bulletin of the Seismological Society of America, v. 66, p. 1085-1099.
- Langston, C.A. and Butler, R., 1976, Focal Mechanism of the August 1, 1975 Oroville Earthquake: Bulletin of the Seismological Society of America, Vol. 66, No. 4, pp. 1111-1120.
- Minster J. B. and Jordan, T. H., 1987, Vector constraints on western U. S. deformation from space geodesy; Neotectonics and plate motion: Journal of Geophysical Research, v. 92, p. 4798-4804.
- Morrison, P.W., Jr., Stump, B.W., and Uhrhammer, R., 1976, The Oroville earthquake sequence of August 1975: Bulletin of the Seismological Society of America, v. 66, p. 1065-1084.
- NORCAL Geophysical Consultants, Inc., 2013, Seismic Refraction Investigation, Combie Dam, Placer/Nevada Counties, California, 12 p.
- Pacific Gas and Electric Company (PG&E), 1994a, Characterization of potential earthquake sources for Ralston Afterbay Dam: FERC Project No. 2079, State Dam No. 1030-4.
- Pacific Gas and Electric Company (PG&E), 1994b, Characterization of potential earthquake sources for Rock Creek (Drum) Dam: FERC 2310, Drum Spaulding Project, State Dam No. 97-43.
- Packer, D.R., Cluff, L.S., Knuepfer, P.L., and Withers, R.J., 1979, Study of reservoir induced seismicity: U.S. Geological Survey Open-File Report 80-1092, 279 p.
- Page, W.D. and Sawyer, T.L., 2001, Use of geomorphic profiling to identify Quaternary faults within the northern and central Sierra Nevada, California: Association of Engineering Geologists Special Volume, "Engineering Geology Practice in Northern California", eds Ferriz, H. and Anderson, R., pg 275-293.
- Perman, R.C., Packer, D.R., Coppersmith, K.J., and Knuepfer, P.L., 1981, Collection of data for data bank on reservoir induced seismicity: U.S. Geological Survey Final Technical Report, 44 p.
- Peterson, M.D., Frankel, A.D., Harmsen, S.C., Mueller, C.S., Haller, K.M., Wheeler, R.L., Wesson, R.L., Zeng, Y., Boyd, O.S., Perkins, D.M., Luco, N., Field, E.H., Wills, C.J., and Rukstales, K.S., 2008, Documentation for the 2008 update of the United States National Seismic Hazard Maps: U.S. Geological Survey Open-File Report 2008-1128, 61 p.
- Rajendran, K. and Gupta, H.K., 1986, Was the earthquake sequence of August 1975 in the vicinity of Lake Oroville, California, reservoir induced?: Physics of the Earth and Planetary Interiors, v. 44, p. 142-148.

- Saucedo, G.J., and Wagner, D.L., 1992, Geologic map of the Chico quadrangle, California: California Division of Mines and Geology, Sacramento, Regional Geologic Map Series, map no. 7, scale 1:250,000.
- Schwartz, D. P., Swan, F. H., III, Harpster, R. E., Rogers, T. H., and Hitchcock, D. E., 1977, Surface faulting potential, Earthquake evaluation studies of the Auburn dam area: Woodward-Clyde Consultants Report for U. S. Bureau of Reclamation, v. 2, 135 p.
- Schwartz, D.P., Joyner, W.B., Stein, R.S., Brown, R.D., McGarr, A.F., Hickman, S.H., and Bakun, W.H., 1996, Review of seismic-hazard issues associated with the Auburn Dam Project, Sierra Nevada foothills, California: U.S. Geological Survey Open-File Report 96-11.
- Simpson, D.W., 1976, Seismicity changes associated with reservoir impounding: Engineering Geology, v. 10, p. 371-385.
- Stover, C. W. and Coffman, J.L., 1993, Seismicity of the United States, 1568-1989 (Revised): U.S. Geological Survey Professional Paper 1527, 493 p.
- Tierra Engineering Consultants, Inc., 1983, Geologic and seismologic investigations of the Folsom, California area: Report to the U.S. Army Engineer District, Sacramento, CA.
- Topozada, T.R. and Morrison, P.W., 1982, Earthquakes and lake levels at Oroville, California: California Geology, v. 35, p. 115-118.
- Tuminas, A., 1983, Structural and Stratigraphic Relations in the Grass Valley – Colfax Area of the Northern Sierra Nevada Foothills, California: Ph.D. Thesis, University of California, Davis.
- Unruh, J.R. and Lettis, W.R., 1998, Kinematics of transpressional deformation in the eastern San Francisco Bay region, California: Geology, v. 26, p. 19-22.
- Unruh, J.R. and Moores, E.M., 1992, Quaternary blind thrusting on the southwestern Sacramento Valley, California: Tectonics, v. 11, p. 192-203.
- USCOLD (U.S. Committee on Large Dams), 1985, Guidelines for selecting seismic parameters for dam projects.
- USCOLD (U.S. Committee on Large Dams), 1998, Updated guidelines for selecting seismic parameters for dam projects.
- Wong, I.G. and Ely, R.W., 1983, Historical seismicity and tectonics of the Coast Ranges-Sierra block boundary: Implications to the 1983 Coalinga earthquakes; *in* Bennet, J. and Sherburne, R. (eds.), The 1983 Coalinga, California Earthquakes: California Division of Mines and Geology Special Publication 66, p. 89-104.
- Wong, I.G., Ely, R.W., and Kollman, A.C., 1988, Contemporary seismicity and tectonics of the northern and central Coast Ranges-Sierran block boundary zone, California: Journal of Geophysical Research, v. 93, p. 7813-7833.
- Wong, I.G., Green, R.K., Sawyer, T.L., and Wright, D.H., 1994, Probabilistic seismic hazard analysis: Mormon Island Auxiliary Dam, Central Valley Project, east-central California: Unpublished report prepared for U.S. Bureau of Reclamation by Woodward-Clyde Federal Services and William Lettis and Associates, 41 p.

Wong, I.G. and Strandberg, J.F., 1996, Assessing the potential for triggered seismicity at the Los Vaqueros Reservoir, California, in *Seismic Design and Performance of Dams*, Sixteenth Annual USCOLD Lecture Series, p. 217-231.

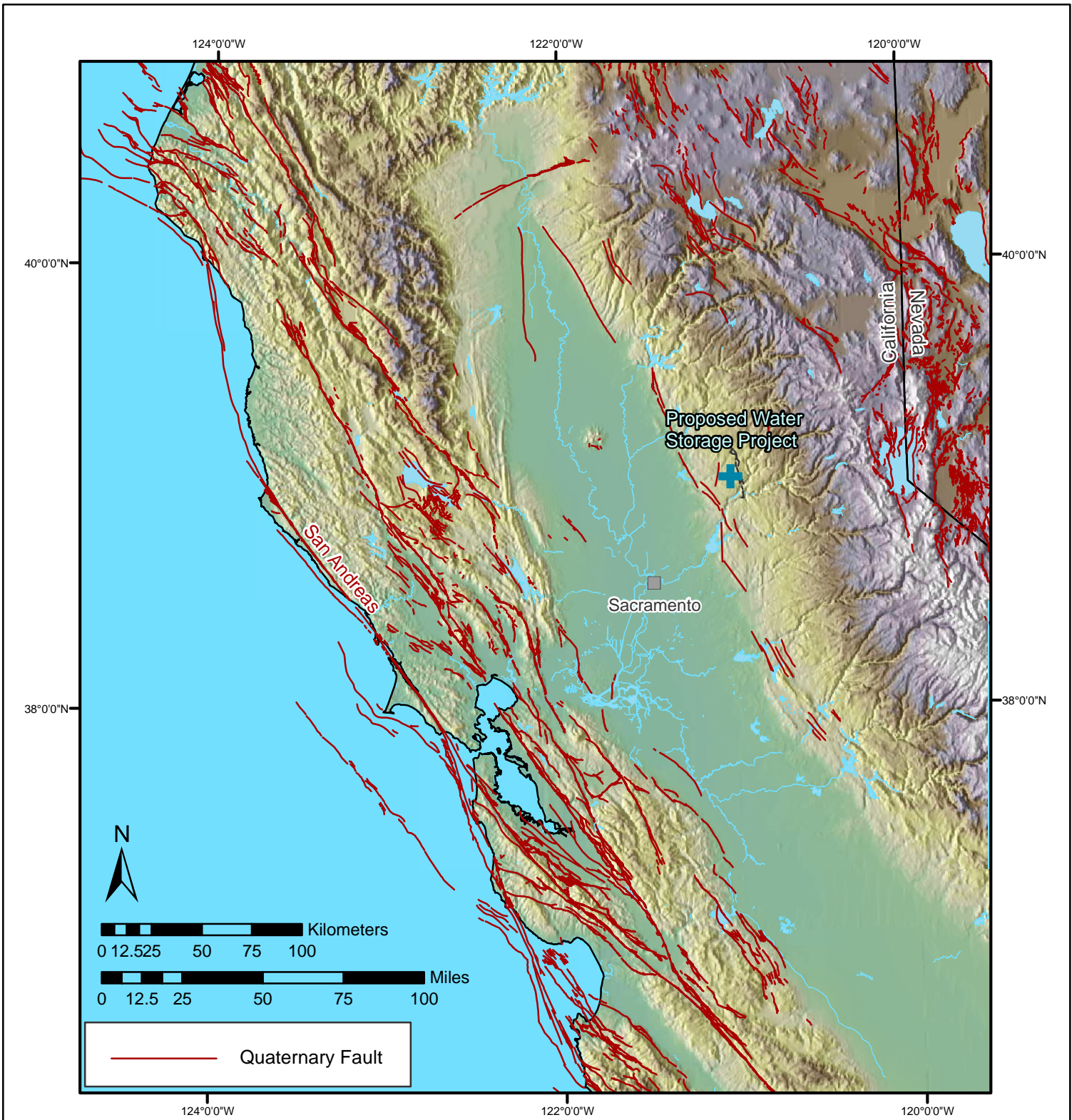
Wong, I.G., Voos, K., Kulkarni, R., and Lawton, G., 1991, An updated probabilistic approach for evaluating reservoir-induced seismicity (abs.), *Seismological Research Letters*, v. 62, p. 36.

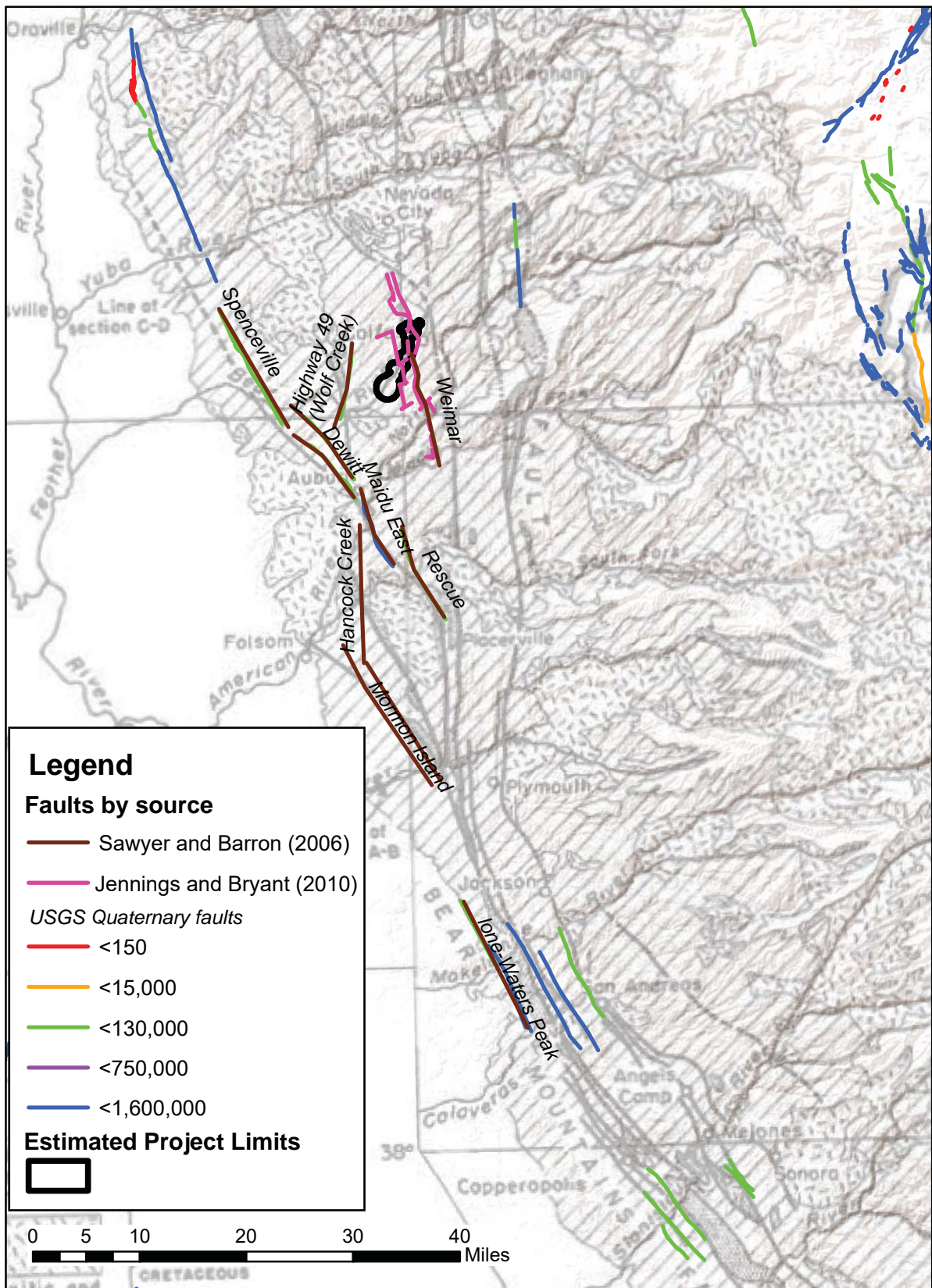
Woodward-Clyde Consultants, 1978, Foothills fault system study: Appendix C.4 of volume 6, Stanislaus Nuclear Project, Site Suitability-Site Safety Report: Report to the Pacific Gas and Electric Company, 166 p.

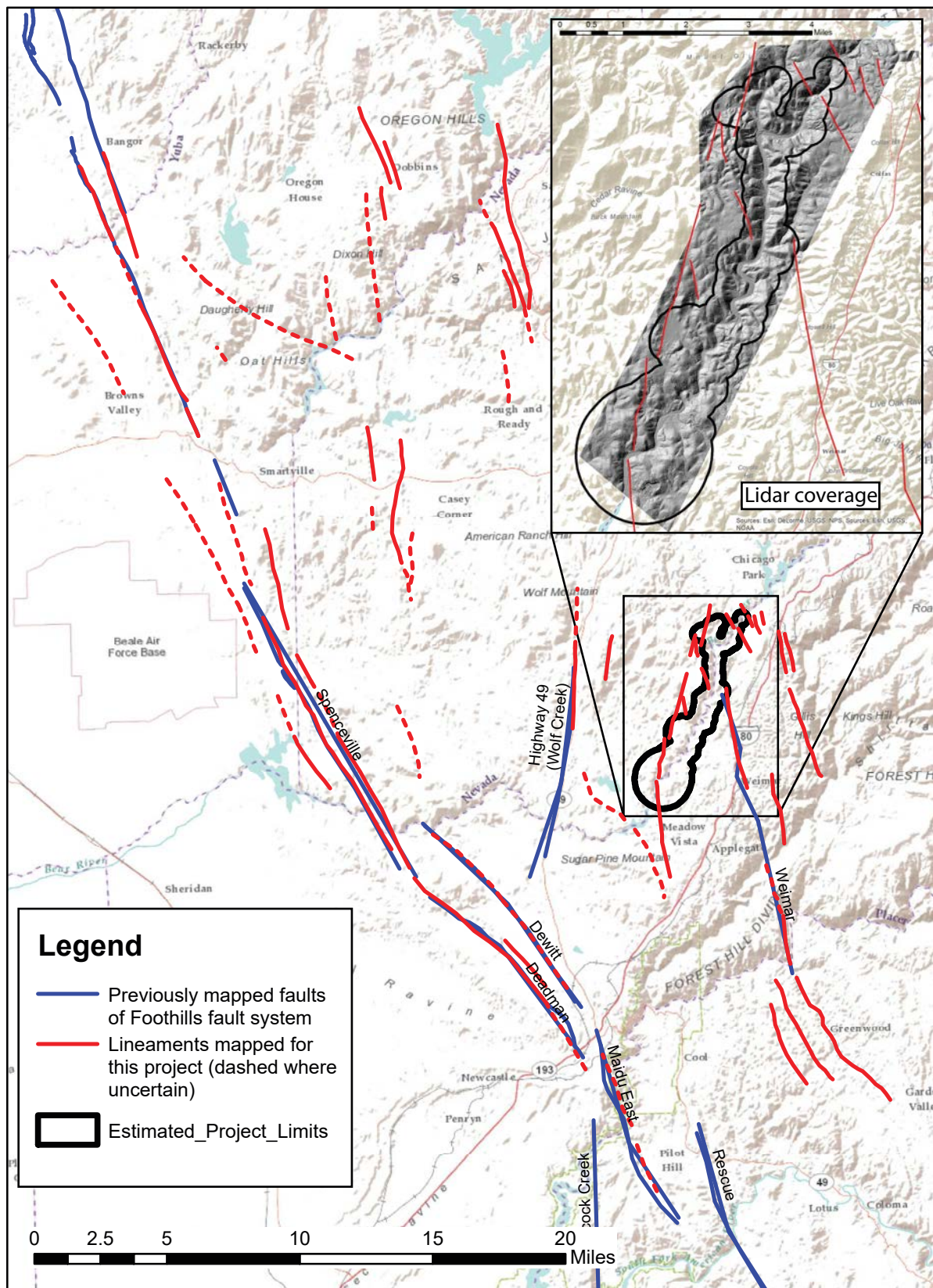
Working Group for California Earthquake Probabilities (WGCEP), 2003, Earthquake probabilities in the San Francisco Bay area: 2002-2031: U.S. Geological Survey Open-File Report 03-214.

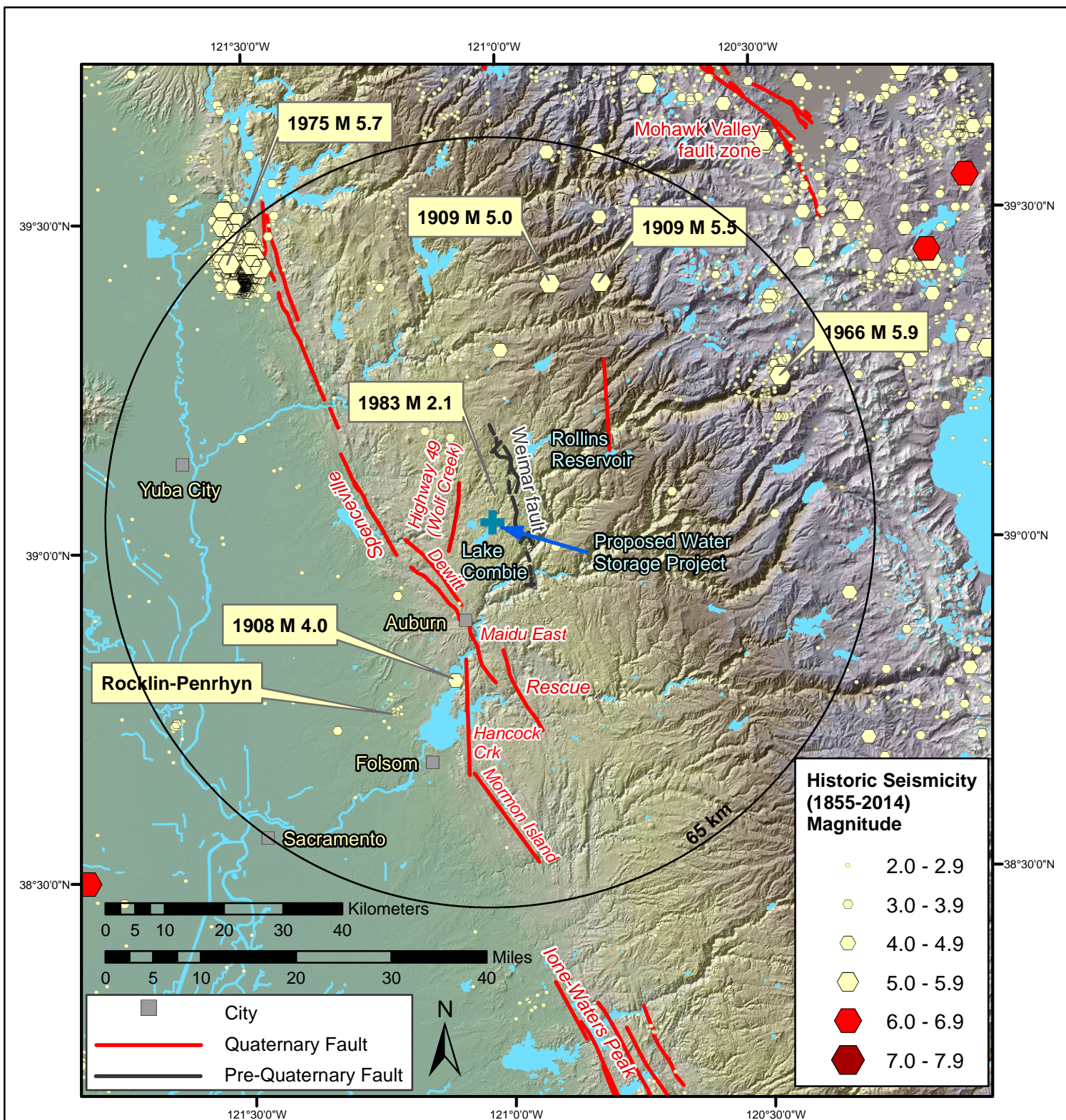
Working Group for California Earthquake Probabilities (WGCEP), 2008, The uniform earthquake rupture forecast, version 2 (UCERF2): U.S. Geological Survey Open-File Report 2007-1437.

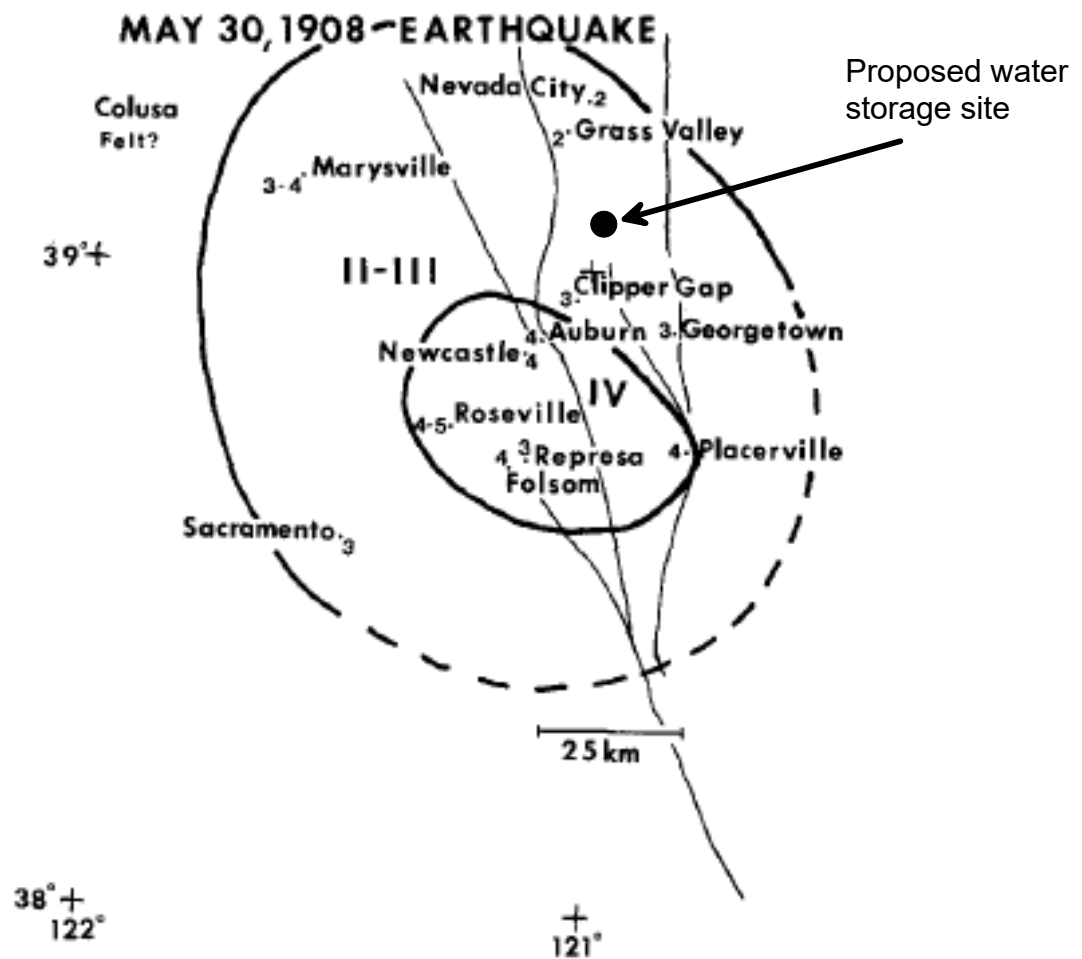
Working Group on Northern California Earthquake Potential (WGNCEP), 1996, Database of potential sources for earthquakes larger than magnitude 6 in northern California: U. S. Geological Survey, Open-File Report 96-705, 53 p.



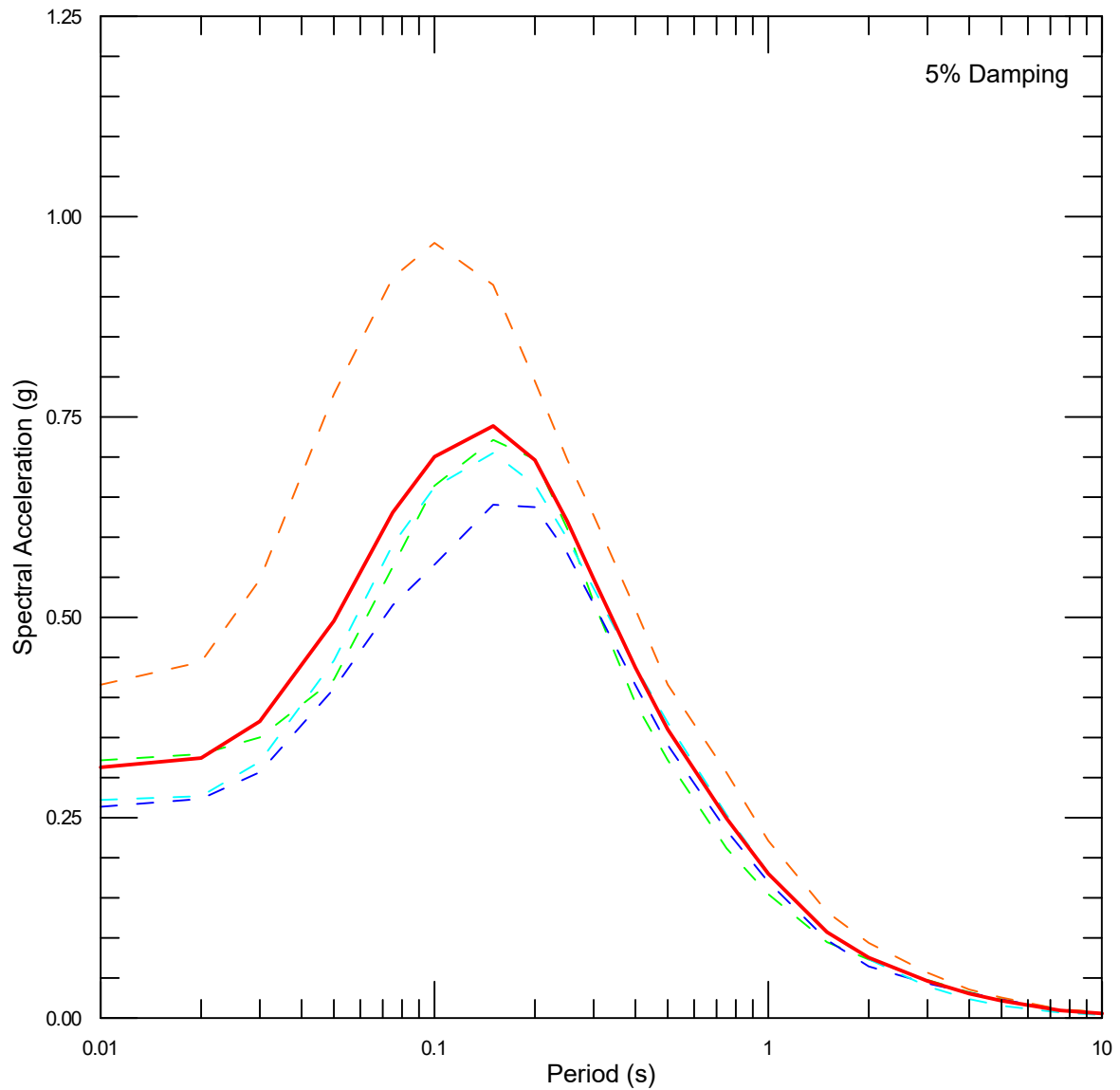






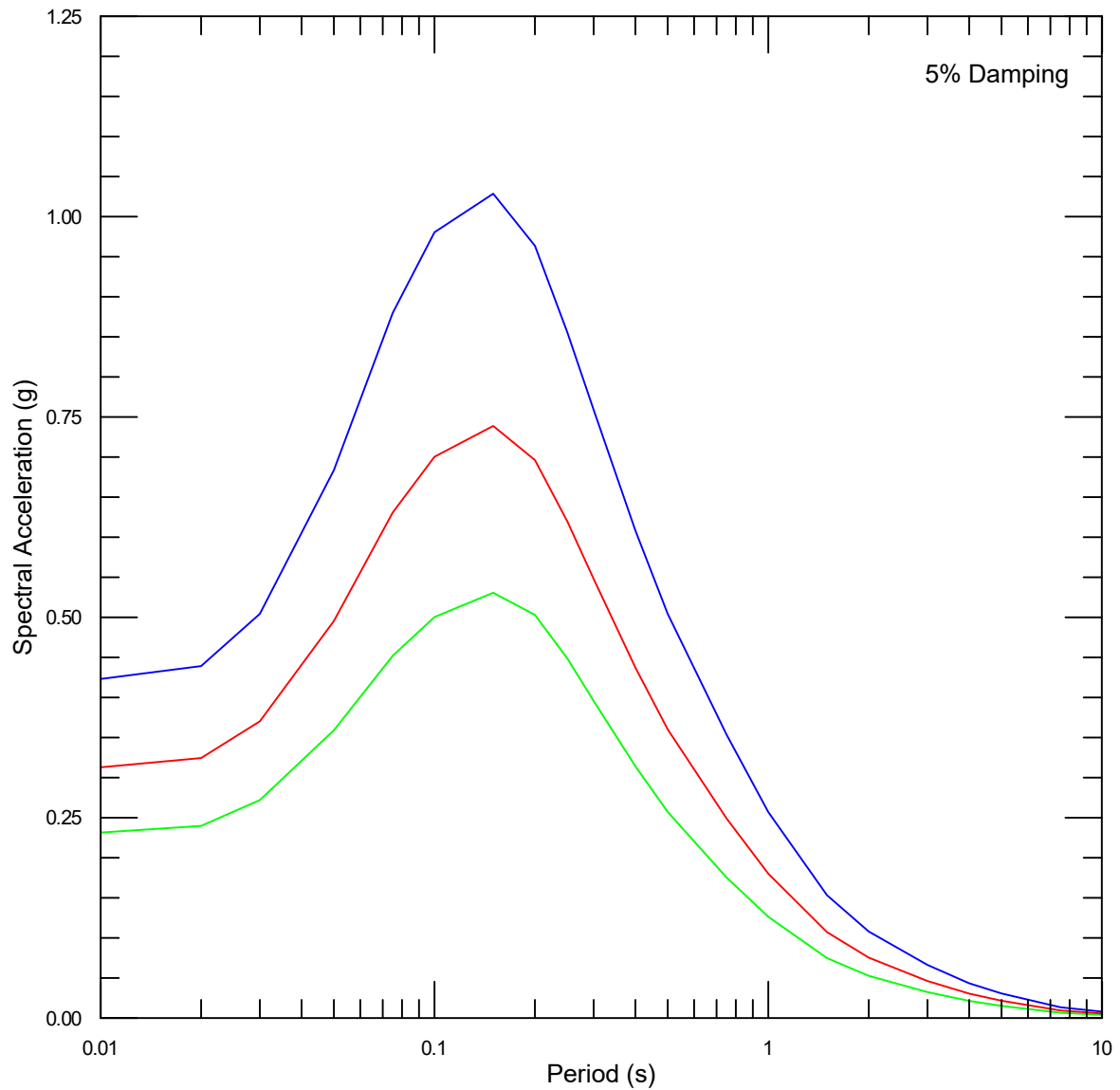


From Cramer et al. (1976)



Wolf Creek fault
M 6.5
 $R_{RUP} = 5.9$ km
 $R_{JB} = 5.9$ km
 Normal Fault
 Dip 80° west
 $V_{S30} = 1000$ m/s

--- Abrahamson *et al.* (2014)
 --- Boore *et al.* (2014)
 --- Campbell and Bozorgnia (2014)
 --- Chiou and Youngs (2014)
 — Average



Wolf Creek fault
M 6.5
 $R_{RUP} = 5.9$ km
 $R_{JB} = 5.9$ km
 Normal Fault
 Dip 80° west
 $V_{S30} = 1000$ m/s

— Median
 — 69th-Percentile
 — 84th-Percentile

Appendix A-2 Independent Evaluation of the Potential for Active Faulting at the Proposed Centennial Dam Site

Appendix A-2

Independent Evaluation of the Potential for Active Faulting at the Proposed Centennial Dam Site



Lettis Consultants International, Inc.
1981 N. Broadway, Suite 330
Walnut Creek, CA 94596
(925) 482-0360; fax (925) 482-0363

January 26, 2017

To: Mr. Michael Forrest
AECOM
300 Lakeside Drive, Suite 400
Oakland, CA 94612

Cc: Mr. David Simpson
Mr. Benjamin Kozlowicz

RE: Memorandum, Independent Evaluation of the Potential for Active Faulting at the Proposed Centennial Dam Site, Nevada and Placer Counties, California

Dear Mr. Forrest,

This memorandum was prepared by Lettis Consultants International, Inc. (LCI) to assist AECOM with the ongoing Geotechnical Investigation for the Centennial Reservoir Project. This memorandum describes our independent evaluation of the potential for active faulting in the vicinity of the proposed reservoir. LCI was directed to focus its investigation near proposed Axis 2 and former Axis 6, with an emphasis on Axis 2, the preferred proposed dam location. The preliminary findings indicate that there is a low hazard associated with active faulting (e.g., activity in the last 35 ka based on Division of Safety of Dams [DSOD] fault criteria), and that a shear zone identified in a nearby quarry, that may underlie proposed dam Axis 2, does not appear to be active. However, this study is limited in scope and is not considered an exhaustive surface-fault rupture evaluation for the proposed reservoir.

1.0 Background and Purpose

The proposed Centennial Reservoir is located on the Bear River in Nevada and Placer Counties, California on the western flank of the Sierra Nevada, approximately 15 km north-northeast of Auburn, California (Figure 1). The proposed dam site lies close to and within the active to potentially active Foothills fault system (FFS), a suite of steeply dipping, north- to northwest-trending faults that bound the western flank of the Sierra Nevada. The FFS is the source of the 1975 Oroville earthquake that ruptured the Cleveland Hill fault as a M5.7 earthquake. The FFS consists of numerous fault strands that comprise a several km-wide zone, and includes the Spenceville, Wolf Creek, Weimar and Gillis Hill faults near the proposed Centennial Dam site. Specifically, the proposed reservoir is located between the Wolf Creek fault to the west and Weimar fault to the east.

AECOM previously assessed the presence or absence of active faulting at the proposed Centennial Dam site in their Phase I Geotechnical Investigation Report (see Appendix A, AECOM, 2016). AECOM (2016) concluded that there were no faults considered to be active by the U.S. Geological Survey (USGS) or California Geological Survey (CGS) in the vicinity of the proposed dam site. Additionally, AECOM (2016) concluded that several faults that occur within

the nearby Teichert Quarry (~0.5-mi south of Axis 2) are minor, inactive faults that appear to be subparallel with observed geomorphic lineaments. An analysis developed by DSOD, documented in an informal presentation (Ellis, July 12, 2016), suggested that bedrock faults and features (anomalous abrupt bends in Bear Creek) previously identified in AECOM (2016), combined with geomorphic lineaments and structures interpreted from geophysical data by Ellis (2016), indicate potentially active faults may be intersecting the proposed dam axes. LCI was retained by AECOM to provide an independent analysis of the faulting at the proposed dam site in support of the geotechnical investigation.

This study does not evaluate possible reactivation of older bedrock structures due to reservoir-triggered seismicity.

Mr. John Baldwin (CEG) and Dr. Matthew Huebner of LCI performed the independent review and prepared this technical memorandum. Dr. William Lettis (LCI) provided technical peer review of the memorandum. Mr. David Simpson (CEG) and Benjamin Kozlowicz (PG) of AECOM provided technical support during the field reconnaissance.

2.0 Scope of Work

The scope of work for the independent geologic evaluation at the proposed Centennial Dam site included the following activities:

2.1. Office-based Analysis of Existing Data

LCI reviewed local and regional published and unpublished geological, geotechnical, geophysical, and seismological data recently compiled and interpreted by AECOM in a Phase 2 Preliminary Geotechnical Report, dated February 9, 2016 (AECOM, 2016). LCI also compiled and reviewed readily available peer-reviewed journal articles, theses and/or dissertations, geologic information from the U.S. Geological Survey (USGS), California Geological Survey (CGS), as well as unpublished information from Pacific Gas & Electric (PG&E).

2.2. Review and Analysis of LiDAR Imagery and Digital Elevation Model (DEM) Data

LCI reviewed and analyzed existing project LiDAR (~1 ft resolution) and National Elevation Dataset (NED) 10 m DEM (USGS, 2016a) to assess the presence or absence of prominent geomorphic lineaments coincident with previously mapped potentially active faults of the FFS, as well as potentially unrecognized lineaments that lie near the proposed footprint(s) of the Centennial Dam.

2.3. Field Reconnaissance

Following the completion of the office-based review of geologic and geotechnical data and geomorphic analysis, LCI performed a two-day field reconnaissance of the site. The purpose of the reconnaissance was to: (1) develop an initial geologic model of the site; (2) obtain a general understanding of the bedrock and Quaternary geology; (3) review key exposures of bedrock faulting at the nearby Teichert Quarry (~0.5-mi south of proposed Axis 2), and (4) evaluate linear geomorphic anomalies identified during the office-based review.

2.4. Technical Memorandum

Based on the results of the office-based evaluation and site reconnaissance, LCI prepared this review letter to summarize the work performed and key conclusions developed from the independent evaluation of the coseismic rupture hazard at the proposed dam.

3.0 Findings

The findings presented below are the result of our office-based review of existing data (which included a literature review, geomorphic evaluation of project LiDAR and publically available 10 m DEM topographic data, and review of borehole logs and photographs of rock core) and a two-day field reconnaissance at the proposed dam site.

3.1. Office-Based Analysis of Existing Data

LCI reviewed Woodward-Clyde Consultants comprehensive evaluation of the FFS (WCC, 1978), the USGS Quaternary fault and fold database (USGS, 2016b) and the CGS Digital Database of Quaternary and Younger Faults (Jennings and Bryant, 2010) for previously mapped potentially active faults in the vicinity of the subject site. Additional compilations of geologically recent faulting in the FFS reviewed for this study include Page and Sawyer (2001, 2007). The proposed dam site lies within the FFS (Clark, 1960), which consists of a zone of steeply dipping north- to northwest-trending faults that bound the western flank of the Sierra Nevada (Figure 1). The FFS initially developed as a series of east-dipping, west-vergent thrust faults that juxtaposed several island-arc terranes as they were accreted to the continental margin during Jurassic time (e.g., Edelman et al., 1989). Based on historical seismicity and offset Tertiary-Quaternary strain markers along the ~350-km length of the FFS, several segments of this fault system were reactivated during the Cenozoic, with localized areas of late Quaternary activity. The FFS is the source of the 1975 Oroville earthquake that ruptured the Cleveland Hill fault as a M5.7 earthquake.

Near the proposed Centennial Reservoir, potentially active segments of the FFS consist of several northwest-trending faults across a several km-wide belt that includes the Spenceville, Dewitt, and Wolf Creek faults; these exhibit predominantly normal-sense dip-slip and normal right-lateral oblique displacement during the Late Quaternary (Jennings and Bryant, 2010; Page and Sawyer, 2007; USGS, 2016b) (Figure 1). These faults do not intersect dam Axes 2 or 6 considered during our analysis. Additionally, the nearby Weimar fault (~6 km east of Axis 2) is not considered to be active by either the USGS or CGS (USGS, 2016b, Jennings and Bryant, 2010).

The geology in the vicinity of the proposed Centennial Dam is complex and consists of several fault-bounded ophiolitic (ancient ocean seafloor) sequences that were subjected to various degrees of deformation and metamorphism during Jurassic time (e.g., Clark, 1960; Menzies et al., 1980; Day et al., 1985; Edelman et al., 1989; Lloyd, 1995). On the basis of geologic mapping and analysis, Day et al. (1985) designate this portion of the Bear River geology as lying within a major Sierra Nevada tectonic belt ("Central belt"), which consists of penetratively deformed, low- to medium-grade metasedimentary, ultramafic, and mafic igneous rocks that are intruded by Late Jurassic to Early Cretaceous granitic plutons. These rocks are included in the Slate Creek terrane of Edelman and Sharp (1989). Geologic mapping by Tuminas (1983), Saucedo and Wagner (1992), and Lloyd (1995) indicates the geology at the proposed dam site

consists of moderately to shallow dipping, undifferentiated mafic to intermediate metavolcanic flows, flow-breccias, and volcanoclastic metasedimentary rocks (Figure 2). These rocks are part of the Lake Combie complex, a fault-bounded, pseudostratigraphic sequence representing a pre-Late Jurassic island arc assemblage (Day et al., 1985).

In the vicinity of the proposed dam, the Lake Combie complex is bound to the west by the Wolf Creek fault, which juxtaposes it against ophiolitic Smartville complex rocks on the east (Day et al., 1985; Saucedo and Wagner, 1992). The eastern boundary of the Lake Combie complex is the Weimar fault, with Colfax sequence deep-sea fan-channel deposits to the east (Day et al., 1985). Geologic mapping by Tuminas (1983) shows dam Axes 2 and 6 lie along the eastern flank of a broad synclinorium, with foliation near the site striking approximately north-south with steep (~80°) east and west dips (Figure 2). The northeast-trending synclinorium appears to be confined to the Lake Combie complex (see Figure 2), which suggests folding is pre- to syn-deformational in terms of slip along the bounding Wolf Creek and Weimar fault zones.

A review of geologic mapping by Tuminas (1983) and Saucedo and Wagner (1992) indicates that the Weimar fault lies approximately 3-5 km east of the proposed Centennial Dam (~ 5 km east of Axis 2) and does not offset Tertiary volcanic rocks directly east of the proposed dam. Furthermore, Tuminas (1983) mapped several short (~3.5 km), northeast-southwest-striking faults that offset the Weimar fault, which also do not offset Tertiary volcanic rocks (Figure 2). The USGS (2016b) and CGS (Jennings and Bryant, 2010) do not consider the Weimar fault as late Quaternary active. The Wolf Creek fault is approximately 6 km west of the proposed dam. Trenching along its trace by Woodward-Clyde Consultants (1978; referenced in Bryant, 1983) indicates the fault deforms the "Paleo-B" horizon, a proposed 130,000-10,000 year-old paleosol, and thus is considered active based on DSOD criteria (e.g., active within the last 35 ka). Based on their distance from the site, neither the Wolf Creek nor Weimar faults appear to pose a surface-fault rupture hazard to the proposed dam.

AECOM's report to the Nevada Irrigation District, dated February 9, 2016, describes the results of their Phase II geotechnical investigations and their assessment of site conditions for the proposed Centennial Dam. This report summarizes the location of previously mapped and potentially active faults in the region, includes a preliminary analysis of LiDAR and regional DEM data, and summarizes results of geologic mapping. AECOM (2016) concluded that previously identified faults coincided with prominent northwest-trending geomorphic lineaments (e.g., the Wolf Creek fault), and that shorter, east-west and north-south trending lineaments were likely associated with a well-developed joint pattern in the Lake Combie complex rock exposed in the Bear River drainage. Two northwest- to northeast-striking faults were identified in the nearby Teichert Quarry, south of the proposed dam sites, and were considered to be inactive. AECOM (2016) concluded that the initial analysis of existing geologic and geotechnical data supported the absence of active faults through dam Axes 2 and 6.

3.2. Review and Analysis of LiDAR Imagery and Digital Elevation Model (DEM) Data

As part of this independent investigation, LCI reviewed project LiDAR data in the direct vicinity of the dam sites, and supplemented the review with more regional-scale 10 m DEM data north and south of the LiDAR extent (Figure 3). LCI developed an initial topographic lineament map at both regional and local scales to support the geomorphic evaluation of the proposed reservoir and vicinity. Additionally, LCI interpreted DEM data along the Bear River to identify any possible fluvial terraces, which can be useful strain gauges to document the presence or absence of recent faulting.

3.2.1. *Lineament Mapping*

AECOM's (2016) scope of work included the development of a seismic source characterization model (see their Appendix A). To support the seismic source characterization, AECOM (2016) identified topographic and tonal lineaments using 1:80,000-scale, black-and-white aerial photographs of the region surrounding the dam site, and project LiDAR data from the direct vicinity of the proposed reservoir. The results of AECOM's (2016) lineament analysis are provided in their Subsection 3.1.2 and Appendix A.2.1. As shown in AECOM's (2016) Figure A-3, lineaments range from approximately 1 to 30 km in length, and the majority trend northwest to north-northwest. In the direct vicinity of the dam site, AECOM (2016) identified a few short (~8 km) lineaments that trend north-northeast; however these lineaments do not intersect dam Axes 2 or 6.

As part of LCI's evaluation of potential active faulting near the proposed reservoir, LCI developed a lineament map independently of AECOM (2016) that spans the surrounding dam site region (Figure 3). LCI supplemented the LiDAR analysis with color satellite imagery from Google Earth (imagery dates from 2015 to 2016) and a grayscale, hillshaded DEM image developed from USGS NED 10 m resolution data (USGS, 2016a). These data were viewed at approximately 1:50,000 scale or less to identify regional-scale lineaments. LiDAR data were used to identify lineaments in the direct vicinity of the dam sites. For identifying these local lineaments, viewing was restricted to a scale of approximately 1:20,000 or less.

In general, our lineament map shown in Figure 3 is similar to AECOM's (2016) Figure A-3. For example, the preponderance of the lineaments trend north-northwest, with the longest and most prominent being located west and northwest of the dam site and spatially associated with the Spenceville fault, Wolf Creek fault, and other elements of the Foothill fault system. These lineaments typically range in length from approximately 1 to 30 km, similar to the findings of AECOM (2016). One key difference between the two analyses is that LCI identifies a series of relatively short, and closely-spaced, roughly east-west-trending and northwest-southeast-trending lineaments located orthogonal to each other and at a high angle to the overall regional tectonic grain (see Figure 3). This pattern is readily recognizable in the multiple abrupt bends in the Bear River that appear to control, at least in part, the location of the drainage. We interpret this pattern as reflective of the dominant local and regional jointing as observed in Tiechert Quarry and noted in the stereonet developed by AECOM (2016; see their Figure 4-2), as opposed to active faulting. Additionally, there does not appear to be any convincing geomorphic expression of the proposed linear geologic structures interpreted from project seismic refraction data by Ellis (2016), or for the proposed northwest extension of the "Quarry fault" identified in AECOM (2016). Alternatively, several of these features appear to be correlative with geologic contacts or mapped slope failures (see Figure 4). Further assessment of the roughly east-west and north-south trending lineaments can be addressed further through the interpretation of existing borehole data (see section below).

3.2.2. *Terrace Mapping*

Flights of fluvial terraces often can be used as geomorphic datum for identifying and characterizing tectonic deformation that underlie or offset the terrace deposits. Specifically, terrace surfaces (or "treads") are generally planar, low-gradient features that can be evaluated for evidence for and against a vertical component of deformation, and the back edges (or "risers") separating terrace surfaces can be evaluated for evidence for and against a lateral component of deformation. We examined a grayscale hillshaded DEM image produced from

project LiDAR data, in combination with color satellite imagery from Google Earth (imagery date 4/15/2015) to look for evidence of longitudinally continuous terrace surfaces along the Bear River in the immediate vicinity of the Centennial Dam site.

Our terrace investigation was performed as a desktop exercise with limited field confirmation, and the area of investigation was limited to the extent of project LiDAR coverage in the direct vicinity of Axis 2. Our main observations include the following:

- Fluvial terraces are not continuous along the stretch of river examined and do not appear to be paired across the river. Instead, the terraces appear limited to point bar deposits.
- It is difficult to distinguish possible fluvial terrace deposits from possible bedrock strath surfaces. Where present, the deposits appear to be quite thin, as bedrock commonly is exposed in the river bed and banks.
- Along the stretch of river investigated, the discontinuous terrace deposits generally lie approximately 5-10 ft above river level.
- The density of vegetation on terraces is light to moderate, suggesting that the surfaces are young.
- No obvious knickpoints or changes in river gradient are observed in the elevation data.
- Discrete high-angle bends in the river are consistent with preferential erosion along dominant conjugate joint sets observed in Teichert Quarry to the south, and inferred from the LiDAR mapping.

Based on these observations, we conclude that the terrace deposits along this stretch of the Bear River are discontinuous, thin, and likely quite young, possibly of historical age (e.g., post Gold Rush era). As such, the terrace deposits are not suitable for use in evaluating possible longer term tectonic deformation associated with previously unrecognized faults. We see no evidence for tectonic deformation along this stretch of Bear Creek, but cannot preclude the possibility of faulting based on the terraces alone.

3.3. Field Reconnaissance

Following completion of the initial compilation and analysis of available geological, geotechnical, and geophysical data relevant to the identification of potentially active fault traces, LCI performed field reconnaissance to document the geologic setting at the proposed dam sites, with a particular focus on documenting the locations of features potentially related to active faulting (e.g., shear zones in the Teichert Quarry, LiDAR lineaments), and subdivide geologic units within the Lower Combie complex with the purpose of constructing a preliminary geologic model by which to assess faulting and lateral continuity of bedrock units. Site reconnaissance was performed on November 17-18, 2016. A preliminary geologic map of the site area is presented in Figure 4.

3.3.1. *Preliminary Geologic Model*

Field reconnaissance in the vicinity of the proposed dam revealed a sequence of approximately five lithologically discernable volcanic bedrock units. The orientation of planar fabric (likely bedding) at outcrop scale, in addition to map patterns, indicate these units strike roughly NW-SE and dip moderately to gently ($\sim 30^\circ$ to subhorizontal) to the southwest. A schematic stratigraphic

column of the Lake Combie complex (LCC) rocks within the direct vicinity of the site is presented in Figure 5. The identified units, from stratigraphically lowest to highest, are as follows:

- LCC-1: Medium- to fine-grained porphyritic olivine basalt; phenocrysts are generally <5 mm, consist of pyroxene, olivine, and plagioclase. This unit was identified along access road near boreholes CB-08 and CB-09, and along the Bear River ~900 ft upstream of proposed Axis 2.
- LCC-2: Well-bedded, coarse- to fine-grained volcanic sandstone (Figure 6A). Consists of cm-scale fining-upward sequences, base of coarse beds locally appears scoured.
- LCC-3: Variable unit that appears to contain at least two distinct lithologies (3a – amygdaloidal; 3b – basalt), interpreted to consist of several individual volcanic flows of similar composition basalt (possibly portions of two flows exposed in the site area). Internal contacts were not well delineated during field reconnaissance.
 - 3a Porphyritic, locally amygdaloidal basalt (Figure 6B). Highly variable unit, basaltic matrix ranges from fine- to coarse-grained; amygdaloidal texture conspicuous along exposures the Bear River south and southwest of borehole CB-16.
 - 3b Medium-grained porphyritic olivine basalt (Figure 6C); phenocrysts are generally <5 mm, consist of pyroxene, olivine, and plagioclase. This unit was identified along access road near borehole CB-11, and is exposed along the base of the northeastern wall of the Teichert Quarry. This unit is similar to Unit 1, although is generally coarser-grained and includes more porphyroclasts.
- LCC-4: Fine-grained basalt with sparse, 1-2 mm plagioclase and pyroxene porphyroclasts; unit does not appear to be laterally extensive based on reconnaissance mapping.
- LCC-5: Volcaniclastic breccia with large (up to 50 cm) angular, matrix supported boulders of varying lithology (Figure 6D); large clasts tend to be matrix supported, and consist of mafic and felsic volcanics, and locally red chert; matrix varies from very coarse to very fine-grained; amount of large clasts can be highly variable (Figure 6D).

This preliminary stratigraphic framework for the site was tested using existing borehole data collected from proposed dam Axis 2. Geologic cross section A-A' is oriented roughly north-south along dam Axis 2 (Figure 7). Using descriptions from borehole logs, coupled with core photographs and the initial geologic map developed for the project, it is apparent that distinct geologic units comprising the Lake Combie complex can be differentiated and projected down dip across Bear River. Cross-section A-A' depicts Lake Combie complex units distinguished during field reconnaissance as dipping moderately south. Based on photographs of rock core from boreholes CB-13 and CB-3, the lower contact between LCC-3a (amygdaloidal basalt) and underlying LCC-3b (basalt), identified along the south bank of the Bear River immediately across from borehole CB-16 (Figure 8), appears to project across the Bear River without any noticeable offset, which supports the absence of significant vertical separation along a hypothetical east-west trending structure (Figure 7).

Review of borehole core photographs indicates that this initial interpretation of stratigraphy is very simplistic, and that the volcanic stratigraphy in the area is more complex than depicted in Figure 5. Individual LCC units identified during field reconnaissance could likely be further subdivided based on the identification of flow bases and tops. LCI relied on the core photographs; we did not perform an inspection of core samples preserved for the project.

3.3.2. *Teichert Quarry Reconnaissance*

Exposures present in the nearby Teichert Quarry (~0.5-mi south of proposed Axis 2) were evaluated during field reconnaissance to: (1) investigate geologic structures (e.g., bedding, joints) of the Lake Combie complex, and (2) evaluate shear zones identified in the Phase II Geotechnical Investigation Report (AECOM, 2016) and referenced by Ellis (2016). Only the lowermost walls of the quarry were examined in detail, as there was no safe access to higher benches.

The most abundant lithologic unit exposed in the quarry is volcanoclastic breccia (LCC-5). This unit is generally massive, with beds of matrix-supported, angular boulders that appear to be at least several meters thick. Locally, beds occur that include few, if any, angular clasts, and thin coarse granular lenses suggestive of bedding (Figure 6D).

A small exposure of LCC-3b occurs in the far northeastern corner of the quarry (Figures 9 and 10), which is consistent with the northwest-southeast strike and southwest dip of the bedrock units in the area (Tuminas, 1983; Figures 4 and 7). The contact with the overlying volcanoclastic breccia (LCC-5) is undulatory, and is most obvious in the northeastern wall (Figure 10). The rock immediately above the contact is flaggy and fine-grained, and appears to grade upward into the more characteristic volcanoclastic breccia of LCC-5. The contact appears to dip gently to the southwest.

Several mafic dikes are also exposed in the quarry (Figures 11 and 12). Chill margins are well expressed at the dike boundaries, confirming they are late-stage intrusions (Figure 12). In the western wall of the quarry, a 0.5 to <5 m-thick dike dips moderately to the north (Figure 13). This dike does not appear to be continuous across the quarry. A separate large dike occurs on the north wall of the quarry, immediately east of the main shear zone described in AECOM (2016) (Figure 7). This dike appears to be continuous across the quarry, and may bifurcate between the north wall exposure and its exposure on the south wall. Alternatively, a second subparallel dike may occur in the south wall exposure, which does not continue to the north wall.

The “Quarry fault” of AECOM (2016) strikes N10-20°E, subparallel to the large dike exposed in the north wall, and juxtaposes volcanoclastic breccia of Unit LCC-5 on both sides of the shear zone. The dike margins are bounded by the shear zone, with the most prominent deformation expressed along the western margin of the dike. Deformation is characterized by a zone of anastomosing shear-fabric, grains size reduction of the volcanoclastic breccia matrix, calcite recrystallization and apparent hydrothermal alteration. Slickensided surfaces with deformed calcite mineralization were abundant in the quarry rubble in the vicinity of the shear zone, although no convincing linear features were observed on the fault plane itself. The shear zone appears to be continuous upsection in the quarry walls and across upper benches (Figure 9), although careful examination of the quarry walls along projection of the shear zone to the south and southwest revealed no evidence for the continuation of this fault. Additionally, the pair of mafic dikes on the south wall, located along projection of the northern dike, do not exhibit deformation along the dike margins similar to the northern dike at the “Quarry fault”. On the

basis of (1) the lack of lateral continuity of shearing across the quarry, (2) the spatial association of deformation with dike emplacement, and (3) the absence of any geomorphic expression of faulting to the northeast, we conclude there is a low likelihood that this shear zone represents an active surface-fault rupture hazard for the proposed Centennial Dam.

4.0 Conclusions

Based on LCI's review of existing data and two-day field reconnaissance, we conclude that:

- There is a lack of positive evidence to support active faulting at the proposed Centennial Dam site.
- The potential for active faulting at proposed dam Axis 2 and former Axis 6 is low, given the discontinuous nature of the "Quarry fault", association of the "Quarry fault" with late-stage mafic dike(s), and lack of associated geomorphic expression indicative of active faulting. Additionally, proposed linear structures identified in project seismic refraction data appear to correlate, in part, with lithologic contacts and mapped slope failures.
- The meandering expression of the Bear River along the proposed Centennial Reservoir corresponds to roughly north-south and east-west geomorphic lineaments, which appear to be related to the regional orthogonal joint pattern.
- The volcanic stratigraphy near proposed dam Axis 2 and former Axis 6 appears to be relatively consistent through the area, with a moderate to gentle southwest dip. The absence of vertical separation of lithologic contacts documents the absence of faulting through proposed dam Axis 2 (Figures 4 and 7).

5.0 Limitations

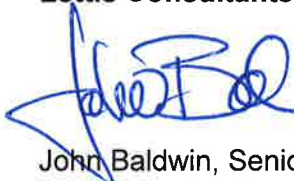
The conclusions presented above are based on an office-based review of existing data, which included a literature review and geomorphic evaluation of LiDAR and 10 m DEM topographic data, and review of borehole logs and photographs of rock core. In addition, a two-day field reconnaissance at the proposed dam site was performed to develop an initial geologic model and investigate possible faults identified in AECOM (2016) and linear features proposed by Ellis (2016). The geologic model and associated stratigraphic column presented within this memorandum should be considered simplistic and preliminary. While our findings indicate no positive evidence for potential active faulting at the proposed dam site, it cannot be precluded by our findings alone.

6.0 Closure

We appreciate the opportunity to support AECOM's Geotechnical Investigation for the Centennial Reservoir Project. Please do not hesitate to contact us if there are any questions or comments regarding the material presented in this memorandum.

Respectfully,

Lettis Consultants International, Inc.

A blue ink signature of John Baldwin, written in a cursive style.

John Baldwin, Senior Principal Geologist (G.E.G.)
baldwin@lettisci.com

A blue ink signature of Matthew T. Huebner, written in a cursive style.

Matthew T. Huebner, Senior Staff Geologist
huebner@lettisci.com

7.0 References Cited

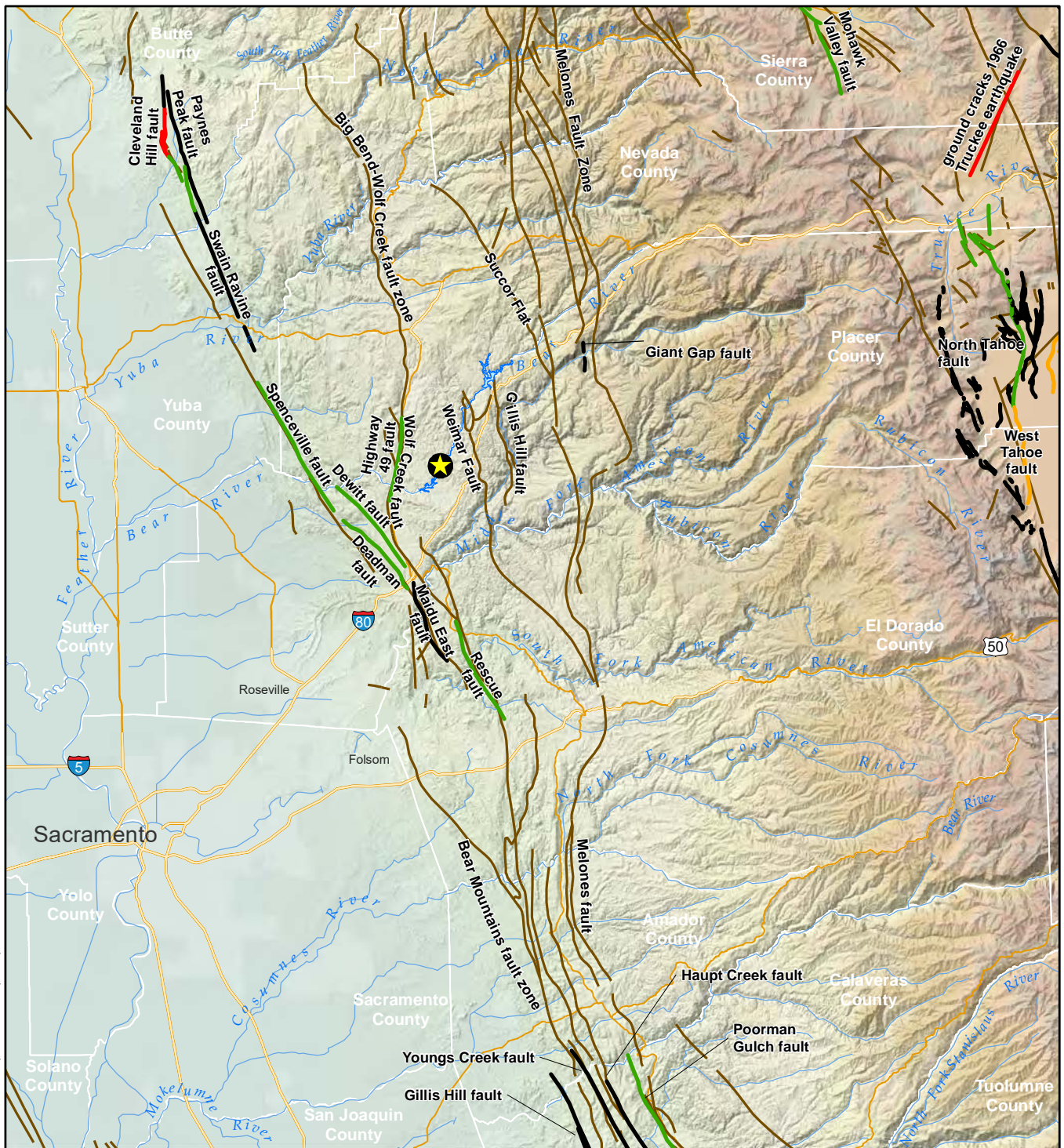
- AECOM, 2016, Centennial Reservoir Project Preliminary Geotechnical Investigation Phase II Report, 95 p. plus Appendices, dated February 9, 2016.
- Bryant, W.A., 1983, Bear Mountain Fault Zone, Auburn Area: California Division of Mines and Geology Fault Evaluation Report FER-147, 14 p. plus figures.
- Clark, L.D., 1960, Foothills fault system, western Sierra Nevada, California: Geological Society of America Bulletin, v. 71, p. 483-496.
- Day, H.W., Moores E., Tuminas A.V., 1985, Structure and Tectonics of the Northern Sierra Nevada, Geologic Society of America Bulletin, v. 96, p. 436-450.
- Edelman, S.H., and Sharp, W.D., 1989, Terranes, early faults, and pre-Late Jurassic amalgamation of the western Sierra Nevada metamorphic belt, California: Geological Society of America Bulletin, v. 101, p. 1420-1433.
- Edelman, S.H., Day, H.W., Moores, E.M., Zigan, S., Murphy, T.P., and Hacker, B.R., 1989, Structure across a Mesozoic ocean-continent suture zone in the northern Sierra Nevada, California: Geological Society of America Special Paper 224, 56 p.
- Ellis, 2016, Centennial Reservoir Proposed Dam Site: Review of Phase II Investigation, Review of Proposed Phase II Exploration: unpublished DSOD presentation, dated July 12, 2016.
- Jennings, C.W., and Bryant, W.A., 2010, Fault activity map of California: California Geological Survey Geologic Data Map No. 6, map scale 1:750,000.
- Lloyd, R., 1995, Mineral land classification of Placer County, California: California Department of Conservation, Division of Mines and Geology Open-File Report 95-10, 66 p. plus plates and appendices.
- Menzies, M., Blanchard, D., & Xenophontos, C., 1980, Genesis of the Smartville arc-ophiolite, Sierra Nevada foothills, California: American Journal of Science, v. 280-A, p. 329-344.
- Page, W.D. and Sawyer, T.L., 2001, Use of geomorphic profiling to identify Quaternary faults within the northern and central Sierra Nevada, California: Association of Engineering Geologists Special Volume, "Engineering Geology Practice in Northern California", eds. Ferriz, H. and Anderson, R., pg. 275-293.
- Page, W.D., and Sawyer, T.L., 2007, Overview of late Cenozoic faulting in the Sierra Nevada foothills (including a reassessment of faults near New Bullards Bar dam): unpublished report dated September 7, 2007, 85 p. plus figures.
- Saucedo, G.J., and Wagner, D.L., 1992, Geologic map of the Chico quadrangle, California: California Division of Mines and Geology, Sacramento, Regional Geologic Map Series, map no. 7, scale 1:250,000.
- Tuminas, A., 1983, Structural and Stratigraphic Relations in the Grass Valley – Colfax Area of the Northern Sierra Nevada Foothills, California [Ph.D. thesis]: Davis, University of California, Davis, 415 p.
- U.S. Geological Survey (USGS), 2016a, National Elevation Dataset Digital Elevation Model, 1/9 arc-second resolution, Page URL accessed on 11/21/2016:
<https://viewer.nationalmap.gov/basic/>

USGS, 2016b, Quaternary Fault and Fold Database of the United States, Page URL accessed 11/21/2016: <https://earthquake.usgs.gov/hazards/qfaults/>

Woodward-Clyde Consultants, 1978, Foothills fault system study: Appendix C4 of Vol. 6, Stanislaus Nuclear Project, Site Suitability – Site Safety Report, Unpublished consulting report to Pacific Gas and Electric Company, 166 p.

Figures

File path: S:\1209\Figures\Draft_01\Figure_01.mxd; Date: 12/12/2016; User: matt, LCI; Rev.1



EXPLANATION



Proposed Centennial Dam Site

Fault symbology



Historic



Holocene



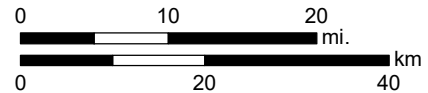
Late Quaternary



Quaternary



Pre-Quaternary



Map projection and scale: NAD 1983 UTM Zone 10N, 1:820,000

Regional Fault Map with CGS and USGS Faults

NEVADA IRRIGATION DISTRICT CENTENNIAL DAM

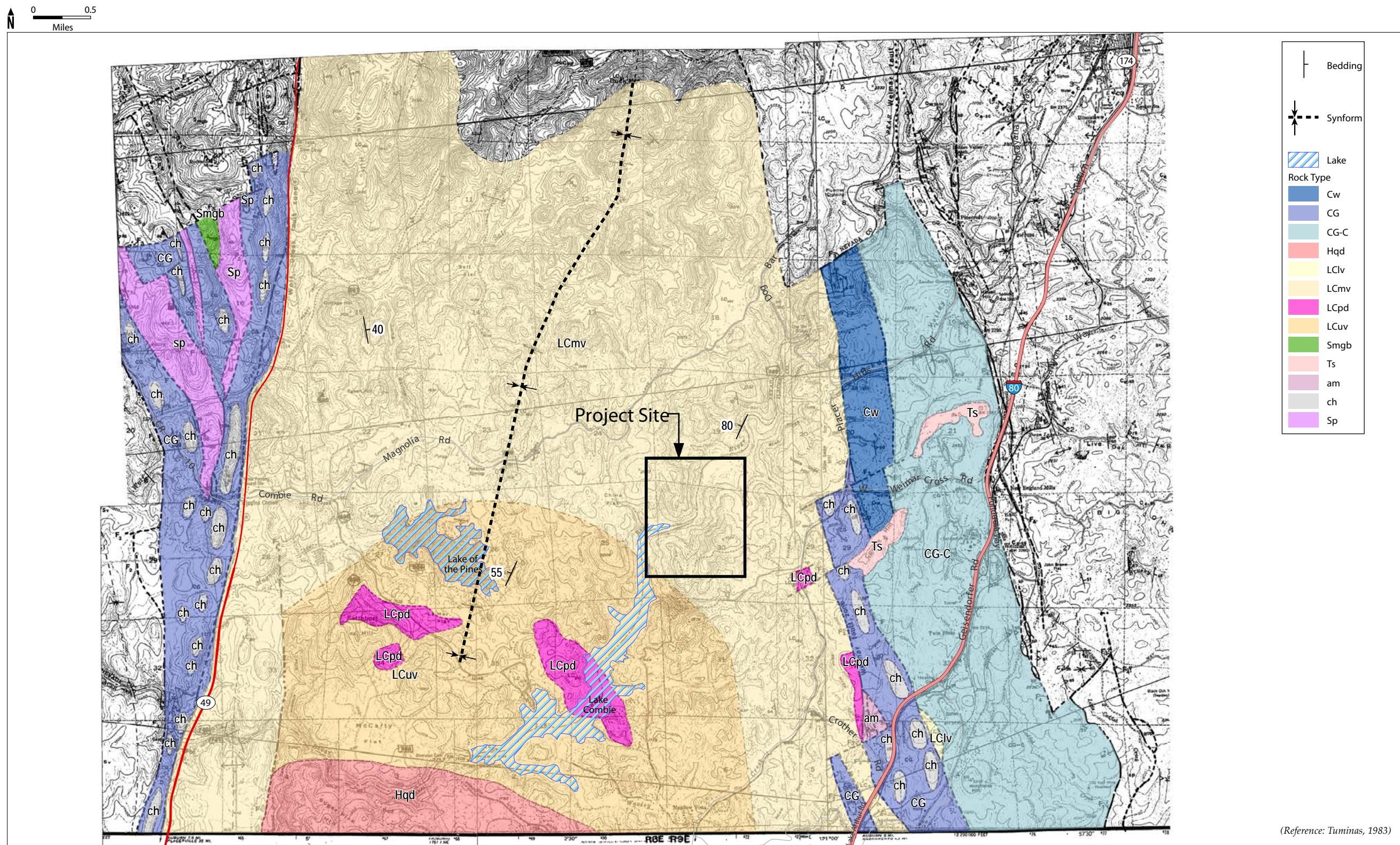


Lettis Consultants International, Inc.

Figure 1

Source: Faults from Bryant (2005) and CGS (2010).

File path: S:\1209\Figures\Draft_01\Figure_02a.ai; Date: 12/14/2016; User: Ase Mitchell, LCI; Rev: 1



Note:
– Figure from AECOM (2016).

Geologic Map of the Site Area

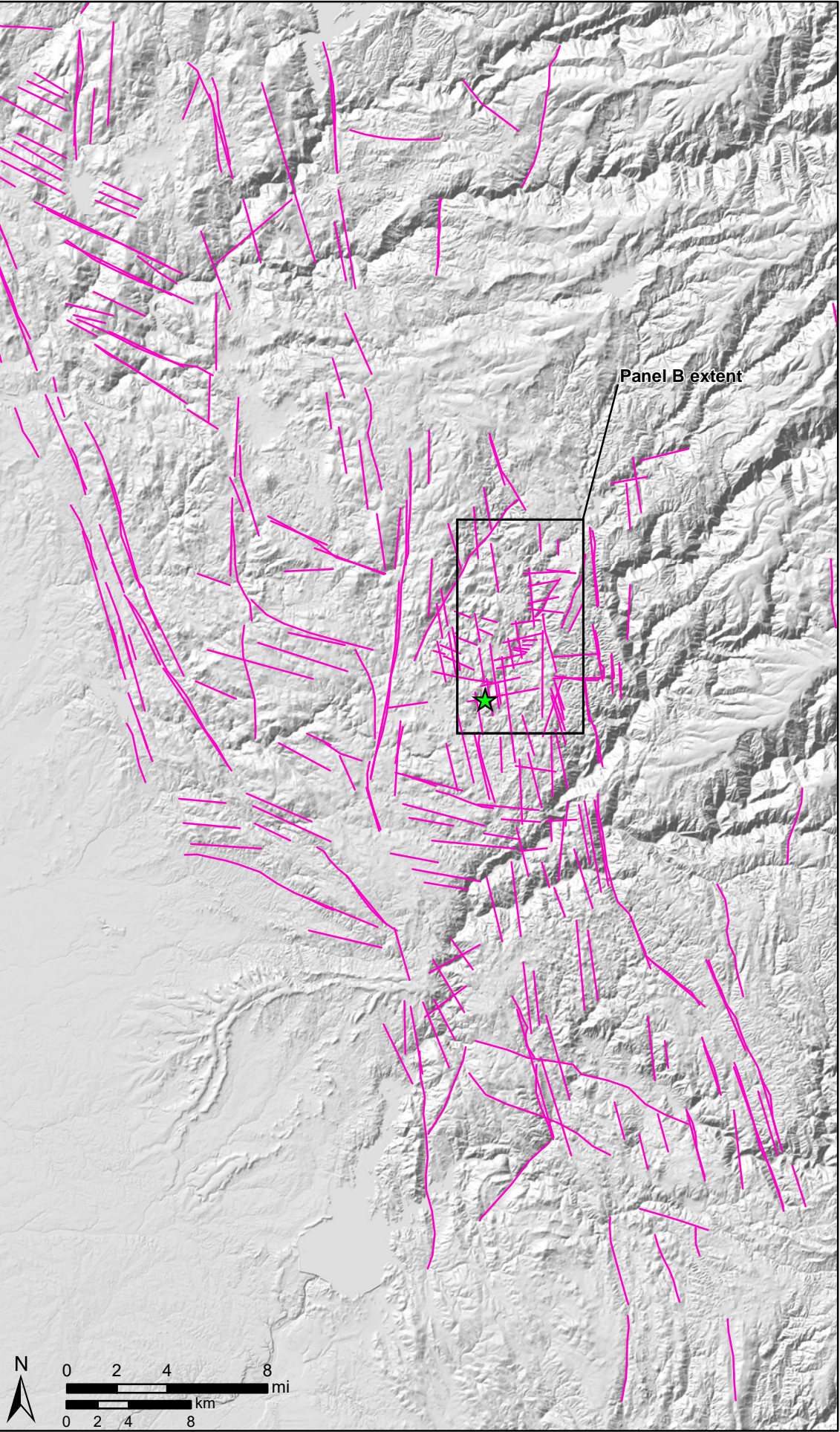
NEVADA IRRIGATION DISTRICT CENTENNIAL DAM

LCI Lettis Consultants International, Inc.

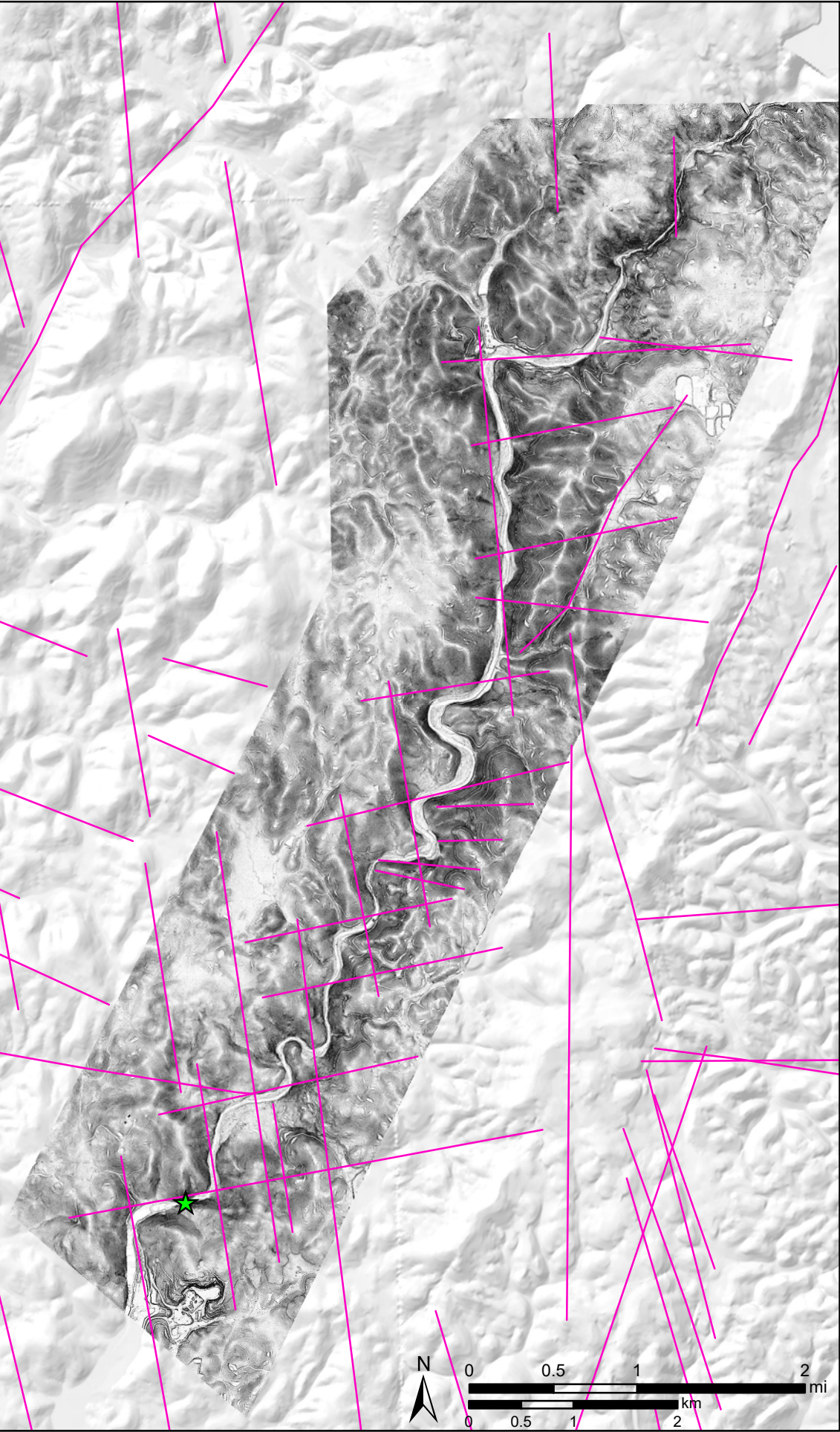
Figure 2a

Figure 2b

(A) Lineaments



(B) LiDAR



EXPLANATION

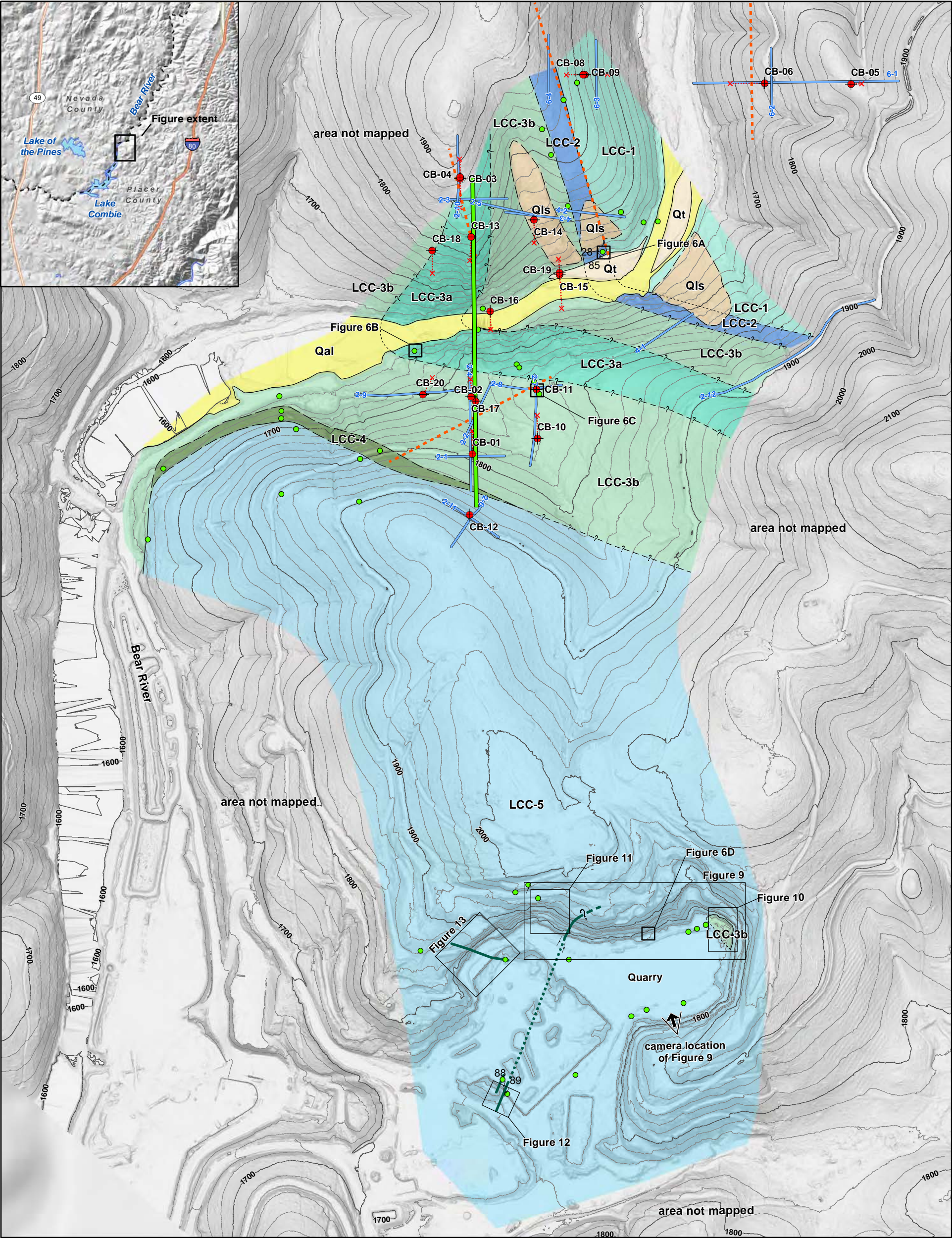
- ★ Centennial Dam
- Interpreted geomorphic lineament

Regional and Local Lineament Maps
Foothills Fault System and
Proposed Centennial Dam

NEVEADA IRRIGATION DISTRICT CENTENNIAL DAM

LCI Lettis Consultants International, Inc.

File path: S:\1209\Figures\Draft_01\Figure_04.mxd; Date: 12/12/2016; User: matt; LCI; Rev.1



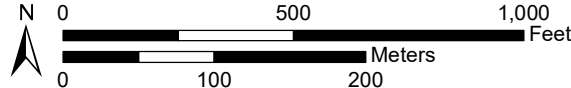
EXPLANATION

Geologic Units

- Qls
- Qal
- Qt
- LCC-5
- LCC-4
- LCC-3b
- LCC-3a
- LCC-2
- LCC-1

- Contacts: solid where certain, dashed where approximate, dotted where concealed, queried where inferred
- Mafic Dikes: solid where certain, dashed where approximate, dotted where concealed, queried where inferred
- Axis of Dam Site No. 2
- Geophysical profiles (AECOM, 2016)
- Ellis (2016) lineaments
- Top of Borehole (AECOM, 2016)
- Bottom of Borehole (AECOM, 2016)
- Field reconnaissance location
- Strike and dip location

Notes:
Contours in 20ft intervals,
See Figure 5 for description
of volcanic units.



Map projection and scale: NAD 1983 UTM Zone 10N, 1:5,000

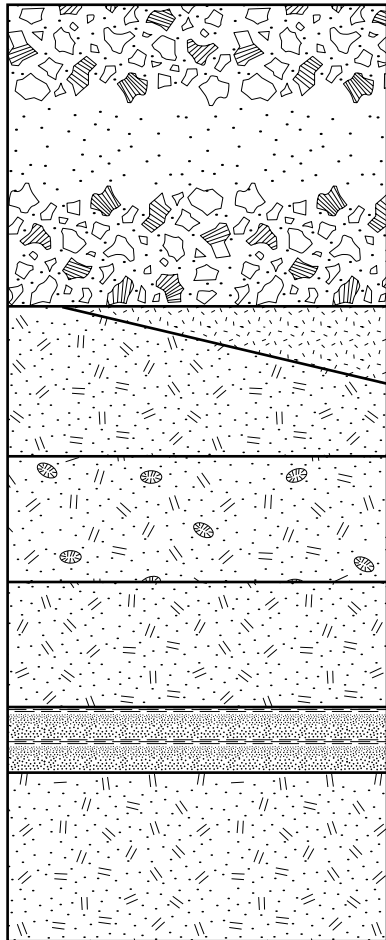
Preliminary Geologic Map
near Proposed Centennial Dam

NEVADA IRRIGATION DISTRICT CENTENNIAL DAM



Lettis Consultants International, Inc.

Figure 4



LCC 5 –

Volcaniclastic breccia with large (up to 50 cm) angular, matrix supported boulders of varying lithology; large clasts tend to be matrix supported, and consist of mafic and felsic volcanics, and locally red chert; matrix varies from very coarse to very fine-grained; amount of large clasts can be highly variable.

LCC 4 –

Fine-grained basalt with sparse, 1-2 mm plagioclase and pyroxene porphyroclasts; unit does not appear to be laterally continuous.

LCC 3b – upper flow of LCC 3 basalt

LCC 3a –

Porphyritic, locally amygdaloidal basalt; highly variable unit, basaltic matrix ranges from fine- to coarse-grained.

LCC 3b –

Medium-grained porphyritic olivine basalt; phenocrysts are generally <5 mm, consist of pyroxene, olivine, and plagioclase

LCC 2 –

Well-bedded, coarse- to fine-grained volcanic sandstone. Consists of cm-scale fining-upward sequences, base of coarse beds locally appears scoured.

LCC 1 –

Medium- to fine-grained porphyritic olivine basalt; phenocrysts are generally <5 mm, consist of pyroxene, olivine, and plagioclase.

**Schematic Stratigraphic Column
of Bedrock near Proposed
Centennial Dam**

NEVADA IRRIGATION DISTRICT CENTENNIAL DAM



Lettis Consultants International, Inc.

Figure **5**



A) Photography of gently to moderately southwest dipping, well-bedded, coarse to fine-grained volcanic sandstone of Unit LCC-2 exposed along north side of Bear River. Rock hammer for scale.



B) Close-up of porphyritic and locally amygdaloidal basalt of Unit LCC-3a exposed along the southwest side of Bear River within the axis of proposed dam location No. 2. Mechanical pencil for scale.



C) Rock sample from Unit LCC-3b of a fine-grained basalt with 1-2 mm long plagioclase and pyroxene phenocrysts. Rock hammer for scale.



D) Exposure of Unit LCC-5 within Teichert Quarry showing crude bedding in the volcaniclastic breccia (fining upwards with coarse-grained volcanic sandstone); geologist noting approximate bedding location.

Characteristic Lithologic Units from the Map Area

NEVADA IRRIGATION DISTRICT CENTENNIAL DAM

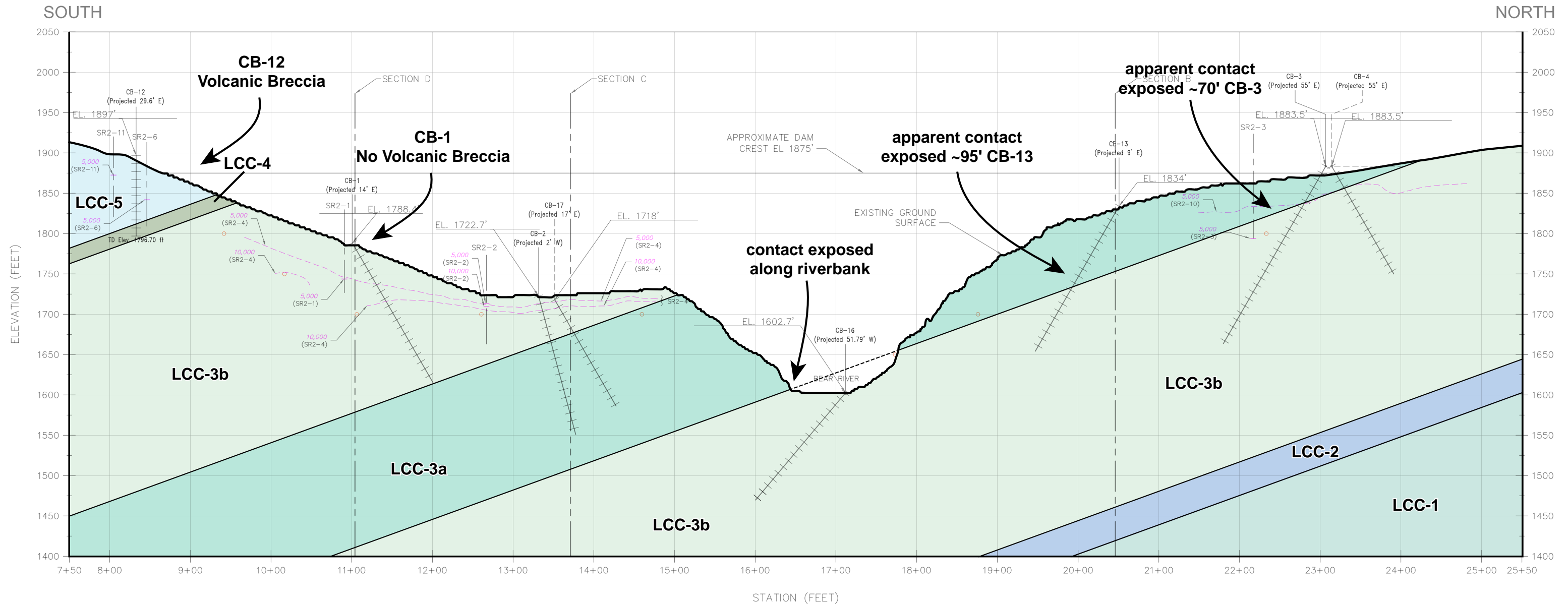


Lettis Consultants International, Inc.

Figure

6

File path: S:\1209\Figures\Figure_06.ai; Date: 12/07/2016; User: Serkan Bozkurt, LCI; Rev.1



LEGEND:

- WEATHERING PROFILE:
- COLLUVIUM
 - RESIDUAL SOIL
 - COMPLETELY WEATHERED
 - HIGHLY WEATHERED
 - MODERATELY WEATHERED
 - SLIGHTLY WEATHERED
 - FRESH
- GW
- GROUNDWATER LEVEL DURING DRILLING
(MAY NOT REFLECT NATURAL GROUNDWATER LEVEL)
- BH
- BOTTOM OF HOLE
- UCS/PLI*
- UNCONFINED COMPRESSIVE STRENGTH; * INDICATES RESULT FROM POINT LOAD TEST; SEE
APPENDICES H AND I FOR DETAILS
- 5,000
- P-WAVE VELOCITY (ft./sec.) FROM SEISMIC REFRACTION SURVEY; SEE APPENDIX C FOR DETAILS
- SR6-4
- SEISMIC REFRACTION LINE 6-4
- LOCATION OF SR LINE, AT CROSSING OF PROFILE

NOTES:

- ELEVATION DATUM IS NAVD (1988).
- WHERE SEISMIC REFRACTION PROFILE DATA ARE PROJECTED INTO ANALYSIS SECTIONS FROM SURVEYS ACQUIRED AT DIFFERENT SURFACE ELEVATIONS, THE DEPTH TO THE PROFILE DATA IS MAINTAINED.

Notes:
– Figure modified from AECOM, Phase III Draft Geotechnical Report

**Preliminary Geologic Cross Section
along Proposed Axis 2**

NEVADA IRRIGATION DISTRICT CENTENNIAL DAM

LCI Lettis Consultants International, Inc.

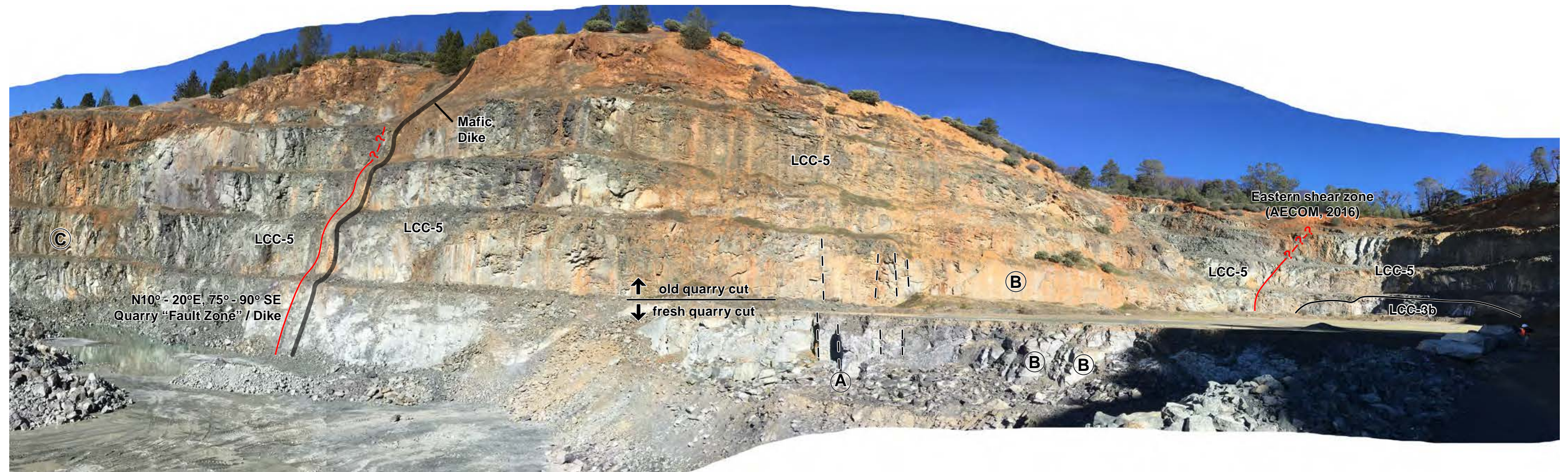
Figure

7



**Units LCC-3a and LCC-3b
Contact on Left Bank of Bear River
near Borehole CB-16**

NEVADA IRRIGATION DISTRICT CENTENNIAL DAM



Ⓐ Typical N-S trending vertical joints (approximate)



Ⓑ Typical E-W trending vertical joints (forms resistant vertical quarry faces)



Ⓒ Intersection of N-S and E-W trending joints (approximate)

Note: See figure 4 for photo location.

**Teichert Quarry Panorama
View to North - Northeast**

NEVADA IRRIGATION DISTRICT CENTENNIAL DAM



Lettis Consultants International, Inc.

Figure

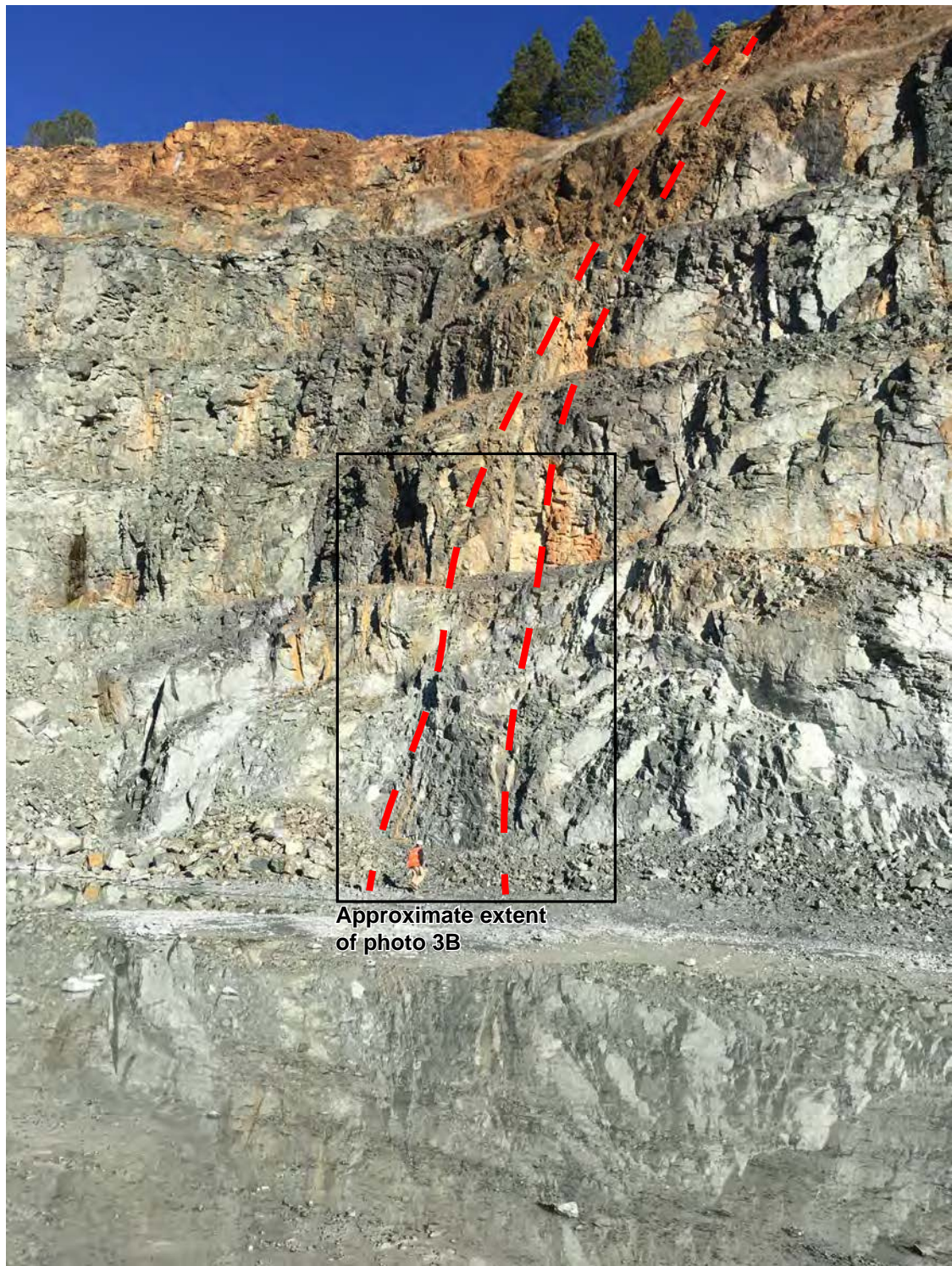
9



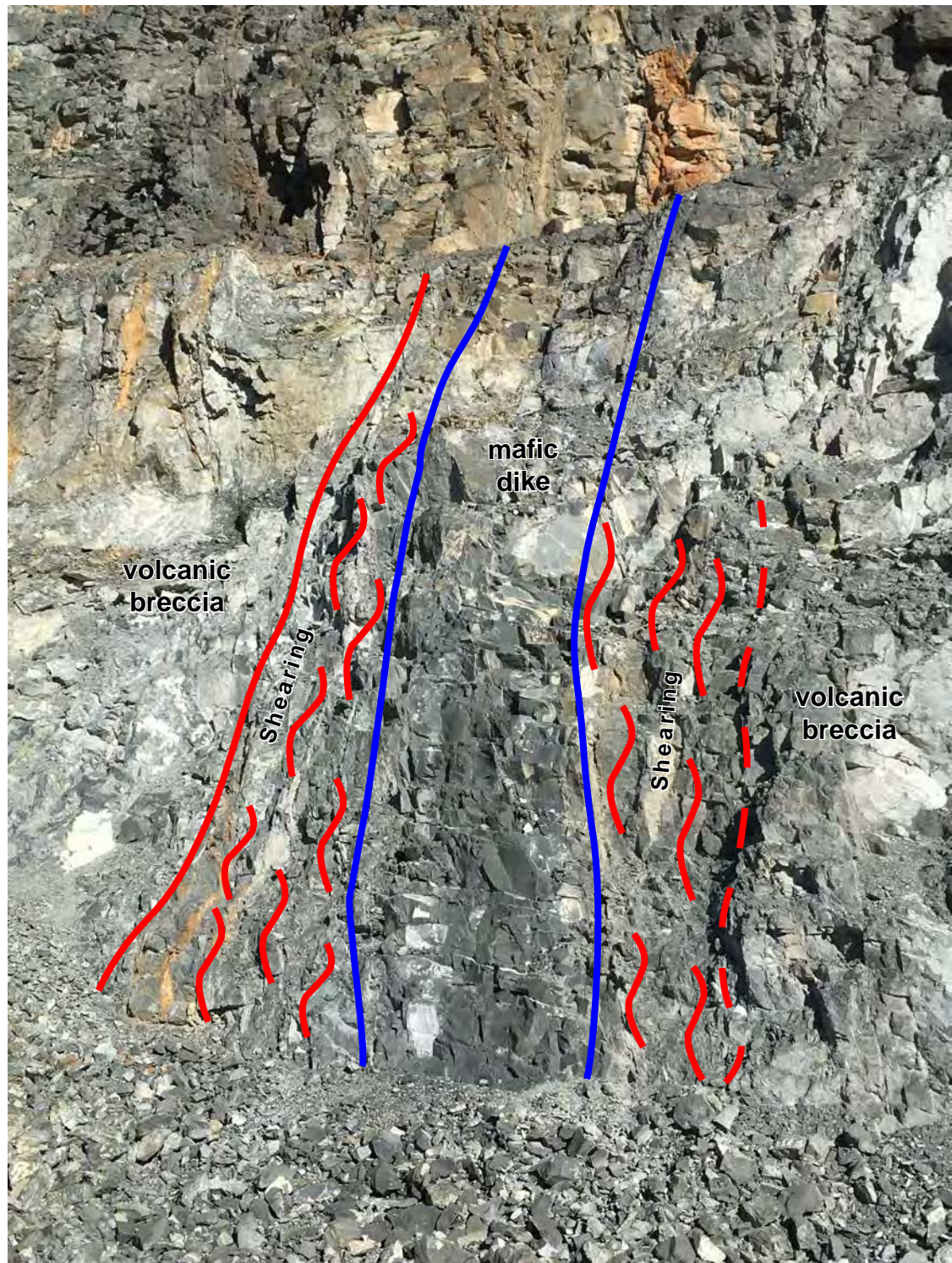
View to the east of the bedding contact between Units LCC-5 (top) and LLC-3b (base) dipping southerly within the eastern part of Teichert Quarry (see Figure 4 for location).

Contact LCC-5 and LCC-3b Teichert Quarry

NEVADA IRRIGATION DISTRICT CENTENNIAL DAM



A) View to the north-northeast showing Quarry “fault zone” of AECOM (2016). Dashed line represents the approximate margins of the “fault zone” upsection and across the quarry benches. Note the absence of weathering of the fresh exposure, whereas older benches show the zone as highly oxidized and weathered. The “fault zone” trends N10-20E and dips steeply 75-90SE. Note the geologist for scale.



B) Close-up of Quarry “fault zone” showing sheared volcanic breccia (LCC-5) along the eastern and western margins of an aphanitic mafic dike. The shear zone exhibits calcite recrystallization and hydrothermal alteration.

Mafic Dike and Shear Zone in Teichert Quarry

NEVADA IRRIGATION DISTRICT CENTENNIAL DAM



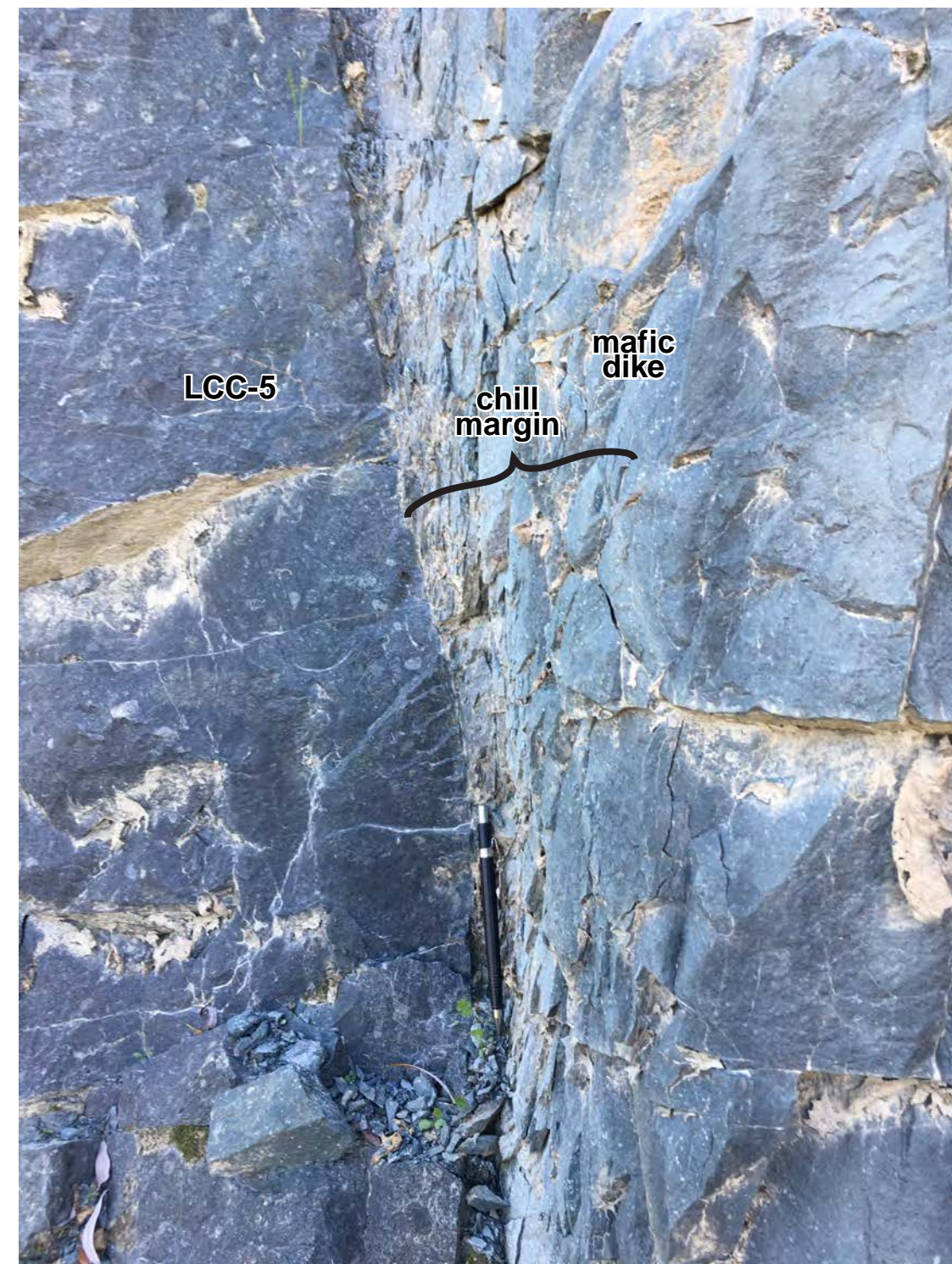
Lettis Consultants International, Inc.

Figure

11



A) Exposure of southern continuation of a mafic dike in the southwest corner of the quarry.



B) Photo of the eastern margin of the mafic dike in the southwest corner of the quarry. Note the absence of deformation and presence of the chill margin of the dike with volcanic breccia (LCC-5) on the left side of the photo.

Mafic Dike and Chill Margin in Teichert Quarry

NEVADA IRRIGATION DISTRICT CENTENNIAL DAM



Lettis Consultants International, Inc.

Figure

12



View to the northwest within Teichert Quarry showing the location of the western mafic dike, intersection of approximately north-south and east-west oriented joints, and large continuous rock faces along preferred jointing.

Western Dike of Teichert Quarry

NEVADA IRRIGATION DISTRICT CENTENNIAL DAM



Lettis Consultants International, Inc.

Figure 13

Appendix B. Surface Discontinuity Data

Appendix B. Surface Discontinuity Data

Appendix B.

Surface Discontinuity Data

Discontinuity data collected during the field mapping effort was compiled using the program DIPS (Rocscience, 2012). The purpose was to analyze the general distribution of rock mass discontinuities as visualized by their poles and establish major discontinuity trends and relationships throughout the project area. Equal area stereonet is used to visualize the distribution of poles and their orientations, to determine significant discontinuity sets as well as a general sense of the degree of fracturing throughout the rock mass. Wide spread discontinuities are indicative of highly fractured rock masses without a consistent fabric. Using a Fisher concentration plot, pole densities can be observed for different discontinuity types and major discontinuity sets determined. These discontinuity sets can then be visualized in an equal angle stereonet to determine any problematic kinematic relationships.

A total of 123 data points were collected during the preliminary and Phase 2 and 3 mapping efforts, representing discontinuity attitudes observed at the ground surface across the Axis 2, north and south borrow and quarry project areas. Of these data points, 4 represent regional shear surface, 23 represent rock mass bedding or bedding parallel joint attitudes and 96 represent rock mass joint attitudes. Figures 4-3a and 4-3b are equal angle stereonet of the bedding and joint data from left and right abutment slopes (respectively) with fisher concentrations to determine the major discontinuity sets. A total of 1 bedding and 2 joint sets were determined from this analysis (Table 4-1). The locations and orientations of bedding and bedding parallel discontinuity features are plotted on Figure 4-1. All of the surface bedding and discontinuity data from the Axis 2 area, borrow areas and Teichert quarry are presented in Table B-1 below. Shears were considered as individual and unique discontinuities due to insufficient data for determination of shear sets.

Table B-1: Surface Discontinuity Data

Number	Strike			Dip		Type	Latitude	Longitude	Location
1	S	10	W	51	W	Discontinuity	39.03952	-121.02501	Axis 2
2	S	20	W	85	W	Discontinuity	39.03931	-121.02497	Axis 2
3	N	60	W	85	N	Discontinuity	39.03931	-121.02497	Axis 2
4	N	81	W	78	N	Discontinuity	39.03948	-121.02445	Axis 2
5	N	10	E	84	E	Discontinuity	39.03948	-121.02444	Axis 2
16	N	18	W	65	SW	Discontinuity	39.04096	-121.02342	Axis 2
17	N	3	E	30	SE	Discontinuity	39.04095	-121.02342	Axis 2
18	N	70	W	85	S	Discontinuity	39.04064	-121.02327	Axis 2
19	N	75	W	12	S	Discontinuity	39.04058	-121.02328	Axis 2
20	N	75	E	20	S	Discontinuity	39.04012	-121.02309	Axis 2
21	N	27	E	84	SE	Discontinuity	39.03939	-121.02261	Axis 2
22	N	60	W	87	N	Discontinuity	39.03940	-121.02261	Axis 2
23	N	25	W	75	N	Discontinuity	39.03940	-121.02257	Axis 2
24	N	20	E	87	S	Discontinuity	39.03991	-121.02196	Axis 2
25	N	60	W	20	SW	Discontinuity	39.03991	-121.02194	Axis 2
26	N	10	E	60	S	Discontinuity	39.04001	-121.02215	Axis 2
27	N	85	E	75	S	Discontinuity	39.03998	-121.02218	Axis 2
48	N	30	E	77	E	Discontinuity	39.03890	-121.02247	Axis 2
49	N	55	W	65	W	Discontinuity	39.03892	-121.02243	Axis 2
50	N	0	E	8	E	Bedding	39.03891	-121.02243	Axis 2
51	N	90	E	8	S	Bedding	39.03892	-121.02244	Axis 2
52	N	90	E	20	S	Bedding	39.03894	-121.02248	Axis 2
53	N	70	E	90	S	Discontinuity	39.03898	-121.02216	Axis 2
54	N	30	E	70	E	Discontinuity	39.03898	-121.02216	Axis 2
55	N	50	W	18	S	Bedding	39.03898	-121.02216	Axis 2
56	N	90	E	77	S	Discontinuity	39.03900	-121.02198	Axis 2
57	N	28	E	68	E	Discontinuity	39.03900	-121.02198	Axis 2
58	N	50	W	11	S	Bedding	39.03900	-121.02198	Axis 2
59	S	40	E	68	S	Discontinuity	39.03897	-121.02182	Axis 2
60	N	85	E	57	N	Discontinuity	39.03897	-121.02182	Axis 2
61	N	80	E	80	S	Discontinuity	39.03888	-121.02155	Axis 2
65	N	37	E	90	S	Discontinuity	39.03837	-121.02193	Axis 2
66	N	45	W	75	N	Discontinuity	39.03849	-121.02187	Axis 2
67	N	30	E	83	S	Discontinuity	39.03848	-121.02188	Axis 2
68	N	60	W	10	S	Bedding	39.03851	-121.02185	Axis 2
69	N	5	E	78	W	Discontinuity	39.03856	-121.02193	Axis 2
70	N	78	E	68	N	Discontinuity	39.03855	-121.02193	Axis 2
71	N	2	E	75	E	Discontinuity	39.03816	-121.02253	Axis 2
72	N	90	W	86	N	Discontinuity	39.03817	-121.02254	Axis 2
73	N	72	E	90	S	Discontinuity	39.03817	-121.02281	Axis 2
74	N	26	E	9	S	Bedding	39.03817	-121.02281	Axis 2
75	N	6	W	60	W	Discontinuity	39.03817	-121.02281	Axis 2
76	N	20	W	70	E	Discontinuity	39.03839	-121.02288	Axis 2
77	N	20	E	80	E	Discontinuity	39.03840	-121.02288	Axis 2

Number	Strike			Dip		Type	Latitude	Longitude	Location
78	N	80	W	68	N	Discontinuity	39.03840	-121.02288	Axis 2
79	N	68	W	27	S	Bedding	39.03840	-121.02288	Axis 2
80	N	58	W	88	N	Discontinuity	39.03848	-121.02296	Axis 2
81	N	15	E	15	W	Bedding	39.03848	-121.02296	Axis 2
82	N	35	E	75	S	Discontinuity	39.03848	-121.02296	Axis 2
83	N	75	W	25	S	Bedding	39.03848	-121.02314	Axis 2
84	N	24	E	80	S	Discontinuity	39.03848	-121.02314	Axis 2
85	N	73	W	68	N	Discontinuity	39.03848	-121.02314	Axis 2
86	N	32	E	70	S	Discontinuity	39.03836	-121.02309	Axis 2
87	N	90	E	6	S	Bedding	39.03835	-121.02310	Axis 2
88	N	60	W	71	N	Discontinuity	39.03833	-121.02307	Axis 2
89	N	10	E	72	E	Discontinuity	39.03805	-121.02459	Axis 2
90	N	30	E	77	S	Discontinuity	39.03805	-121.02459	Axis 2
91	N	90	E	90	S	Discontinuity	39.03805	-121.02459	Axis 2
92	N	25	W	20	S	Bedding	39.03840	-121.02551	Axis 2
93	N	65	W	83	N	Discontinuity	39.03840	-121.02547	Axis 2
94	N	5	W	88	E	Discontinuity	39.03840	-121.02542	Axis 2
95	N	65	W	80	N	Discontinuity	39.03847	-121.02505	Axis 2
96	N	12	E	80	3	Discontinuity	39.03848	-121.02505	Axis 2
97	N	45	W	27	S	Bedding	39.03848	-121.02505	Axis 2
98	N	90	E	9	S	Bedding	39.03855	-121.02508	Axis 2
99	N	85	W	85	S	Discontinuity	39.03653	-121.02650	Axis 2
100	N	5	E	75	E	Discontinuity	39.03652	-121.02652	Axis 2
BR04	N	60	W	68	N	Discontinuity	39.03925	-121.02485	Axis 2
BR05	N	5	W	90	N	Discontinuity	39.03910	-121.02463	Axis 2
BR06	N	80	W	70	N	Discontinuity	39.03816	-121.02354	Axis 2
BR07	N	5	E	83	E	Discontinuity	39.03832	-121.02384	Axis 2
BR08	N	15	E	20	W	Discontinuity	39.03844	-121.02387	Axis 2
BR08	N	90	E	75	S	Discontinuity	39.03844	-121.02387	Axis 2
BR08	N	25	E	80	E	Discontinuity	39.03844	-121.02387	Axis 2
BR09	N	75	W	67	N	Discontinuity	39.03845	-121.02409	Axis 2
BR09	S	20	E	18	S	Discontinuity	39.03845	-121.02409	Axis 2
BR09	N	80	E	85	N	Discontinuity	39.03845	-121.02409	Axis 2
BR10	N	70	W	80	N	Discontinuity	39.03855	-121.02418	Axis 2
BR10	N	10	E	90	N	Discontinuity	39.03855	-121.02418	Axis 2
BR11	N	15	W	80	E	Discontinuity	39.03899	-121.02451	Axis 2
BR12	N	20	E	85	E	Discontinuity	39.03846	-121.02477	Axis 2
BR13	N	58	W	70	S	Discontinuity	39.03837	-121.02486	Axis 2
BR13	N	35	E	80	E	Discontinuity	39.03837	-121.02486	Axis 2
BR13	N	60	E	34	N	Discontinuity	39.03837	-121.02486	Axis 2
BR14	N	70	E	21	S	Discontinuity	39.03768	-121.02505	Axis 2
BR20	N	5	E	90	N	Discontinuity	39.03697	-121.02665	Axis 2
BR20	N	85	E	72	S	Discontinuity	39.03697	-121.02665	Axis 2
BR20	N	0	W	0	N	Bedding	39.03697	-121.02665	Axis 2
BR21	N	60	E	86	S	Discontinuity	39.03712	-121.02671	Axis 2

Number	Strike			Dip		Type	Latitude	Longitude	Location
BR21	N	65	E	90		Discontinuity	39.03712	-121.02671	Axis 2
BR21	N	15	E	72	E	Discontinuity	39.03712	-121.02671	Axis 2
BR21	N	20	E	72	E	Discontinuity	39.03712	-121.02671	Axis 2
BR21	S	72	E	7	S	Bedding	39.03865	-121.02442	Axis 2
BR22	N	63	E	83	S	Discontinuity	39.03864	-121.02467	Axis 2
BR22	S	0	E	30	W	Bedding	39.03864	-121.02467	Axis 2
BR22	N	70	W	85	S	Discontinuity	39.03864	-121.02467	Axis 2
BR22	N	60	W	87	N	Discontinuity	39.03864	-121.02467	Axis 2
BR23	S	0	E	15	W	Bedding	39.03865	-121.02419	Axis 2
BR23	N	27	E	69	E	Discontinuity	39.03865	-121.02371	Axis 2
BR23	N	25	E	80	E	Discontinuity	39.03865	-121.02323	Axis 2
BR23	N	65	E	30	N	Discontinuity	39.03866	-121.02275	Axis 2
BR24	S	10	E	12	W	Bedding	39.03914	-121.02441	Axis 2
BR25	S	42	E	28	W	Bedding	39.03915	-121.02436	Axis 2
BR26	N	90	E	6	S	Bedding	39.03948	-121.02444	Axis 2
BR27	N	90	E	4	N	Bedding	39.03949	-121.02445	Axis 2
BR28	N	83	W	20	S	Bedding	39.03940	-121.02260	Axis 2
BR01	N	62	W	30	S	Discontinuity	39.05581	-121.01295	North Borrow Area
BR02	N	87	E	77	N	Discontinuity	39.05429	-121.01217	North Borrow Area
BR03	N	77	W	82	S	Discontinuity	39.04989	-121.02135	South Borrow Area
6	N	75	E	85	SE	Discontinuity	39.03041	-121.02462	Teichert quarry
7	N	27	W	90	N	Discontinuity	39.03044	-121.02460	Teichert quarry
8	N	15	E	12	NW	Discontinuity	39.03074	-121.02467	Teichert quarry
9	N	60	W	85	NE	Discontinuity	39.03074	-121.02467	Teichert quarry
10	N	20	E	85	SE	Discontinuity	39.03075	-121.02467	Teichert quarry
11	N	80	E	50	SE	Discontinuity	39.03074	-121.02467	Teichert quarry
12	N	15	E	72	E	Discontinuity	39.03095	-121.02443	Teichert quarry
13	N	70	E	15	NW	Discontinuity	39.03103	-121.02434	Teichert quarry
14	N	20	W	60	SW	Discontinuity	39.03019	-121.02225	Teichert quarry
15	N	85	E	80	S	Discontinuity	39.03017	-121.02228	Teichert quarry
	N	12	W	85	NE	Fault	39.03107	-121.02345	Teichert quarry
	N	10	E	85	E	Fault	39.03129	-121.02336	Teichert quarry
	N	11	E	85	E	Fault	39.02910	-121.02373	Teichert quarry
	N	55	E	90	N	Fault	39.02969	-121.02440	Teichert quarry

Appendix C. Seismic Refraction Surveys

Appendix C. Seismic Refraction Survey Report

Appendix C-1 Seismic Refraction Survey Report – Phase II

Appendix C-1 Seismic Refraction Survey Report – Phase II



December 2, 2015

Mr. Michael Forrest
AECOM
1333 Broadway, Suite 800
Oakland, California 94612

Subject: Seismic Refraction Survey (Phase 2)
Nevada Irrigation District (NID) Water Storage Project, Bear River, Nevada
County, CA
NORCAL Job Number 15-533.74

Dear Mr. Forrest:

This letter is an addendum to our report dated September 23, 2015. Based on the results of that survey, it was determined by AECOM that additional seismic refraction information was needed on the north side of Bear River in Nevada County, California. As a result, a Phase 2 survey was performed on November 4, 2015 by NORCAL Professional Geophysicist Donald J. Kirker, Staff Geophysicist Hunter Philson and Geophysical Technician Travis Black. Background information was provided by Michael Forrest and David Simpson of AECOM. The purpose, methodology, data acquisition and analysis procedures were consistent with our initial work.

Attached are the Site Location Map and Seismic Refraction Profiles, Plates 1 and 2, respectively. As shown on Plate 1, the SR survey was conducted along two lines designated as Lines 2-5 and 6-4. Line 2-5 was positioned from the center of Line 2-3 to the center of Line 4-3, and Line 6-4 was positioned approximately 200-ft upslope of Line 6-3, as directed by AECOM. The seismic refraction profiles (Plate 2) show how the compressional P-wave velocities vary beneath each line.

We appreciate the opportunity to provide our services to AECOM for this project. Should you require additional geophysical services or have questions regarding this survey, please do not hesitate to call.

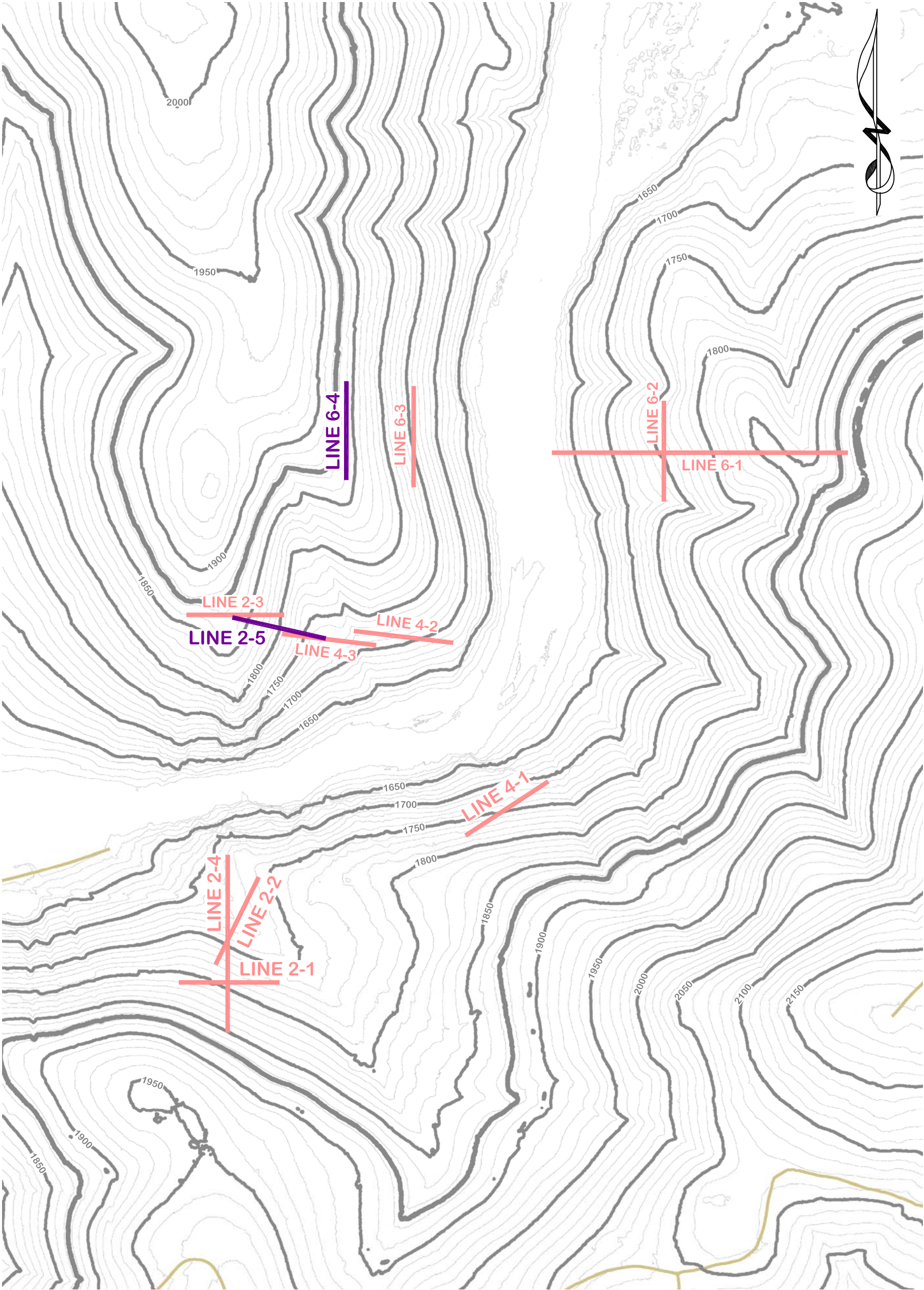
Sincerely,



NORCAL Geophysical Consultants, Inc

Donald J. Kirker
Professional Geophysicist, PGp-997

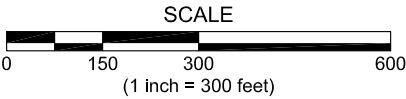
DJK/KGB/tt


Enclosures: Plates 1 and 2

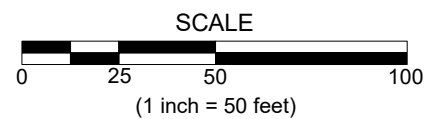
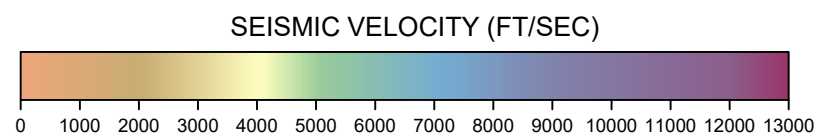
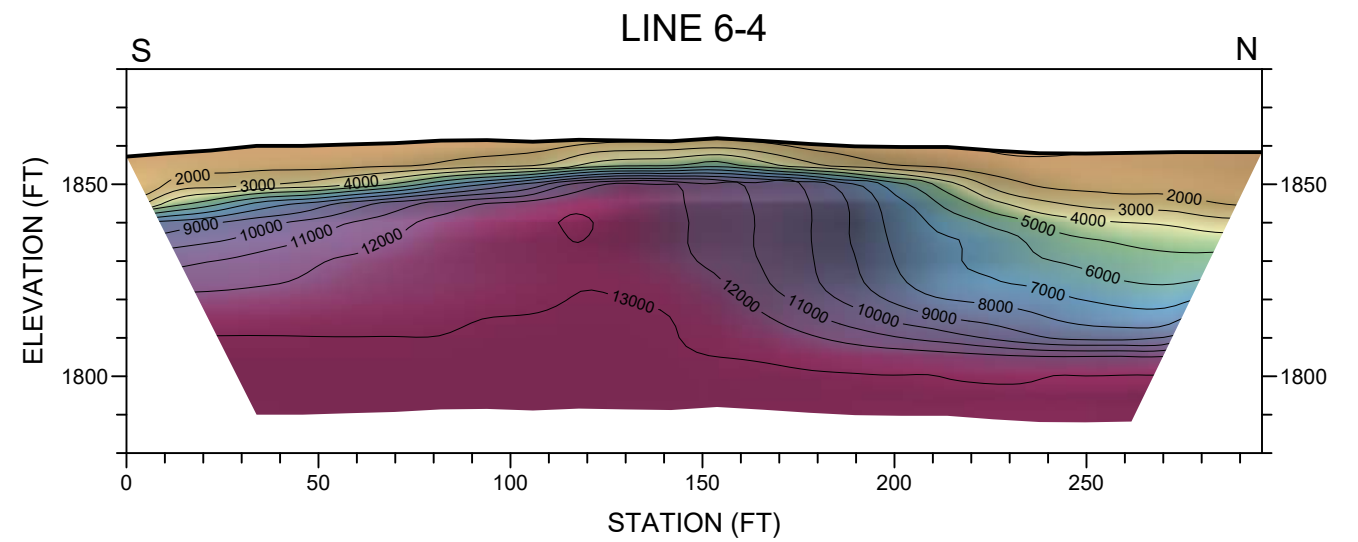
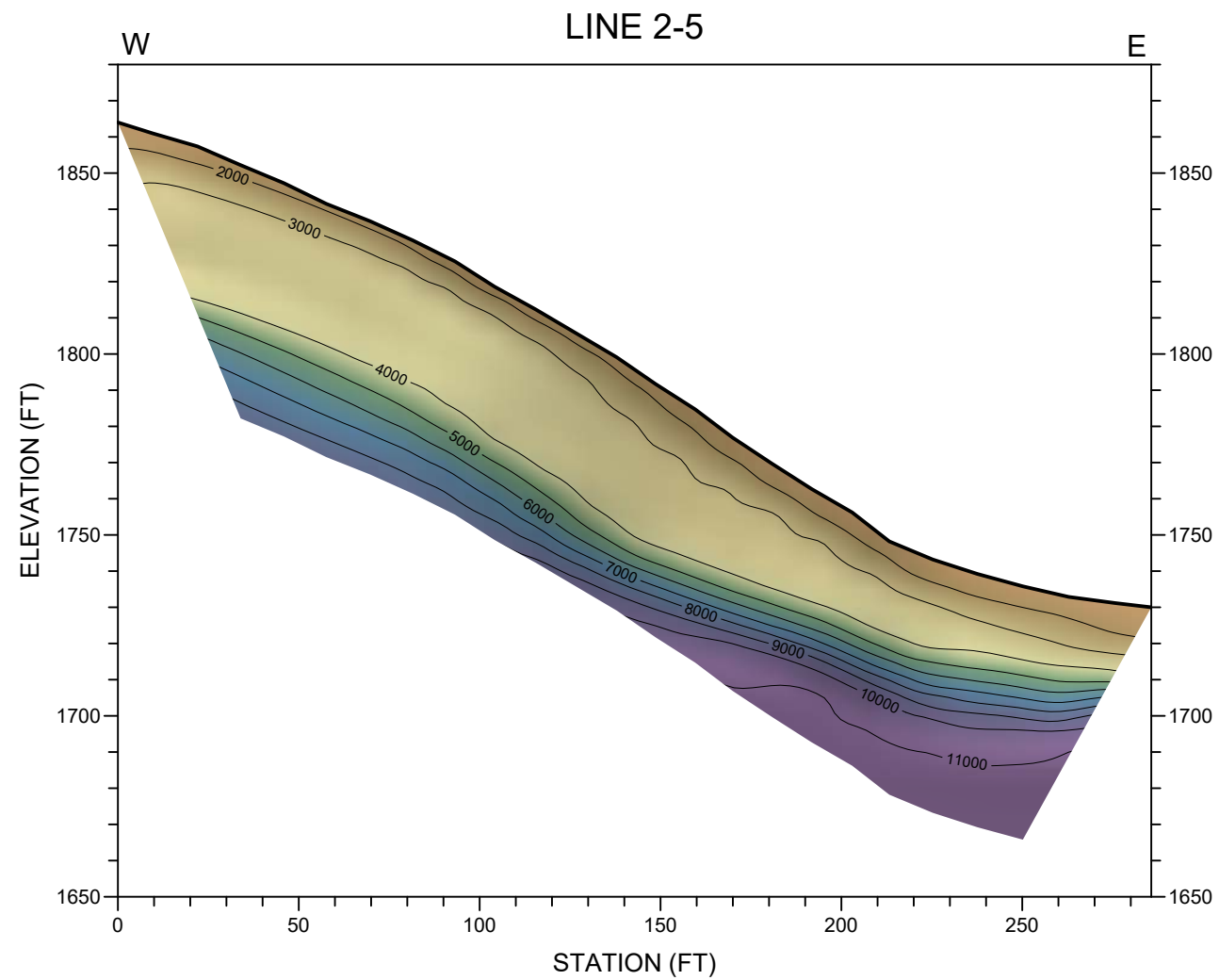



LEGEND	
	SEISMIC REFRACTION LINE - PHASE 2
	SEISMIC REFRACTION LINE - PHASE 1

NOTE: BASE MAP PROVIDED BY AECOM



	SITE LOCATION MAP	
	SEISMIC REFRACTION SURVEY - PHASE 2	
	NID WATER STORAGE PROJECT-BEAR RIVER	
	LOCATION: NEVADA COUNTY, CALIFORNIA	
	CLIENT: AECOM	PLATE 1
JOB #: 15-533.74	NORCAL GEOPHYSICAL CONSULTANTS INC.	
DATE: NOV. 2015	DRAWN BY: G.RANDALL APPROVED BY: DJK	



 NORCAL	SEISMIC REFRACTION PROFILES - PHASE 2		
	LINES 2-5 & 6-4		
	NID WATER STORAGE PROJECT-BEAR RIVER		
	LOCATION: PLACER & NEVADA COUNTIES, CAL FORNIA		
JOB #: 15-533.72	NORCAL GEOPHYSICAL CONSULTANTS INC.		PLATE <div style="font-size: 2em; font-weight: bold; text-align: center;">2</div>
DATE: SEP. 2015	DRAWN BY: G.RANDALL	APPROVED BY: DJK	

Appendix C-2 Seismic Refraction Survey Report – Phase III

Appendix C-2 Seismic Refraction Survey Report – Phase III

August 18, 2016

Mr. Michael Forrest
AECOM
1333 Broadway, Suite 800
Oakland, California 94612

Subject: Seismic Refraction Survey (Phase 3)
Nevada Irrigation District (NID) Centennial Dam Project, Bear River, Placer and
Nevada Counties, CA
NORCAL Job # NS165019A

Dear Mr. Forrest:

This report presents the findings of the Phase 3 seismic refraction (SR) survey performed by NORCAL Geophysical Consultants, Inc. at the NID Centennial Dam Project in Placer and Nevada Counties, California. This report is an addendum to our Phase 1 report dated September 23, 2015 and Phase 2 letter dated December 2, 2015.

1.0 INTRODUCTION

Based on the results of the Phase 1 and 2 surveys and the ongoing field work by AECOM, additional SR surveys were conducted in three separate areas. They are referred to as the Axis 2, South Barrow and North Barrow Areas by AECOM. The surveys at the Axis 2 and North Barrow Areas were conducted during the periods of June 13 through 16, 2016 and July 6 through 8, 2016, respectively, by NORCAL Professional Geophysicist Donald J. Kirker, and Geophysical Technicians Nick Novotny and Erasmo Tapia. The survey at the South Barrow Area was conducted during the period of May 18 through 20, 2016, by NORCAL Professional Geophysicist Donald J. Kirker, Staff Geophysicist Hunter Philson and Geophysical Technician Chris Bissiri. Background information and logistical support for all areas was provided by David Simpson and Ben Kozlowicz of AECOM.

The purpose, methodology, data acquisition and analysis procedures were consistent with our Phase 1 and 2 work. SR data were obtained along a total of 14 lines. Each line was marked in the field by AECOM/NID land surveyors using survey lath and flagging prior to the start of the SR survey. A topography map showing these surveyed locations was subsequently provided by AECOM.

AECOM
August 18, 2016
Page 2

2.0 SR SURVEYS

The results of the Phase 3 SR surveys at the Axis 2, South Borrow, and North Barrow Areas are presented on Plates 1 through 12. These plates represent the respective Site Location Maps and Seismic Refraction Profiles for each area. The SR profiles indicate seismic velocities that gradually increase from less than 2,000- to over 13,000-ft/s within the upper 60- to 70-ft. Based on the results of the previous work and soil boring logs provided by AECOM, we interpret the shallowest and lowest velocities (less than 5,000-ft/s) as representing surficial soils, colluvium and/or highly weathered/fractured bedrock. Velocities of 5,000- to 9,000-ft/s are interpreted as representing moderately weathered and/or fractured bedrock. The highest velocity material (over 9,000-ft/s) is indicative of rock that is slightly weathered and/or fractured.

A description of our findings for the Phase 3 work performed at the Axis 2, South Borrow and North Barrow Areas is provided below. This includes a brief description of the respective site, data acquisition and survey results and interpretation.

2.1 AXIS 2 AREA

2.1.1 Site Description

The Axis 2 Area is located on both sides of the Bear River, as shown on Plate 1. The terrain comprises relatively steep slopes covered with thick brush, and scattered conifers and deciduous trees. Surface elevations along the proposed seismic lines range from approximately 1,640- to over 1,950-ft above mean sea level (msl). On the south side of the river, the site was accessed by an unpaved road from the adjacent quarry. On the north side, the site was accessed by an unpaved road from Magnolia Road. The locations of each line, and the site topography, are shown on Plate 2.

2.1.2 Data Acquisition

The SR survey was conducted along seven lines, as designated by AECOM and shown on Plate 2. They are designated as Lines 2-6 through 2-12 and range in length from 296- to 900-ft. Lines 2-6 through 2-11 are located within the proposed dam axis footprint. Line 2-12 is located east of the proposed axis. They comprise one to four spreads that were either overlapping or placed end to end. Each spread consists of 24-geophones and five shot points distributed in a collinear array. The geophones were coupled to the ground surface at 10- to 13-ft intervals. Three shot points were evenly spaced within the interior of the spread. The remaining two were located approximately 5-ft beyond the end geophones.

AECOM
August 18, 2016
Page 3

2.1.3 Results and Interpretation

The results of the SR survey along Lines 2-6 through 2-12 are presented by the seismic velocity profiles on Plates 3 and 6. The velocity distribution along these profiles suggests that the most competent rock, as indicated by velocities of 9,000- to over 13,000-ft/s, is located south of the river along Lines 2-6 through 2-9, and 2-11. It ranges in depth from as shallow as 3-ft at the east end of Line 2-9 to as deep as 60-ft or more along the northwest half of Line 2-11. Conversely, velocities along the remaining two lines (2-10 and 2-12) are lower. Line 2-10, located on the north side of the river, and Line 2-12, east of the proposed axis, exhibits velocities up to 6,000- and 8,000-ft/s, respectively. These velocities are consistent with rock exhibiting an increase in weathering and/or fracturing.

2.2 SOUTH BARROW AREA

2.2.1 Site Description

The South Barrow Area is located north of the Bear River northeast of the proposed dam Axis 2. The terrain comprises moderately steep slopes covered with grass, thick brush, and scattered conifer and deciduous trees. Surface elevations along the proposed seismic lines range from approximately 1,849-to over 1,880-ft above mean sea level (msl). The site was accessed by an unpaved road from Magnolia Road to the north. The locations of each line, and the site topography, are shown on Plate 7.

2.2.2 Data Acquisition

The SR survey was conducted along four lines, as designated by AECOM and shown on Plate 7. They are designated as Lines BA-1 through BA-4 and range in length from 400- to 710-ft. They comprise two to four overlapping spreads. Each spread consists of 24-geophones and five shot points distributed in a collinear array. The geophones were coupled to the ground surface at 10-ft intervals. Three shot points were evenly spaced within the interior of the spread. The remaining two were located approximately 5-ft beyond the end geophones.

2.2.3 Results and Interpretation

The results of the SR survey along Lines BA-1 through BA-4 are presented by the seismic velocity profiles on Plates 8 and 9. The velocity distribution along these profiles suggests that the most competent rock, as indicated by velocities of 9,000- to over 11,000-ft/s, is located along Lines BA-2 and BA-4. It ranges in depth from as shallow as 10-ft along BA-2 to as deep as 53-ft at the west end of BA-4. The velocity distribution along the remaining two lines (BA-1 and -3)

AECOM
August 18, 2016
Page 4

suggests that the rock is probably slightly more weathered and/or fractured, as indicated by velocities up to 8,000-ft/s.

These profiles also indicate that the interpreted rock is relatively deep along the entire length of BA-1, the north end of BA-3 and the west end of BA-4, defining areas where the overlying low velocity materials (surficial soils, colluvium and/or highly weathered/fractured bedrock) are relatively thick.

2.3 NORTH BARROW AREA

2.3.1 Site Description

The North Barrow Area is located northeast of the South Barrow Area. The terrain is similar, comprising moderately steep slopes covered with grass, thick brush, and scattered conifer and deciduous trees. Surface elevations along the proposed seismic lines range from approximately 2,000-to over 2,100-ft above mean sea level (msl).

2.3.2 Data Acquisition

The SR survey was conducted along three lines, as designated by AECOM and shown on Plate 10. They are positioned on the northwest and southeast sides of a prominent knoll and are designated as Lines BA-5 through BA-7. They range in length from 410- to 1080-ft and comprise two to four spreads that are either overlapping or positioned end to end. Each spread consists of 24-geophones and five shot points distributed in a collinear array. The geophones were coupled to the ground surface at 10-ft intervals. Three shot points were evenly spaced within the interior of the spread. The remaining two were located approximately 10-ft beyond the end geophones.

2.3.3 Results and Interpretation

The results of the SR survey along Lines BA-5 through BA-7 are presented by the seismic velocity profiles on Plates 11 and 12. The velocity distribution along these profiles suggests that the most competent rock (9,000- to 10,000-ft/s) is shallowest on the northwest flank of the knoll (Lines BA-5 and most of Line BA-6) where it ranges in depth from 10- to 38-ft. In contrast, the rock is much deeper on the southwest and southeast flanks (southwest end of Line BA-6 and along BA-7) where it ranges from 55- to over 60-ft deep. As a result, the south flank of the knoll is characterized by areas where the overlying surficial soils, colluvium and/or highly weathered rock are relatively thick.

AECOM
August 18, 2016
Page 5

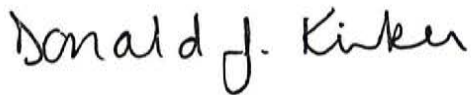
3.0 STANDARD CARE AND WARRANTY

The scope of services for this project consisted of using the seismic refraction method to define subsurface seismic velocities and depths. The accuracy of our findings is subject to specific site conditions and limitations inherent to the seismic refraction technique. We performed our services in a manner consistent with the level of skill ordinarily exercised by members of the profession currently employing similar methods. No warranty, with respect to the performance of services or products delivered under this agreement, expressed or implied, is made by NORCAL.

We appreciate the opportunity to provide our services to AECOM for this project. Should you require additional geophysical services or have questions regarding this survey, please do not hesitate to call.

Sincerely,

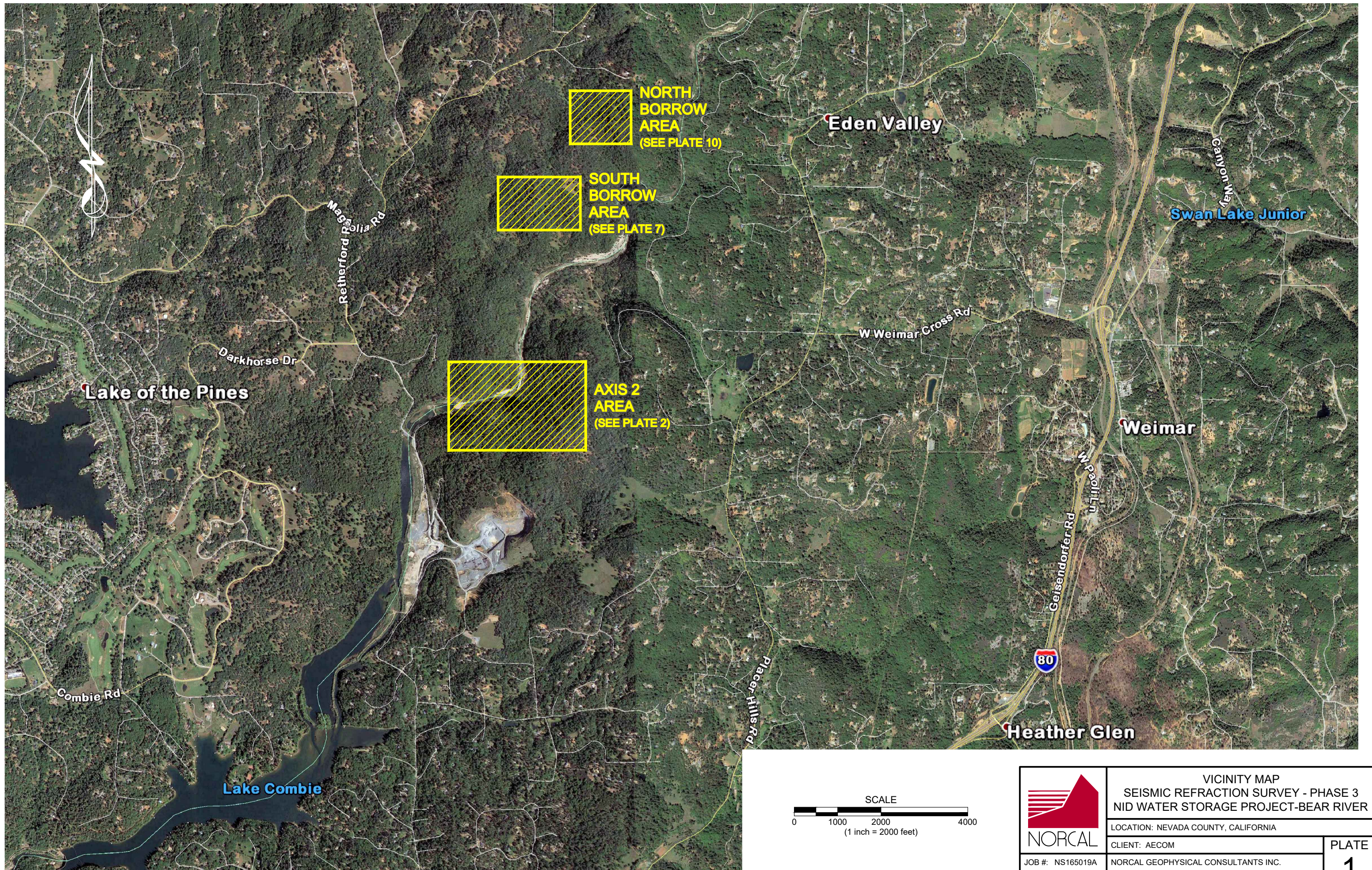
NORCAL Geophysical Consultants, Inc.



Donald J. Kirker
Professional Geophysicist, PGp-997

DJK/KGB/tt

Enclosures: Plates 1 through 12



SCALE
0 1000 2000 4000
(1 inch = 2000 feet)



VICINITY MAP
SEISMIC REFRACTION SURVEY - PHASE 3
NID WATER STORAGE PROJECT-BEAR RIVER

LOCATION: NEVADA COUNTY, CALIFORNIA

CLIENT: AECOM

JOB #: NS165019A

NORCAL GEOPHYSICAL CONSULTANTS INC.

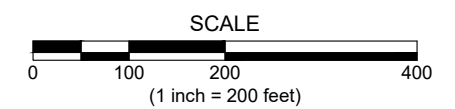
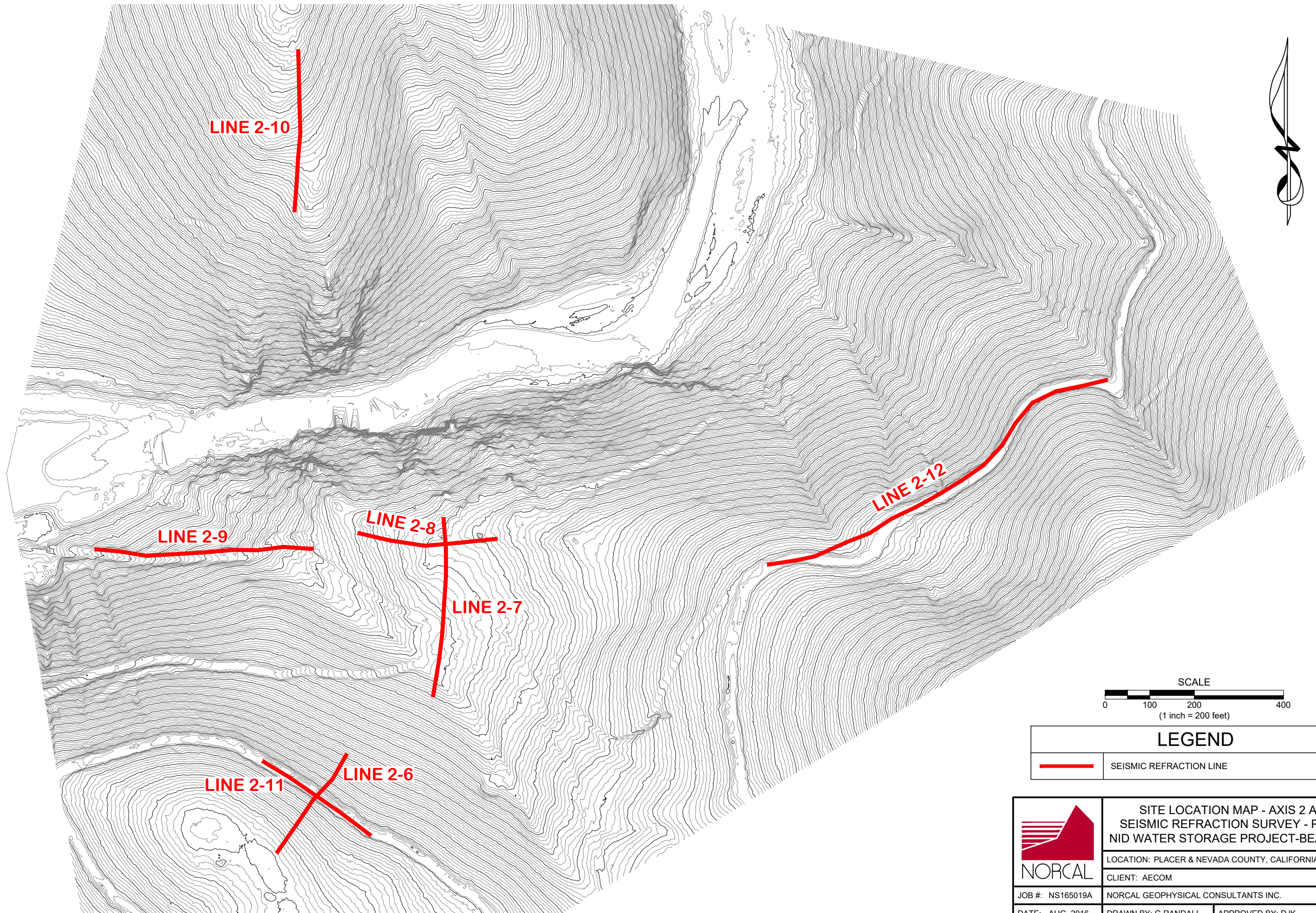
DATE: AUG. 2016

DRAWN BY: G.RANDALL


APPROVED BY: DJK

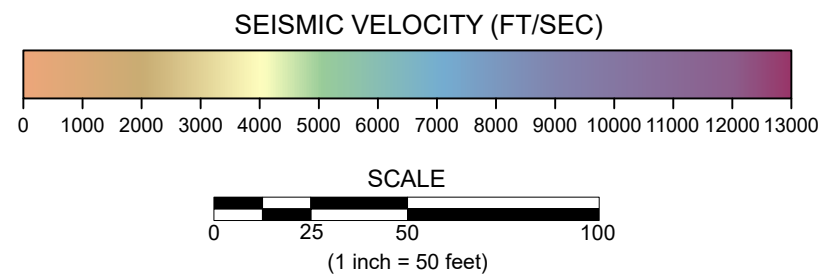
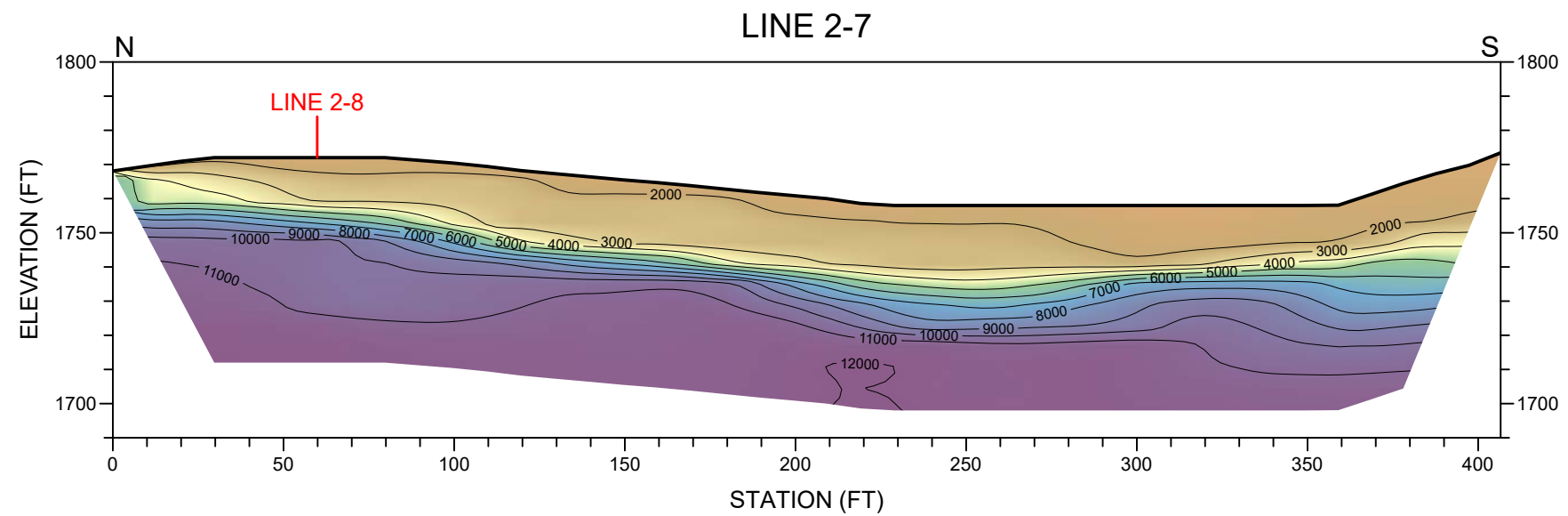
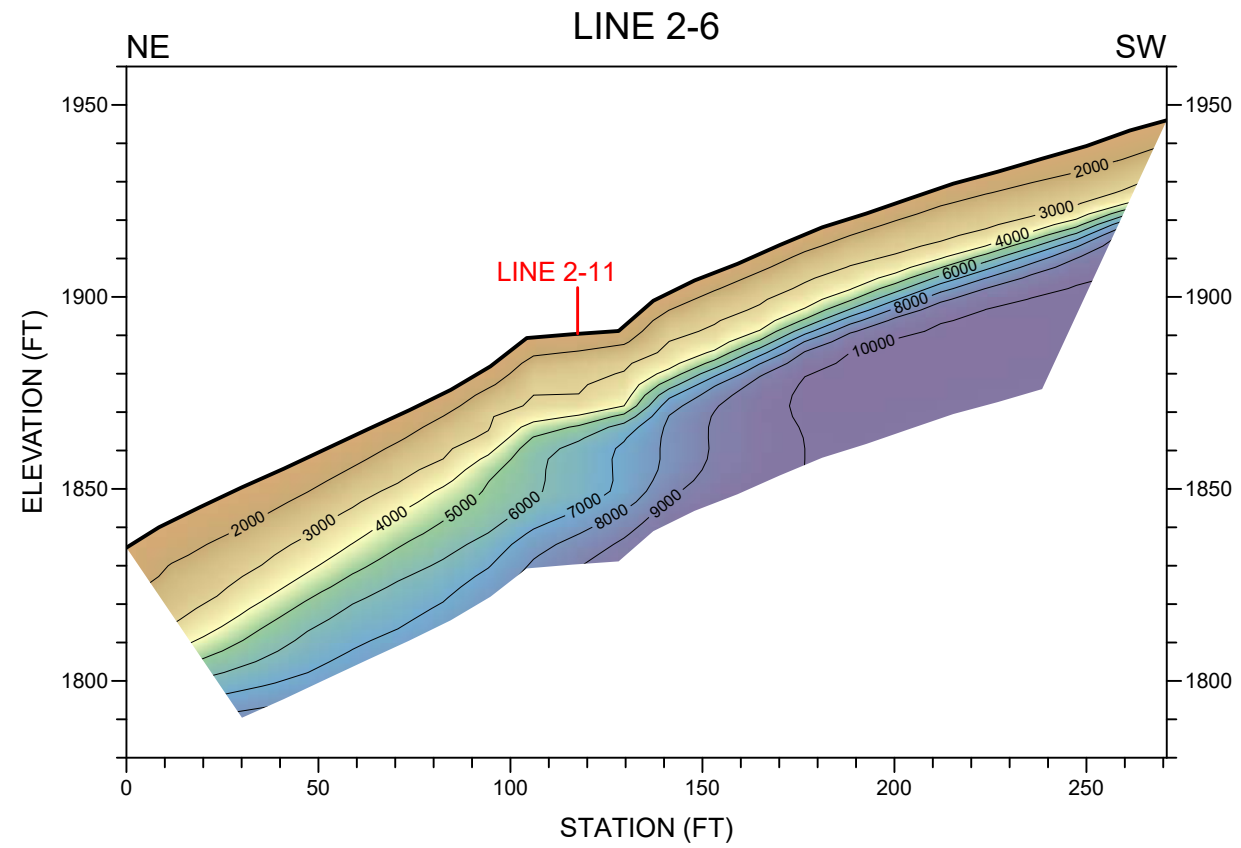
PLATE

1

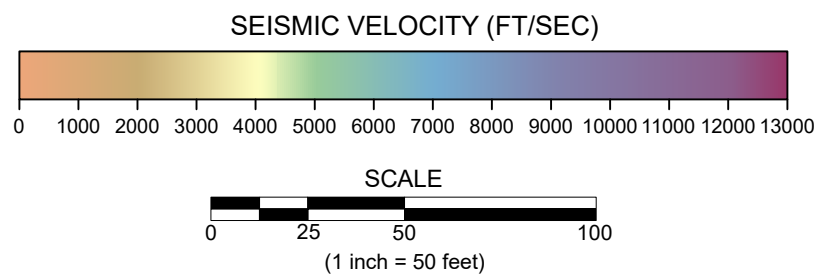
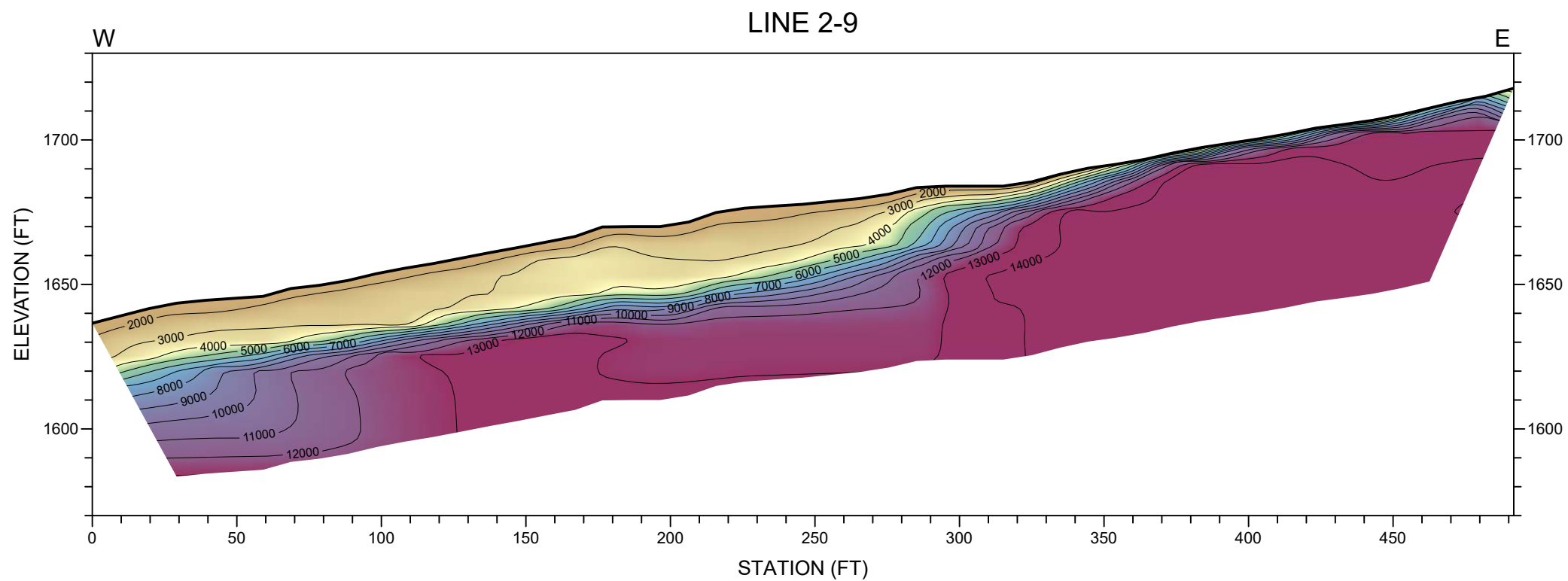
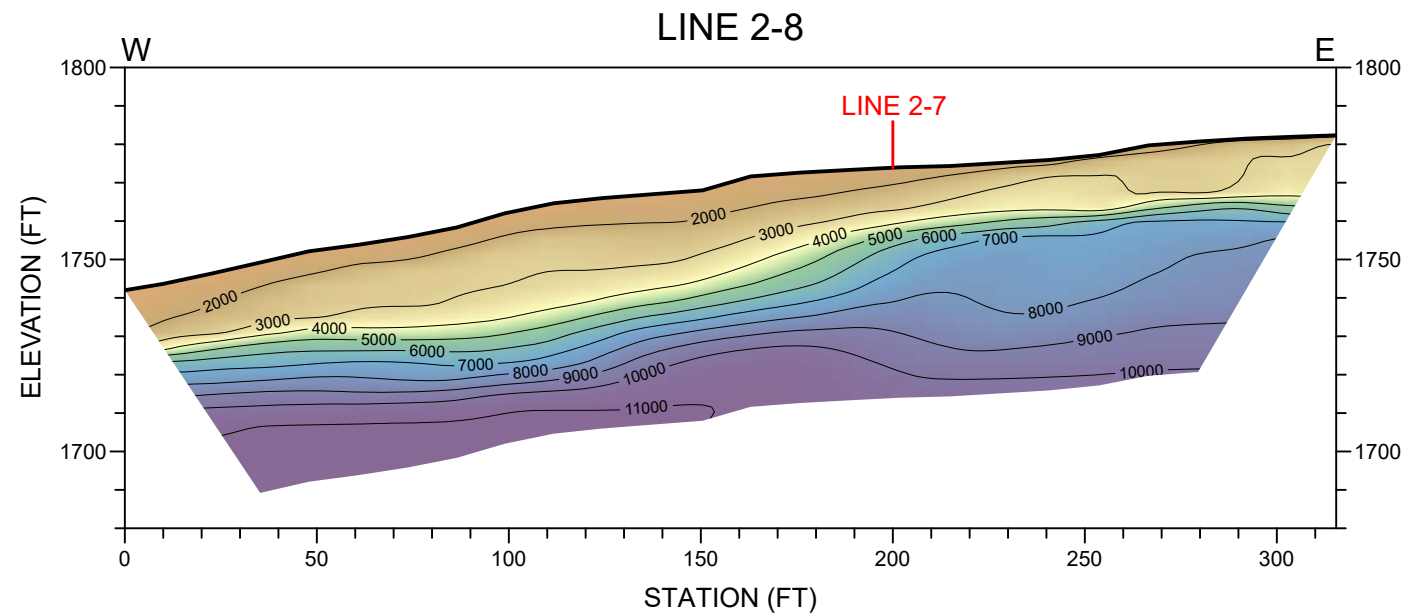



LEGEND	
	SEISMIC REFRACTION LINE

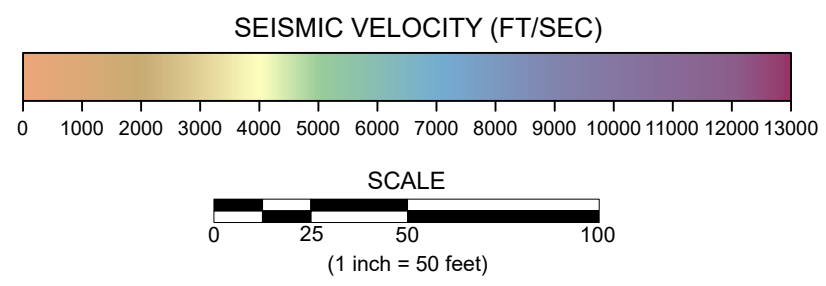
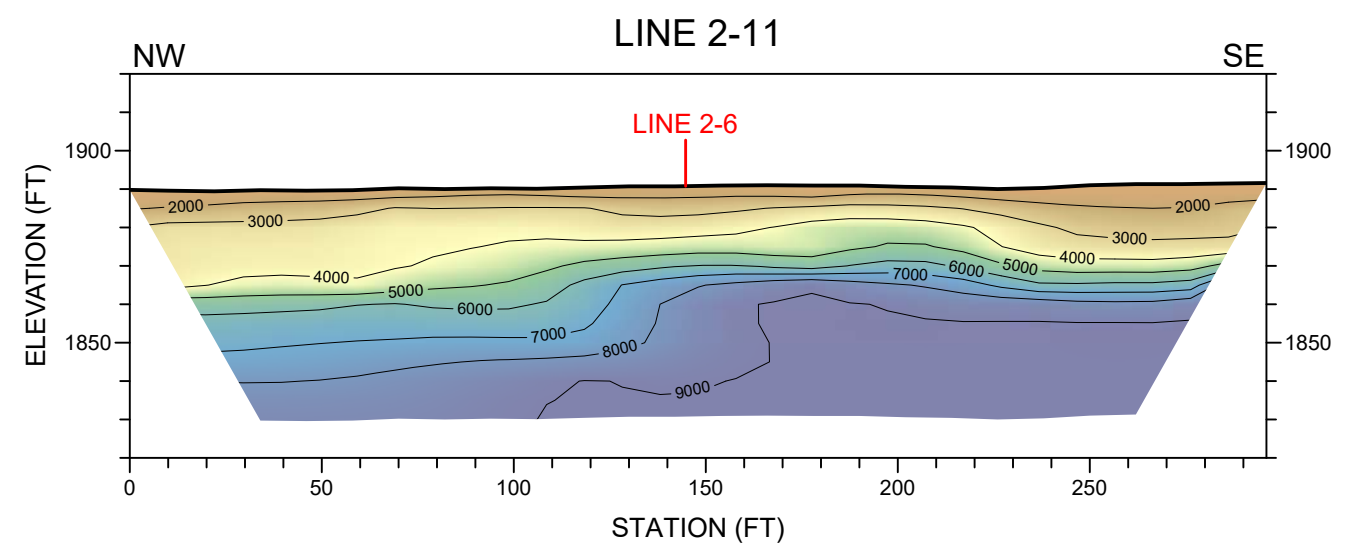
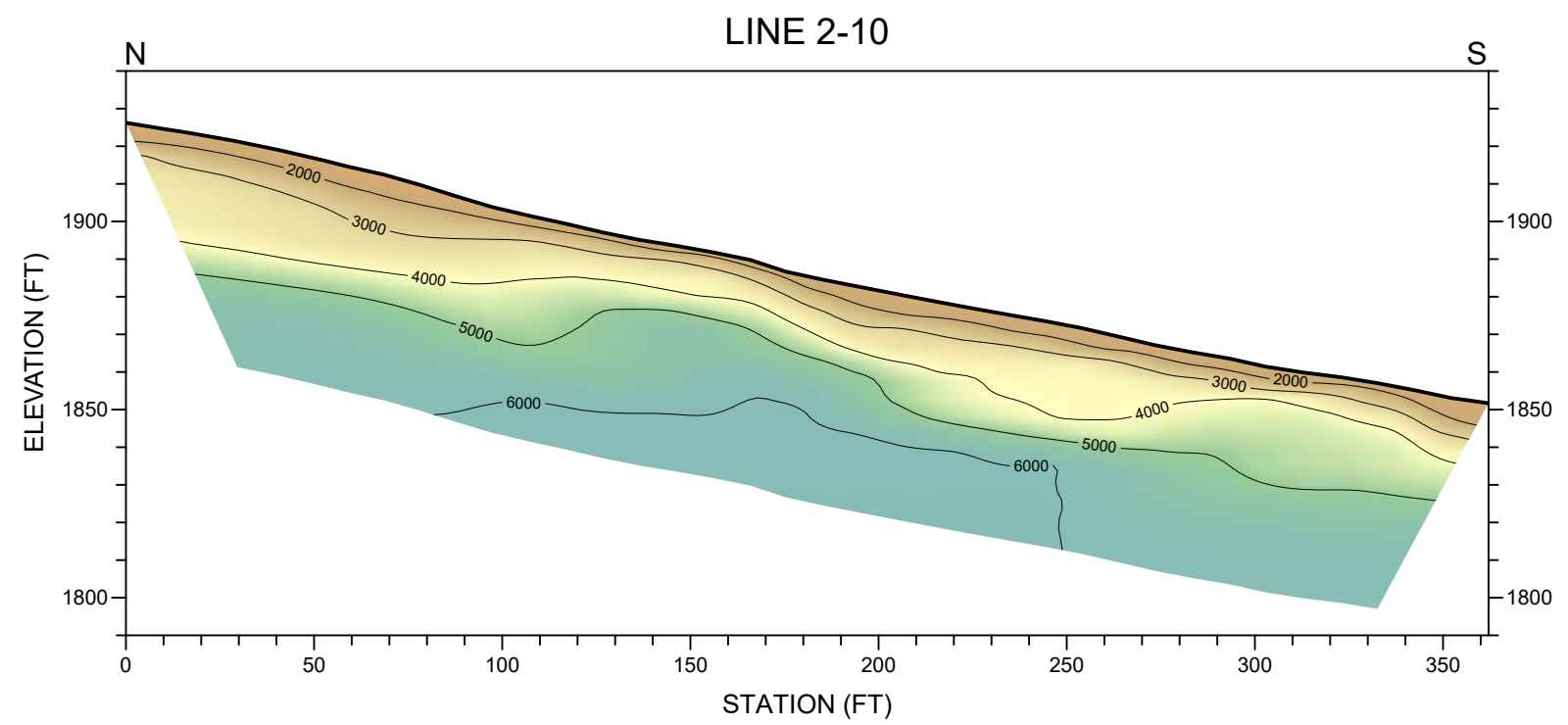
 NORCAL	SITE LOCATION MAP - AXIS 2 AREA SEISMIC REFRACTION SURVEY - PHASE 3 NID WATER STORAGE PROJECT-BEAR RIVER		
	LOCATION: PLACER & NEVADA COUNTY, CALIFORNIA		
	CLIENT: AECOM		PLATE 2
	JOB #: NS165019A	NORCAL GEOPHYSICAL CONSULTANTS INC.	
DATE: AUG. 2016	DRAWN BY: G.RANDALL	APPROVED BY: DJK	




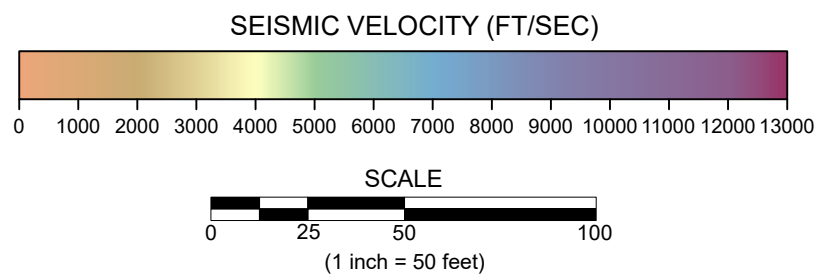
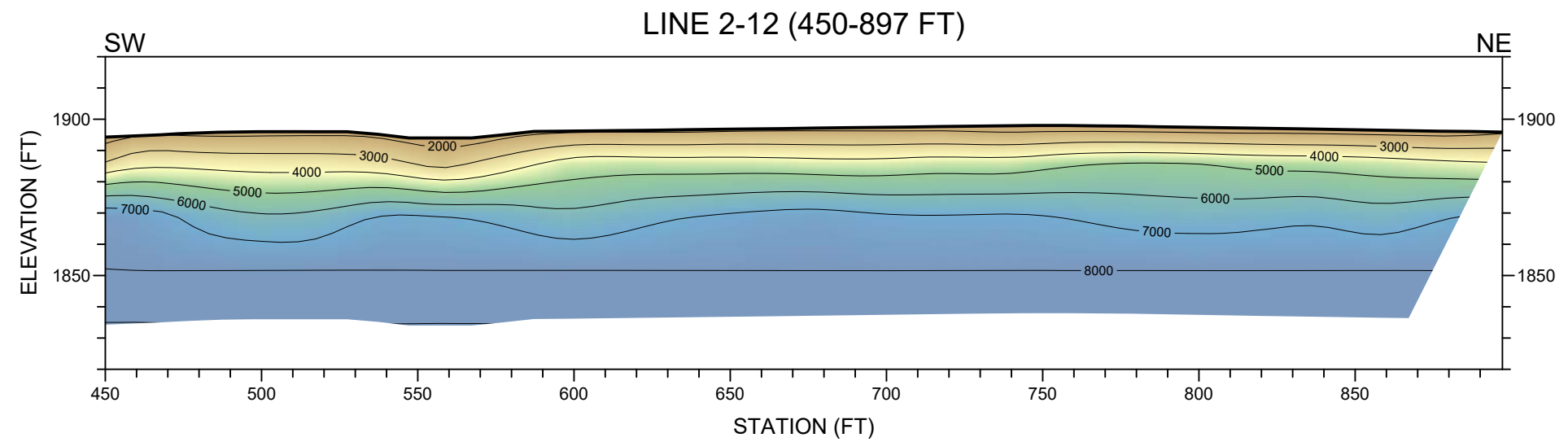
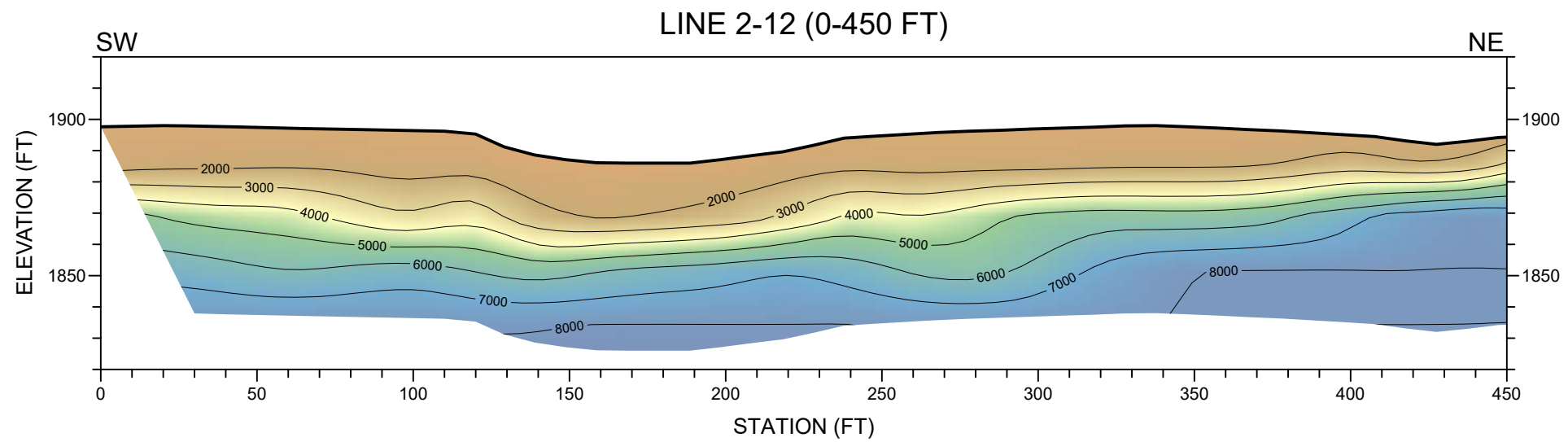
	SEISMIC REFRACTION PROFILES LINES 2-6 & 2-7 NID WATER STORAGE PROJECT-BEAR RIVER PHASE 3 - AXIS 2	
	LOCATION: PLACER & NEVADA COUNTIES, CAL FORNIA	
	CL ENT: AECOM	3
	DATE: AUG. 2016	
JOB #: NS165019A	NORCAL GEOPHYSICAL CONSULTANTS INC.	
DRAWN BY: G.RANDALL	APPROVED BY: DJK	




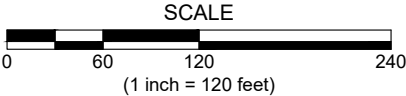
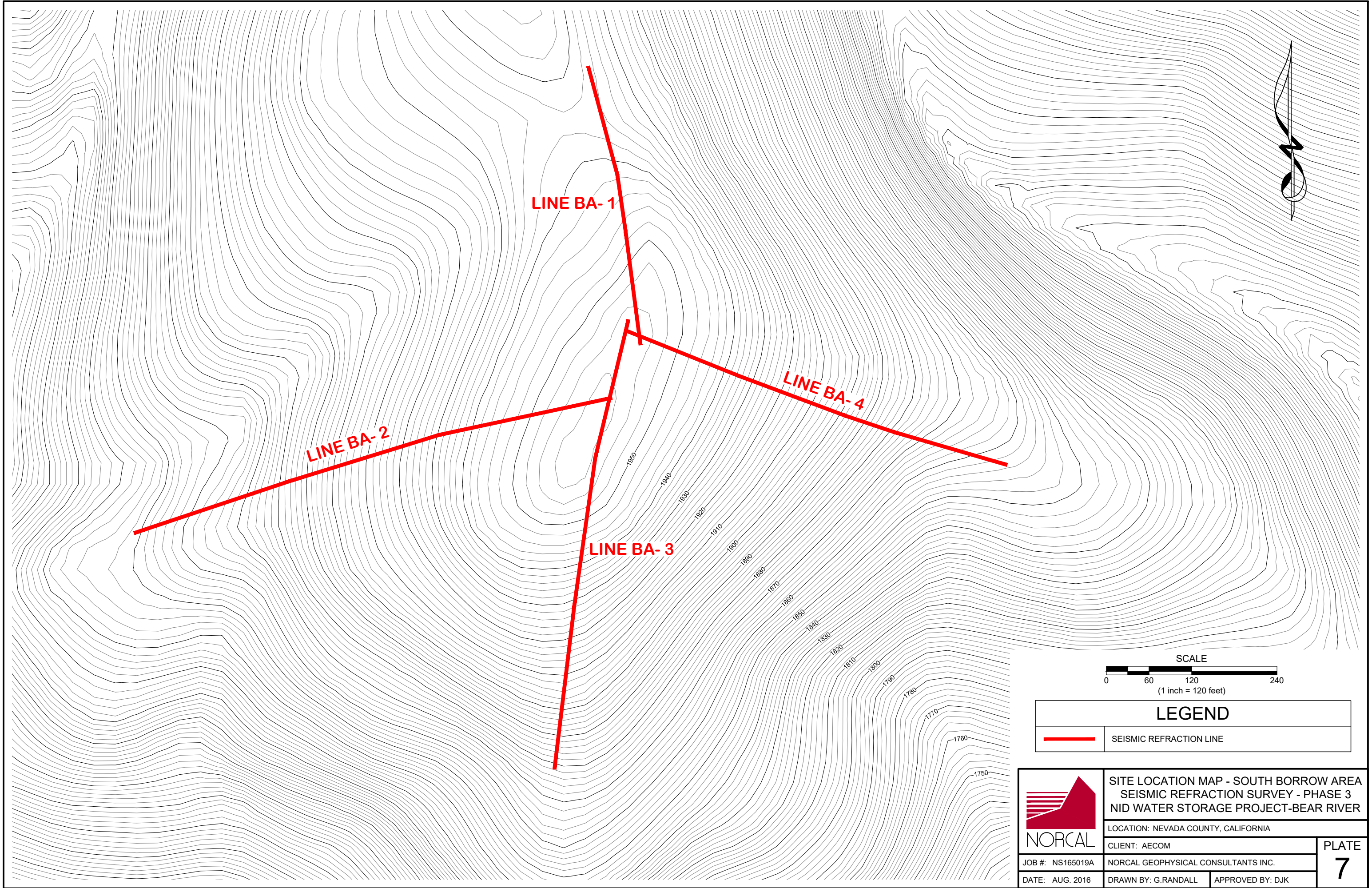
 NORCAL	SEISMIC REFRACTION PROFILES LINES 2-8 & 2-9 NID WATER STORAGE PROJECT-BEAR RIVER PHASE 3 - AXIS 2		
	LOCATION: PLACER & NEVADA COUNTIES, CAL FORNIA		
	CL ENT: AECOM		PLATE 4
	JOB #: NS165019A	NORCAL GEOPHYSICAL CONSULTANTS INC.	
DATE: AUG. 2016	DRAWN BY: G.RANDALL	APPROVED BY: DJK	



 NORCAL	SEISMIC REFRACTION PROFILES LINES 2-10 & 2-11 NID WATER STORAGE PROJECT-BEAR RIVER PHASE 3 - AXIS 2		
	LOCATION: PLACER & NEVADA COUNTIES, CAL FORNIA		
	CL ENT: AECOM		PLATE 5
	JOB #: NS165019A	NORCAL GEOPHYSICAL CONSULTANTS INC.	
DATE: AUG. 2016	DRAWN BY: G.RANDALL	APPROVED BY: DJK	



 NORCAL	SEISMIC REFRACTION PROFILES LINE 2-12 NID WATER STORAGE PROJECT-BEAR RIVER PHASE 3 - AXIS 2		
	LOCATION: PLACER & NEVADA COUNTIES, CAL FORNIA		
	CL ENT: AECOM		PLATE 6
	NORCAL GEOPHYSICAL CONSULTANTS INC.		
JOB #: NS165019A	DATE: AUG. 2016		
	DRAWN BY: G.RANDALL	APPROVED BY: DJK	



LEGEND	
	SEISMIC REFRACTION LINE



SITE LOCATION MAP - SOUTH BORROW AREA
SEISMIC REFRACTION SURVEY - PHASE 3
NID WATER STORAGE PROJECT-BEAR RIVER

LOCATION: NEVADA COUNTY, CALIFORNIA

CLIENT: AECOM

NORCAL GEOPHYSICAL CONSULTANTS INC.

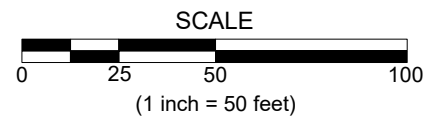
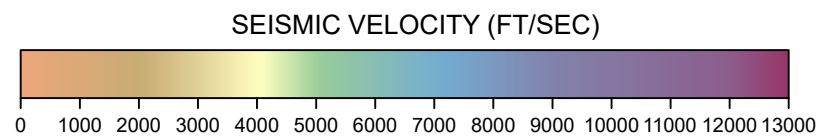
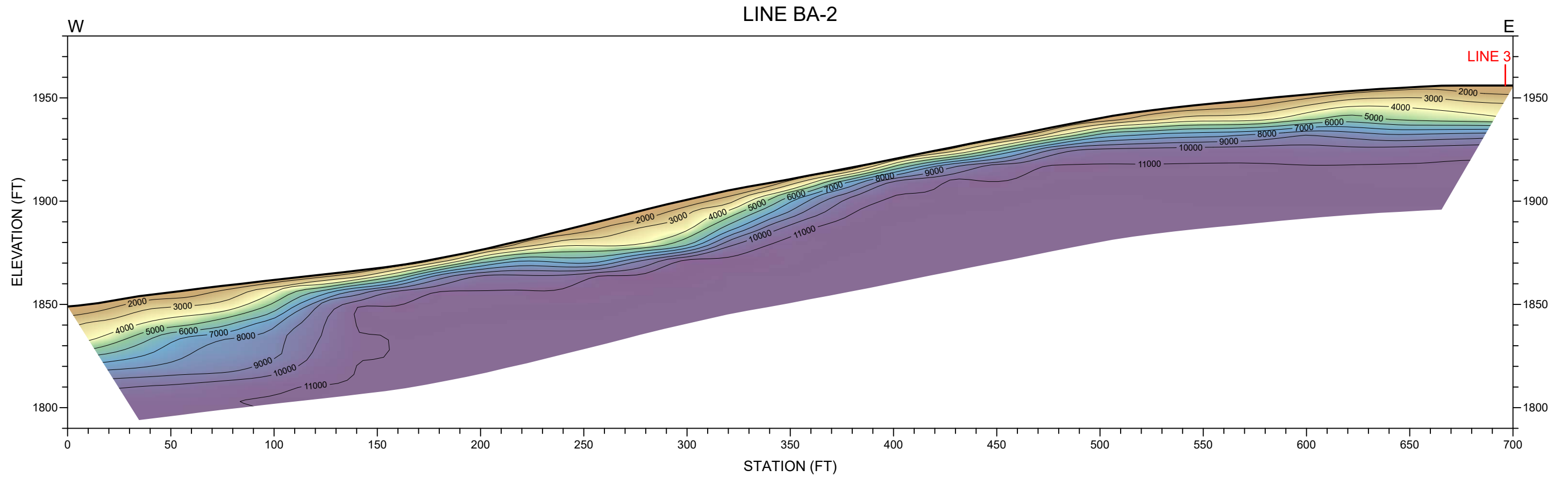
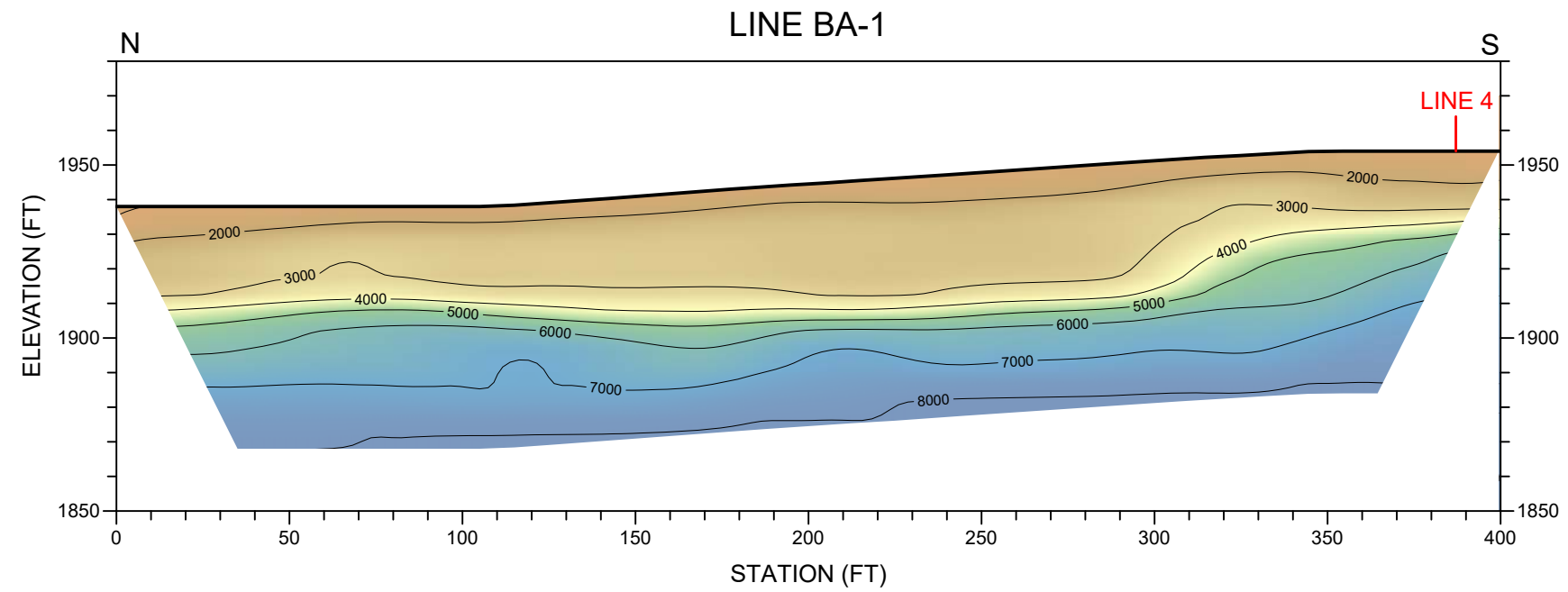
JOB #: NS165019A


DATE: AUG. 2016

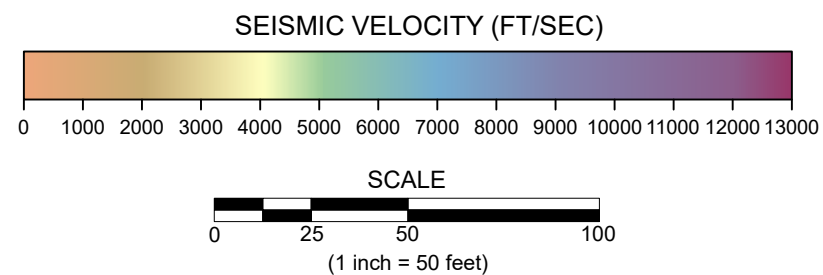
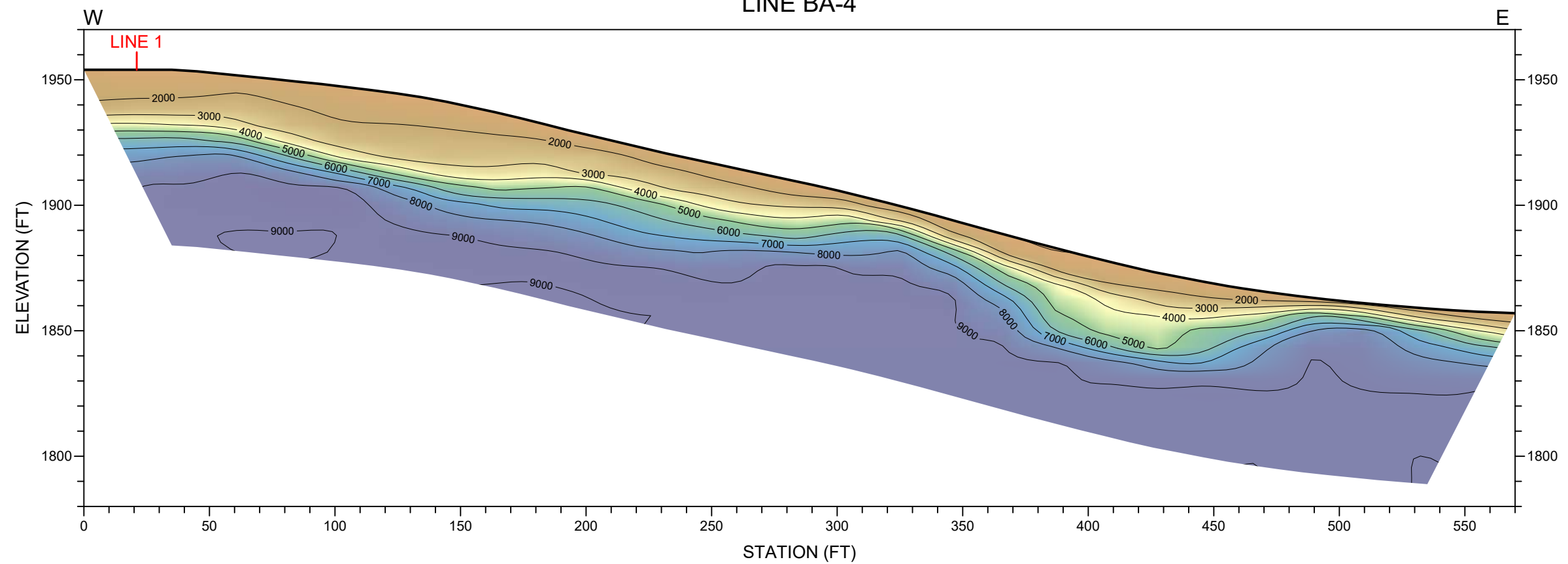
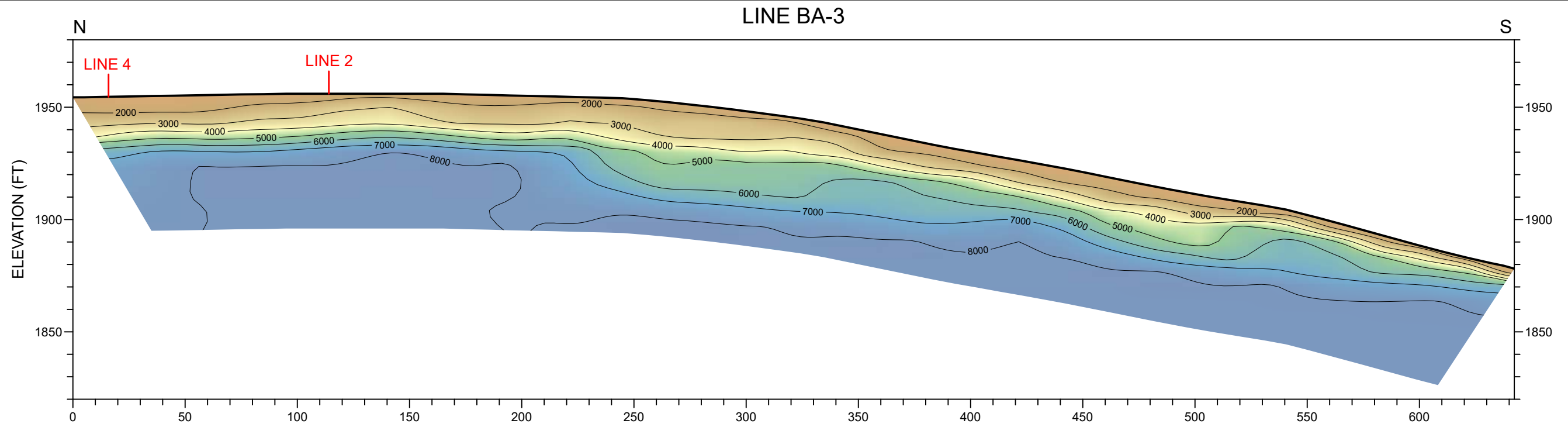
DRAWN BY: G.RANDALL


APPROVED BY: DJK

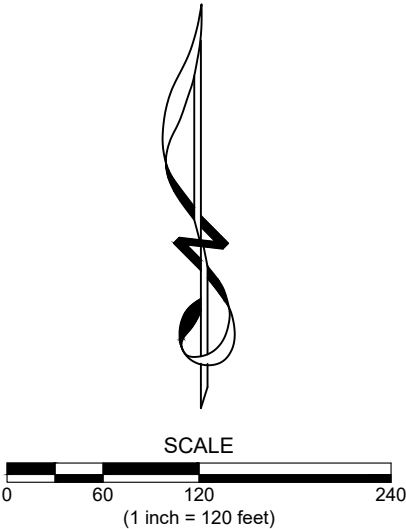
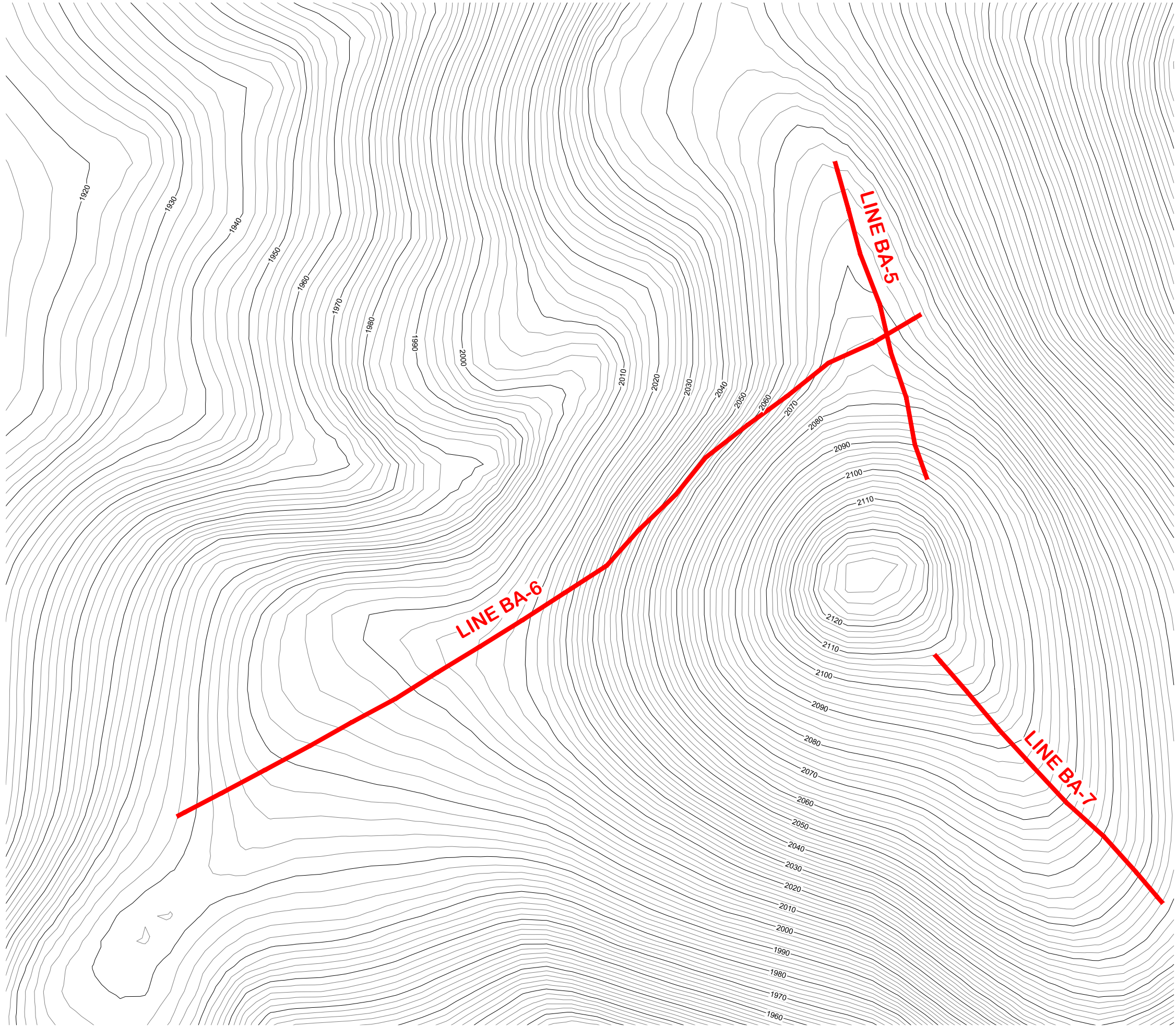
PLATE
7



 NORCAL	SEISMIC REFRACTION PROFILES LINES BA-1 & BA-2 NID WATER STORAGE PROJECT-BEAR RIVER PHASE 3 - SOUTH BORROW AREA		
	LOCATION: NEVADA COUNTY, CAL FORNIA		
	CL ENT: AECOM		PLATE 8
	JOB #: NS165019A	NORCAL GEOPHYSICAL CONSULTANTS INC.	
DATE: AUG. 2016	DRAWN BY: G.RANDALL	APPROVED BY: DJK	



 NORCAL	SEISMIC REFRACTION PROFILES LINES BA-3 & BA-4 NID WATER STORAGE PROJECT-BEAR RIVER PHASE 3 - SOUTH BORROW AREA	
	LOCATION: NEVADA COUNTY, CAL FORNIA	
	CL ENT: AECOM	
	JOB #: NS165019A NORCAL GEOPHYSICAL CONSULTANTS INC.	
DATE: AUG. 2016	DRAWN BY: G.RANDALL	APPROVED BY: DJK
		PLATE 9



LEGEND	
	SEISMIC REFRACTION LINE



SITE LOCATION MAP - NORTH BORROW AREA
SEISMIC REFRACTION SURVEY - PHASE 3
NID WATER STORAGE PROJECT-BEAR RIVER

LOCATION: NEVADA COUNTY, CALIFORNIA

CLIENT: AECOM

NORCAL GEOPHYSICAL CONSULTANTS INC.

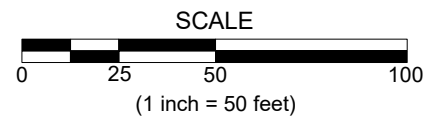
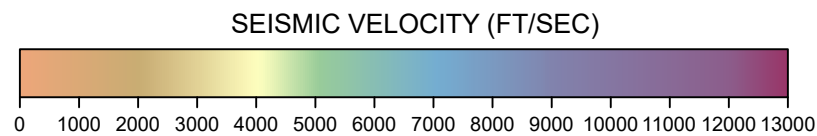
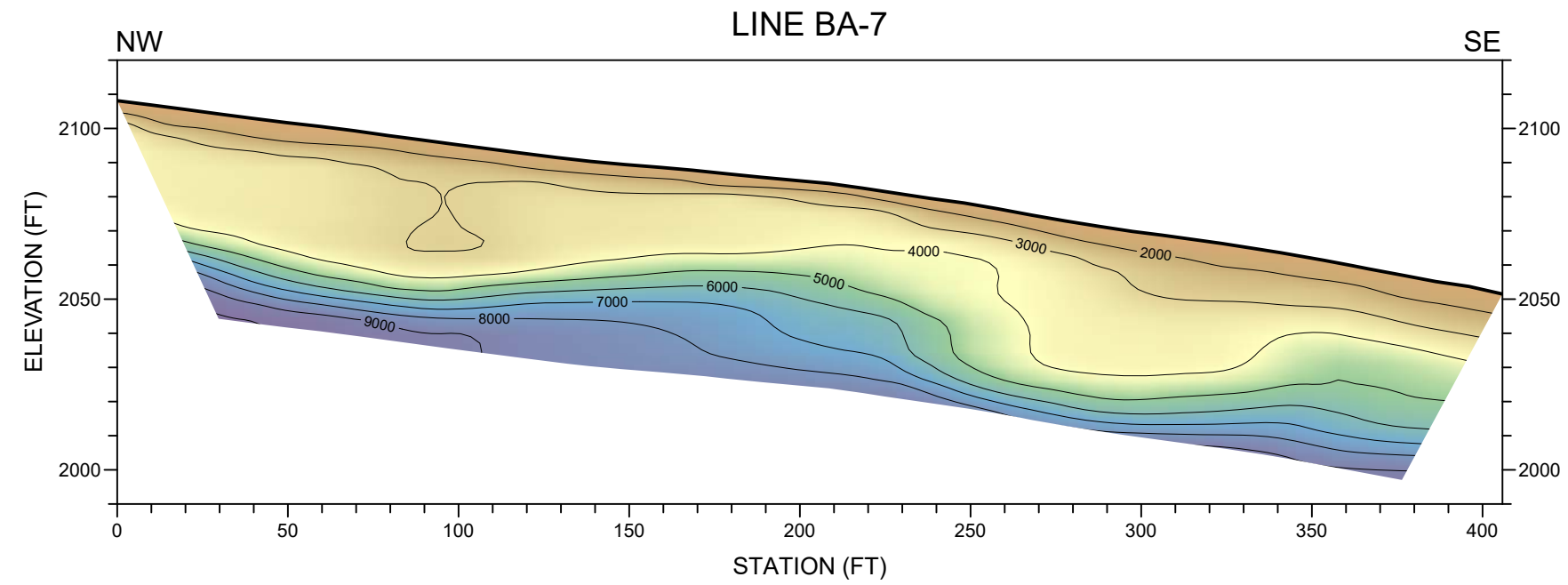
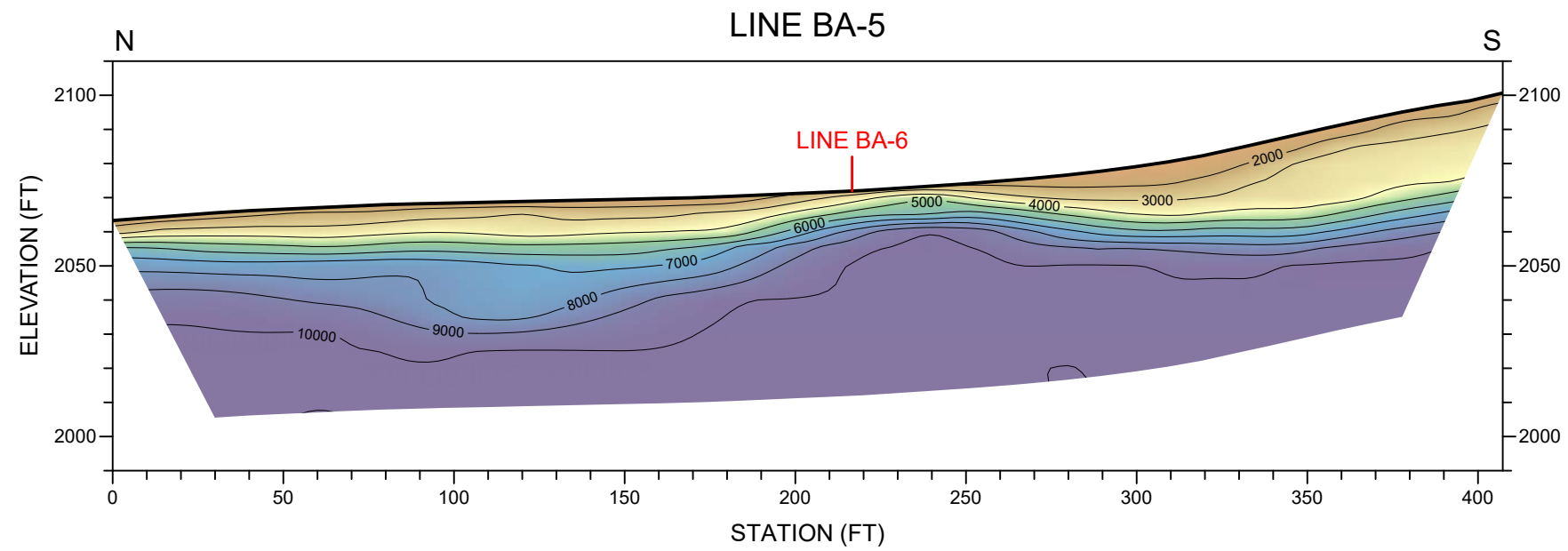
JOB #: NS165019A


DATE: AUG. 2016

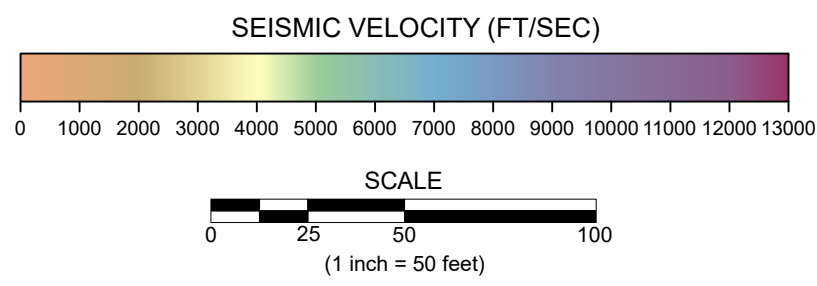
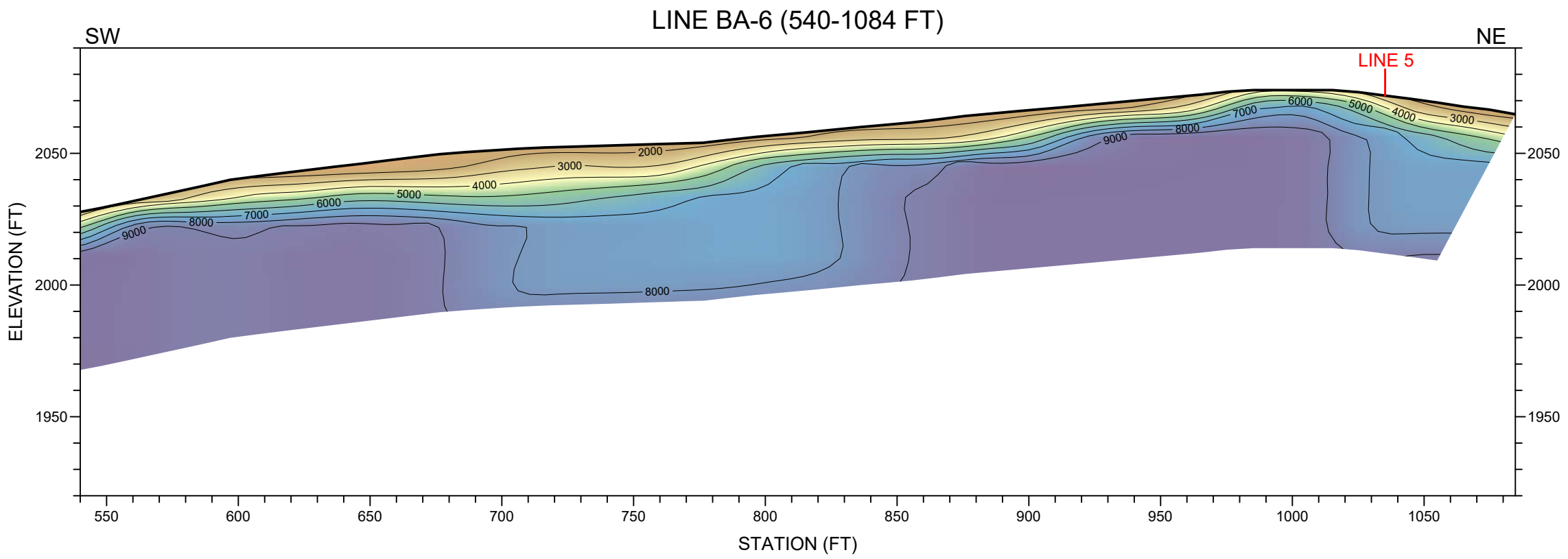
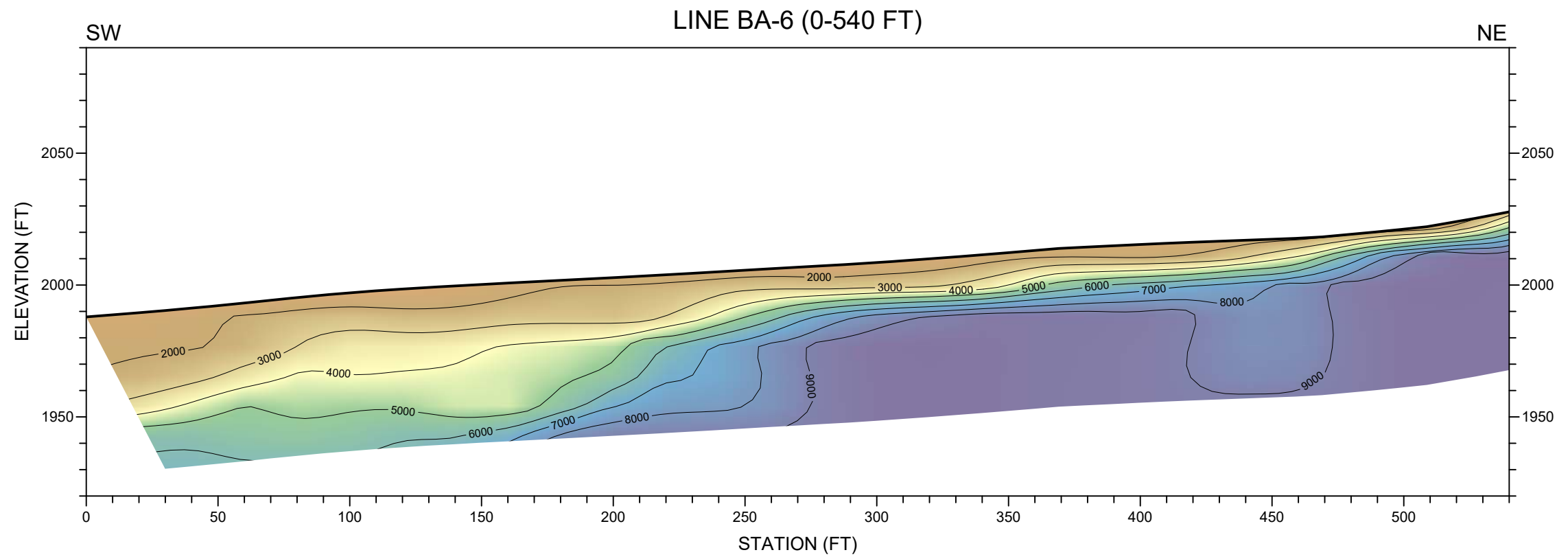
DRAWN BY: G.RANDALL


APPROVED BY: DJK

PLATE
10



 NORCAL	SEISMIC REFRACTION PROFILES LINES BA-5 & BA-7 NID WATER STORAGE PROJECT-BEAR RIVER PHASE 3 - NORTH BORROW AREA		
	LOCATION: NEVADA COUNTY, CAL FORNIA		
	CL ENT: AECOM		PLATE 11
	JOB #: NS165019A	NORCAL GEOPHYSICAL CONSULTANTS INC.	
DATE: AUG. 2016	DRAWN BY: G.RANDALL	APPROVED BY: DJK	



 NORCAL	SEISMIC REFRACTION PROFILES		
	LINE BA-6		
	NID WATER STORAGE PROJECT-BEAR RIVER		
	PHASE 3 - NORTH BORROW AREA		
LOCATION: NEVADA COUNTY, CAL FORNIA			
CL ENT: AECOM			PLATE 12
JOB #: NS165019A	NORCAL GEOPHYSICAL CONSULTANTS INC.		
DATE: AUG. 2016	DRAWN BY: G.RANDALL	APPROVED BY: DJK	

Appendix D. Core Boring Logs and Core Photographs